Effects of Bolt Spacing on Prying Action in Thin Flanged Specimens

by

Richard DeSimone

A Report Submitted to the Faculty of the

Milwaukee School of Engineering

In Partial Fulfillment of the

Requirements for the Degree of

Master of Science in Structural Engineering

Milwaukee, Wisconsin

June 2012

Abstract

A large amount of research has been performed on prying action since the 1950's which lead to modern design procedures. However, many unknowns still exist. One of the unknown considerations is the effect that bolt spacing has on prying forces. This study focused on the effects of bolt spacing in a tee connection subjected to tensile force.

The variable in the experiment was the bolt spacing, and the experiment determined how the prying forces change as the bolt spacing changed. A secondary consideration was to determine and/or validate the idea of the moment at the bolt line be greater than that of the moment at the WT shape's web face, which is a variable in the current design procedure.

The American Institute of Steel Construction provides code provisions for which prying forces are determined. Based on those provisions, the bolt spacing for testing was determined.

In order to properly determine the effects of the prying force with regards to the bolt spacing, the bolt forces were determined using strain measurements from the bolts. Through data analysis, the prying force was determined and a comparison of five specimens was performed.

Results showed that the prying forces dropped considerably as the bolt spacing increased. The first test Specimen had a bolt spacing of 5.25 inches and experienced prying forces larger than that of the AISC provisions. The cause of the larger prying forces was due to alpha, α, being larger than 1.0. A significant drop in prying force occurred from the first Specimen to the second specimen which had a bolt spacing of 7.00 inches. Specimen three had a bolt spacing of 8.75 inches and showed a slight decrease in prying force from specimen two. Specimens four and five which had bolt spacing of 10.50 inches and 14.00 inches, respectively, experienced approximately the same amount of prying force, which was less than that of specimen three.

It was concluded that the prying forces decrease as the bolt spacing increases, and the AISC provisions are conservative for specimens with bolt spacing greater than 7.00 inches, but unconservative for specimen one which had a bolt spacing of 5.25 inches.

Acknowledgments

First and foremost, the author would like to thank the research and project advisor, Dr. Christopher Raebel. Dr. Raebel continually provided guidance as the protect progress. Secondly, the author would like to thank committee members Dr. Hans-Peter Huttelmaier and Mr. Michael Kempfert for their generous preliminary feedback and guidance. Additionally, the author would like to thank Austin Meier, the author's lab partner, for all his hard work and research which helped make the experiment possible.

A special thanks also goes out to Germantown Iron and Steel for providing all the experimental steel. Without Germantown Iron and Steel's generosity, the experiment would not have possible. The Milwaukee School of Engineering was generous enough to fund the testing bolts and strain gages, as well as, allowing the use of the Construction Science and Engineering Center which was where the experiment took place.

Finally, the author would like to thank his family for all their encouragement, and support throughout the academic year.

Table of Contents

List of Figures

List of Tables

Nomenclature

Symbols

A   Effective cross sectional area of A490X bolt

a   Distance from bolt centerline to edge of flange, $a \leq 1.25b$, in.

a'   Distance from edge of flange to inside edge of bolt hole, in.

B   Tensile strength per bolt, kips

b   Distance from bolt centerline to face of fitting, in.

b'   Distance from web edge to inside edge of bolt hole, in.

d_b Bolt diameter, in.

Fu   Specified minimum tensile strength of connecting element, ksi

Fy   Yield strength of connecting element, ksi

g   Transverse center-to-center spacing (gage) between bolts, in.

n   Number of bolts in a row

P1   Tributary length based on AISC provisions (see p).

P2   Actual tributary length (edge of specimen to middle of bolt spacing)

p   Tributary length

p_e Equivalent length

P_{max} Maximum calculated experimental value for tributary length

Q   Multiplication factor for available tension force

q   Additional tension bolt force due to prying action forces, kips/bolt

q_{exp} Experimental prying action forces, kips/bolt

q_{offset} Experimental prying force determined from the experimental graph of bolt force versus Prying Force. (considers engagement zone)

q_{max} Maximum calculated experimental prying force

s   Bolt spacing

T   Tension force due to service loads, kips

$T_{available}$ Available tensile force per bolt, kips

T_{exp} Experimental tensile force per bolt, kips

T_{max} Maximum calculated experimental bolt force

t   Flange thickness of member

t_c Flange thickness required to develop design tensile strength of bolts, in

t_{min} Minimum required flange thickness to prevent prying action, in

α Ratio of moment at the bolt line to the moment at the face of the T-stem, in determining prying action in hanger connections

α_{exp} Experimental value for the ratio of moment at the bolt line used in determining prying action in hanger connections to the moment at the face of the tee stem

α_{max} Maximum calculated experimental value for the α

α' Value of α used for prying action that either maximizes the bolt available tensile strength for a given thickness or minimizes the thickness required for a given bolt available tensile strength

β An α' limit state provision

δ Ratio of the net length at the bolt line to the gross length at the face of the stem or leg of angle used to determine prying action for hanger connections

ρ — Proportion of b' over a'

$\mu\varepsilon$ — Measured bolt strain during the experiment

$\mu\varepsilon_{max}$ — Maximum measured bolt strain during the experiment

σ — Experimental bolt stress

σ_{max} — Maximum calculated experimental bolt stress

ϕ — LRFD factor of safety

Abbreviations

AISC — American Institute of Steel Construction

ASTM — American Society for Testing and Materials

CSEC — Construction Science and Engineering Center

FBD — Free Body Diagram

LRFD — Load and Resistance Factor Design

LVDT — Linear Variable Displacement Transducer

MSOE — Milwaukee School of Engineering

Chapter 1: Introduction

1.1. Background

WT shapes are used in a variety of steel connections. Common applications for WT shapes are beam-to-column connections, beam-to-column moment connections, diagonal braces, and hanger connections [1]. When the flanges of a WT shape are bolted to a column, beam, or base plate, and the WT shape webs are pulled in tension opposing the bolted connection of the flange; a phenomenon known as prying action can occur [2, 3].
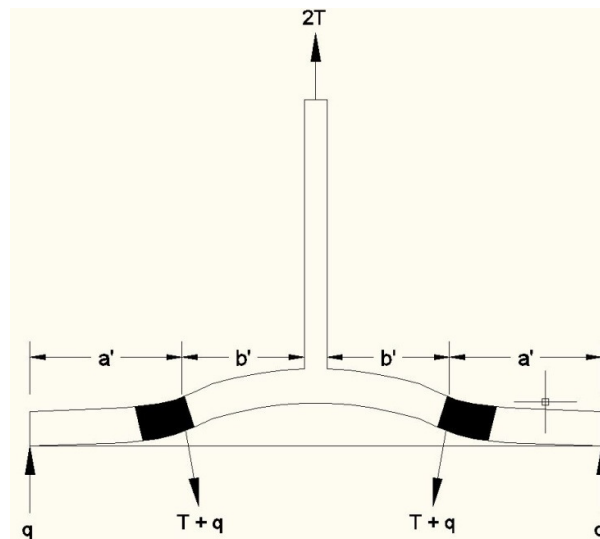
Figure 1.1-1: Deformed Shape with Prying Forces.

Studies such as Thornton [4], Swanson [5], Swanson and Gao [6], Swanson and Leon [7], Zoetemeijer [8], Nair *et al.* [2], Nair *et al.* [9], Dowswell [10], Wheeler *et al.* [11], and Willibald *et al.*[12] have been performed and refined since the 1950's which theorized how to calculate and predict the resulting prying forces in a WT shape. Those same studies have also shown that WT shape bolted connections can be significantly

affected by prying forces and the ultimate capacity of the connection should be checked with prying forces.

When there are large enough tensile loads on a WT shape, three yielding conditions can occur. The first yield condition consists of the bolts elongating while the WT shape's flange remains stiff (Figure 1.1-2). The second yield condition is when a deformation (single curvature) among the WT shape flange occurs between the bolted connections, which then create a prying force (Figure 1.1-2). With the second yield state, the deformation location starts within the gage distance of the two bolts parallel with the WT shape cross-section. As the connected bolts begin to yield, the deformation distance expands from the gage distance to the outer edges of each bolt, towards the flange tips (Figure 1.1-2). The third yield condition consists of deformation at the web edge in addition to that of the bolt line (double curvature). In the third yield condition the prying forces are maximized with the increased WT shape's flange deformation. As the flange begins to yield, plastic hinges begin to develop. Swanson's [5] research indicated that the two developing plastic hinges occur at the location noted as b' (Figure 1.1-2) and a distance of half the radius of the fillet from the web edge. The typical failure modes in the third yield condition are bolt failure and/or flange-to-web member failure. Since the flange of the WT shape is experiencing a large amount of deformation due to yielding, bolt failure will most likely occur first.
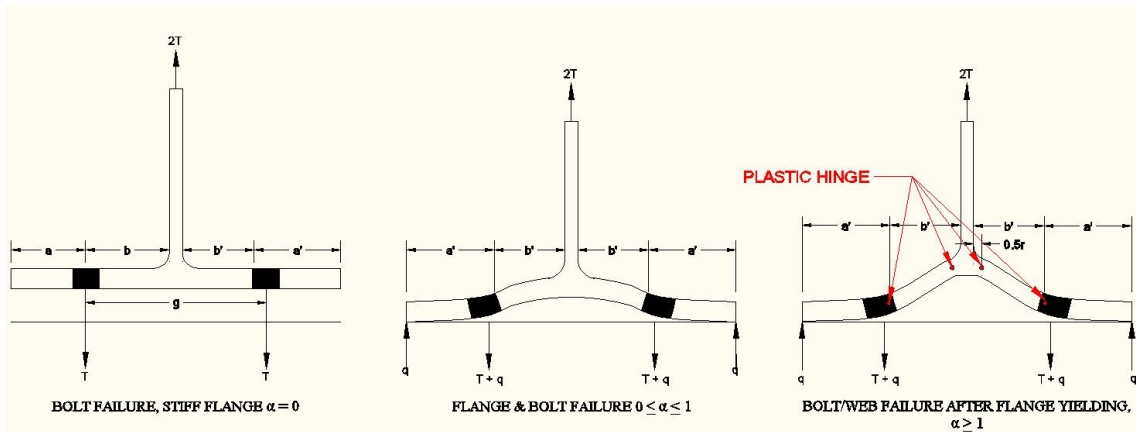
Figure 1.1-2: Yielding Limiting Conditions [12].

The connecting bolts experience axial and bending forces simultaneously when prying action occurs. When the WT shape flange begins to yield, bending moments develop throughout the flange of the WT shape, which develops bending in the connecting bolts. The location of the bending moments are maximized at the location b', shown in Figure 1.1-3. A moment diagram for the entire WT shape flange can be seen in Figure 1.1-3 [10].
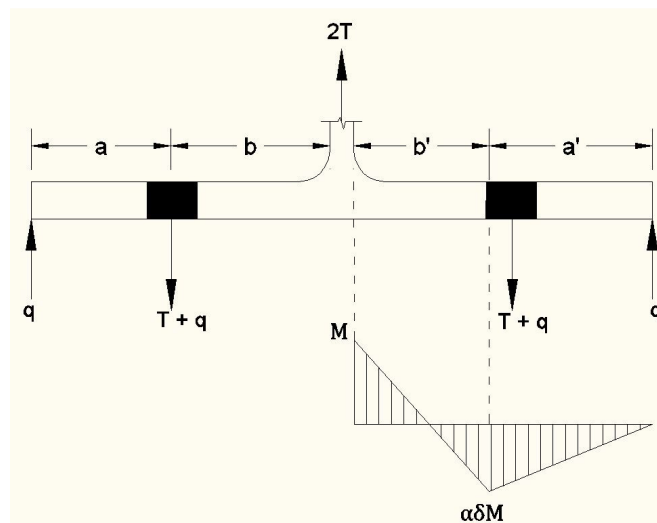
Figure 1.1-3: Prying Action Moment Diagram [10].

By observing the moment diagram across the flange shown in Figure 1.1-3, and the deformed shape shown in Figure 1.1-1, it resembles the shape of a deformed fixed-fixed connected beam element which contradicts Douty and McGuire's [13] research where it was assumed the WT shape acts like a simply supported beam where the bolt lines are the simple supports.

The flange thickness of the WT shape is perhaps the most critical piece of the prying action analysis. If the flange is sufficiently stiff, the deformation of the flange will have little effect and the bolt deformation will control. If the flange lacks sufficient stiffness, the bolt and WT shapes limitations will both have to be evaluated [1]. Some limit states that could occur are the fracturing of the bolts and/or web of the WT shape and flange deformation failure [14].

1.2. AISC Provisions

There are two ways to design a WT shape's connection with regards to prying action. The first way is to design the member with a sufficiently thick flange so that prying action forces are negligible. Figures 1.2-1 and 1.2-2 show a WT shape with bolt hole locations noted by variables. The same variables are noted in the AISC [3] provisions when determining prying forces. This allows for variability between applications.
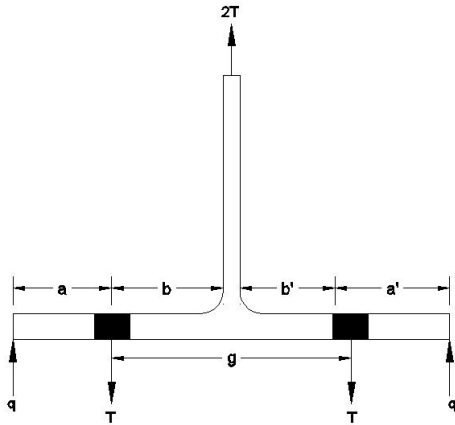
Figure 1.2-1: Prying Action FBD [3].   **Figure 1.2-2: Bolt Spacing [3].**
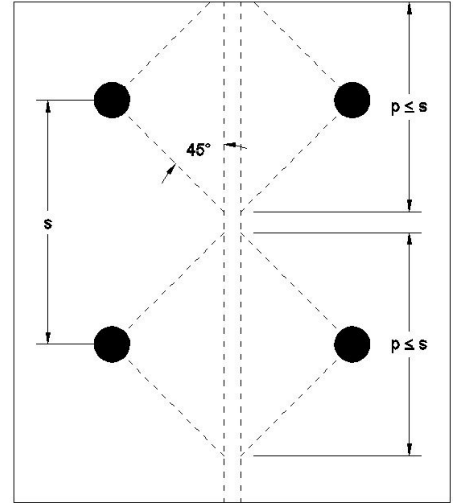
The minimum flange thickness of a WT shape where prying forces are negligible may be calculated as [3]

$$t_{min} = \sqrt{\frac{4Tb'}{\phi p F_u}},$$ (1)

where t_{min} is the minimum flange thickness, T is the required strength per bolt in kips, b' is the location of max bending moment and tensile force within the connecting bolts, and Fu is the maximum tensile strength of the connected element, the tributary length, p, is limited by using the maximum of 2b and the bolt spacing, s, where b is the distance from web face to bolt center [3]. This is expressed as

$$p = \max 2b, \text{ but } \leq s,$$ (2)

unless tests indicate a larger length can be used [10].

The second way to design a WT shape connection with prying forces is to include

the prying forces and check the limit states of the WT shape and bolt capacities. When

checking the connection with prying force, the tension in the bolt, T, can be expressed as

$$T \leq \frac{\phi F_u t^2 p}{2b}, \tag{3}$$

and

$$t_{min} = \sqrt{\frac{4Tb'}{\phi p F_u (1 + \delta \alpha')}}, \tag{4}$$

where ϕ is the LRFD reduction factor, t is the WT shape's flange thickness, δ is the ratio

of the net length at the bolt line to gross length at the face of the stem or leg of an angle,

and α' is the lesser of two values [3]. The values in Equation (4) are defined in the

following manner:

$$\alpha' = 1.0 \text{ if } \beta \geq 1 = \text{ the lesser of 1 and } \frac{1}{\delta}\left(\frac{\beta}{1-\beta}\right) \text{ if } \beta < 1, \tag{5}$$

$$\delta = 1 - \frac{d'}{p}, \tag{6}$$

$$\beta = \frac{1}{\rho}\left(\frac{B}{T} - 1\right), \tag{7}$$

$$\rho = \frac{b'}{a'}, \tag{8}$$

and

$$a' = \left(a + \frac{d_b}{2}\right) \leq \left(1.25b + \frac{d_b}{2}\right). \tag{9}$$

In Equation (9), a' is based on the minimum of two limit states where a is the distance

from the bolt centerline to the edge of the flange tip, b is the distance from the bolt

centerline to the face of the web, and d_b is the bolt diameter.

If it is determined that $t_{min} \leq t$, the preliminary thickness of the flange is

satisfactory and prying forces are negligible. If $t < t_{min}$ then a thicker flange is required to

prevent prying forces from occurring. To determine the maximum allowable bolt force,

the acting prying force, q, will need to be determined. The prying force, q, is calculated

as

$$q = B[\delta\alpha\rho\left(\frac{t}{t_c}\right)^2], \tag{10}$$

where

$$t_C = \sqrt{\frac{4Bb'}{\phi pF_u}}, \tag{11}$$

and

$$\alpha = \frac{1}{\delta}\left[\frac{T}{B}\left(\frac{t_c}{t}\right)^2 - 1\right]. \tag{12}$$

α is the ratio of the moment at the bolt line to the moment at the face of the tee stem, and

shall be greater than zero but ≤ 1.0. The flange thickness t_c is the minimum required to

develop the required design tensile strength of the bolts [3]. When α is equal to zero, no

moments are generated within the flange; thus, no prying action exists on the connection.

When α is equal to 1, the bolt capacities are governing the connection. When α is

between zero and 1, the combination of flange deformation and bolt capacity are acting

together. Realistically, α cannot be greater than 1, but some studies using the α > 1 theory have been presented [5]. If, for instance, we use α > 1, then the prying forces in the each bolt would be larger than that of α = 1, where the bolt capacity governs. The resulting total bolt forces are the applied load plus the prying force [2, 9].

There are alternative ways to determine bolt strength if the WT shapes are known. This follows a similar approach with slightly different provisions. Instead of using the flange thickness limits and strength requirements, one can take the selected size and determine a value of Q, which is a reduction factor of the nominal bolt capacity. The available tensile capacity, $T_{available}$, can be determined by

$$T_{available} = BQ, \tag{13}$$

which is taking the maximum tensile strength per bolt and multiplying it by a reduction factor to determine an available tensile capacity per bolt. Instead of using $0 \leq \alpha \leq 1$, an alternative α' is used with the same limits of $0 \leq \alpha' \leq 1$. A similar set of three limit states apply, only with respect to bolt available tensile strength [3]. One exception to the rule is that α' can be greater than 1 and is as follows,

$$\alpha' = \frac{1}{\delta(1+\rho)}\left[\left(\frac{t_c}{t}\right)^2 - 1\right], \tag{14}$$

$$Q = 1 \text{ when } \alpha' < 0, \tag{15}$$

$$Q = \left(\frac{t}{t_c}\right)^2 (1 + \delta\alpha') \text{ when } 0 \leq \alpha' \leq 1, \tag{16}$$

$$Q = \left(\frac{t}{t_c}\right)^2 (1 + \delta) \text{ when } \alpha' > 1, \tag{17}$$

where α' is a value used to maximize the bolt tensile strength for a given flange thickness or minimize the required flange thickness required for any given available bolt tensile strength. The reduction factor, Q, is based on the limit states of α'.

1.3. Bolt Pre-Tensioning

Bolted connections are typically pre-tensioned. The required pre-tensioning forces are based on bolt diameters [3]. When the connecting bolts are pre-tensioned some initial elongation occurs. If the applied tensile loads are larger than the pre-tensioned loads additional elongation of the connecting bolts will occur. When the effects of prying forces are included, the elongation of the pre-tensioned bolts exists prior to the tensile load exceeding the pre-tensioned bolt force.

The approach taken with regards to combined prying forces, pre-tensioned bolts, and applied tensile loads are as follows. As the applied forces are generated, approximately 5% to 10% of the applied forces are added to the pre-tensioned bolt forces [1]. The increasing applied load is changing the contact pressures between the connecting plates [1]. The ratio of the increasing applied load to the decreasing contact pressures are directly related to the relative stiffnesses of all members involved in the connection [9]. When the plates begin to separate, prying forces will occur if the flange is not sufficiently stiff. When the connected members become completely separated, the bolt forces become equal to the applied load with no resulting prying forces [9]. The results are similar to that of the three yielding conditions mentioned earlier. The resulting bolt force can then be taken as the pre-tensioned force plus the prying action force. From previous studies by Kulak *et al.* [1], Nair *et al.* [2], Nair *et al.* [9], and Willibald *et al.*

[12], the ultimate load capacity of the bolts are unaffected by the value of the pre-
tensioning force, with or without prying forces.

1.4. Objective

Studies by Thornton [4], Swanson [5], Swanson and Gao [6] Swanson and Leon
[7], Zoetemeijer [8], Nair *et al.* [2], Nair *et al.* [9], Dowswell [10], Wheeler *et al.* [11],
Willibald *et al.* [12], and Kulak *et al.* [15] have been done throughout the years regarding
prying action and what limit states are to be considered. Those studies have lead to the
current AISC [3] design provisions. Although prying action has been studied since the
1950's, most of the past studies conducted with regards to the bolt spacing perpendicular
to the applied load have resulted in a variety of results and in some cases changes in bolt
spacing has not been considered. Studies by Swanson [5], Zoetemeijer [8], Dowswell
[10], Thornton and Kane [16], have indicated some effects that bolt spacing has on the
prying action force.

The current research initiative will consider the effects of prying action forces
with regards bolt spacing as well as investigating the case where $\alpha > 1$. Using the
provisions from AISC [3], the prying forces generated based on the selected specimens
will be calculated and compared to experimental results.

Chapter 2: Literature Review

2.1. Bolt Spacing Limitations

A variety of theories have been developed regarding bolt spacing and associated limitations. Whether the bolt spacing is neglected and is assumed that each bolt acts independently, or if the bolt spacing is used to calculate an equivalent length to be used for the prying force calculations, there has not been any conclusions regarding the effects on prying action. AISC [3] has provisions developed by Dowswell [10] that limit the bolt spacing distance to determine an equivalent length, p, in the prying force provisions.

Dowswell [10] compared the various design methods theorized since the 1950's. Different theories were indirectly mentioned on how to handle bolt spacing. The theories focus on the tributary width and equivalent length concepts, which then determined the bolt spacing limits. AISC [17] has provisions for determining the limit states of tension rupture and flange bending with regards to prying action forces of bolted connections. Dowswell [10] stated, "The AISC 13th edition Steel Construction Manual was only valid for fittings with limited bolt spacing and edge distances." It was also mentioned that the AISC [17] did not provide guidance on how to determine equivalent length of fittings with large bolt spacing [10]. Hence, the limitation of p = max 2b but $\leq$ s, resulted.

Using Equation (2) for the bolt spacing limit was said to be slightly conservative for certain applications, and very conservative for determining the WT shape's flange strength in bending [10]. The design method provided by Dowswell [10] states that his methods could be applied to applications with large bolt spacing and edge distances [10].

Strain hardening was ignored in Dowswell's [10] design theory; therefore, the connection

capacity would likely be larger than that of the calculated values.

The equivalent length method was developed by Zoetemeijer [8]. Zoetemeijer's

approach was a simplified approach and the equivalent length provision is

$$p_e = 2b + \frac{5a}{8} + \frac{s}{2},$$ (18)

where p_e is the equivalent length and s is the bolt spacing. By observation, Equation (18)

would be taking the same limit found in Equation (2) from AISC [3] provisions, with

some additional factors added to the distance from bolt centerline to flange edge, and the

bolt spacing. Zoetemeijer's [8] equivalent length theory takes in to account the actual

bolt spacing with no limitation.

The equivalent length idea was revisited by Thornton and Kane [16]. The average

equivalent length is

$$p_e = \frac{s(n-1)+\pi b+2a}{n},$$ (19)

where n is the number of bolts along the member length. Equation (19) also takes into

account the actual bolt spacing like Equation (18) as well as the number of bolts within

that row.

Both equivalent length provisions could be then used in the prying action

provisions in AISC [3]. Dowswell's publication, "A Yield Line Component Method for

Bolted Flange Connections," shows that the prying forces on the outermost bolts take

significantly more force than that of the inner bolts; therefore, the inner bolts can be

neglected [10]. Because both Equations (18) and (19) have actual bolt spacing included, they do not take into account the fact that the outer most bolts experience the highest prying force. The limitations for Equations (18) and (19) would be to use the outer most bolt spacing while ignoring the inner bolts if more than two bolts exist in a given length.

AISC [3] utilizes its bolt spacing limit, for tributary length p, because the design guidelines are based on each bolt independently; therefore, the limit of p = 2b max but ≤ s, would be accurate. Dowswell [10] states that when the bolt spacing is larger than that of the equivalent length, p_e, the equivalent lengths act independently of each other, resulting in the limit of p = 2b max but ≤ s. The equivalent length limitations Dowswell [10] used were

$$2\sqrt{b(a + b)} \;\leq\; p_e \leq 4\sqrt{b(a + b)} \;.$$
(20)

Dowswell [10] mainly focused on the design method based on yield line theory, but mentioned and showed sample calculations on how to calculate the equivalent lengths for various bolt spacing conditions. All the equivalent length calculations Dowswell [10] showed were limited by Equation (20).

2.2. Alpha (α) Considerations

One of the key components of determining the magnitude of prying force is related to alpha and the moment generated in the WT shape's flange. The moment provision derived from statics is [1]

$$(1 + \delta\alpha)M = Tb \;.$$
(21)

Prying forces are zero at $\alpha \leq 0$, are maximum when $\alpha \geq 1$, and when $0 < \alpha < 1$ the prying forces are limited by the WT shape's flange [18]. Another way to understand $\alpha \geq 1$, Swanson [5] indicated that if the connecting bolts are stiff enough the flange can act like a fixed-fixed beam in double curvature. When the value of $\alpha < 0$ the flange physically lifts off the connected base and the flange is in single curvature [5]. In the case where $\alpha \leq 0$, the prying forces are zero which makes the sum of the bolt tension forces equal to the applied load.

Thornton [4, 18], Kulak *et al.* [1], Swanson and Gao [6], and Nair *et al.* [2], Nair *et al.* [9], have stated that $\alpha > 1$ can physically not exist, because "α represents the ratio between the moment per unit width at the centerline of the bolt line and the flange moment at the web face [4]." However, Swanson [5] indicated that $\alpha > 1$ may exist, potentially up to a value of $\alpha = 2$. Even though having a value of $\alpha > 1$ is outside the physical range of $0 \leq \alpha \leq 1$, Swanson [5] shows specimens that experienced values of $\alpha > 1$. Swanson's [5] results show that many WT shapes experienced bolt failure along the line segment EB shown in Figure 2.2-1, which had a value of $1 \leq \alpha < 2$ [5]. It was believed that it was possible due to flange ductility and strain hardening within the flange [5]. When the flange begins to yield and the plastic hinges develop, the prying forces are still increasing and being transferred in to the bolts. With the developed plastic hinge at the location b', the increased forces are creating bending moment within the flange but are unable to transfer to the web. Thus, the moment at b' continues to increase.

Bolt Force vs. Flange Thickness
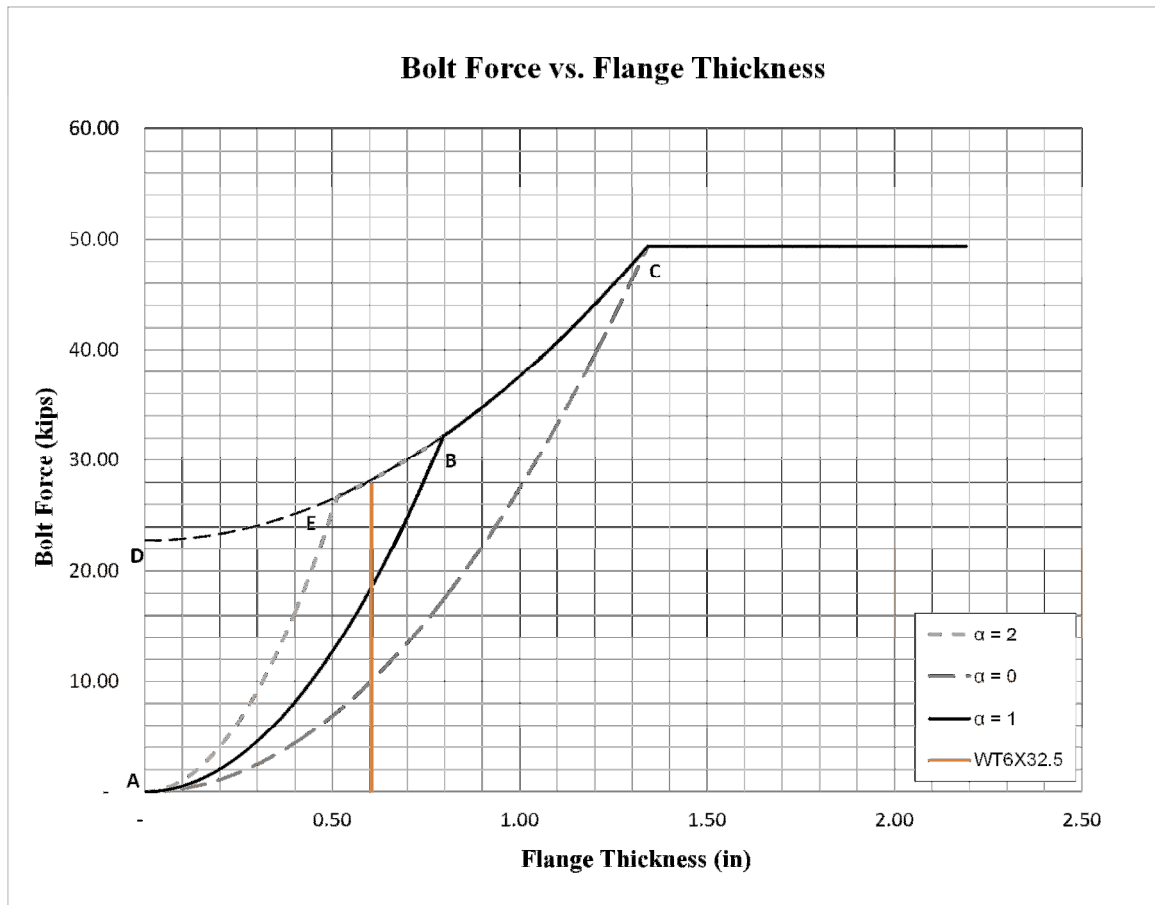
Figure 2.2-1: Bolt Force versus Flange Thickness with Regards to α [5].

The fact that Swanson's [5] research showed α values greater than one were developed in experiments, the max limitation for α = 1 may not be appropriate. Since using a value for α > 1 results in higher prying forces, the actual value should be considered for design purposes.

Chapter 3: Hypothesis

The hypothesis for this research initiative is that by increasing the bolt spacing parallel to the stem in WT shapes the prying forces will decrease. The WT shape's flange will experience deformation along its cross-section and orthogonal length as illustrated in Figure 2.2-2.
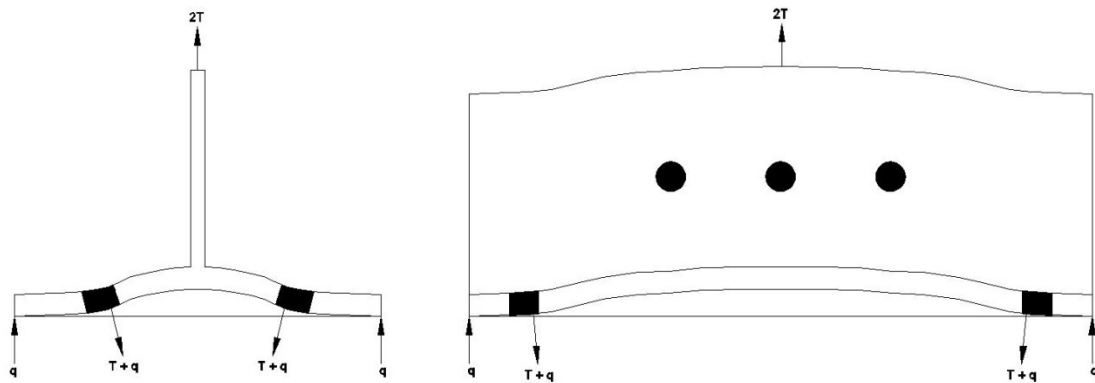
Figure 3-1: Cross-Section and Orthogonal Prying Forces.

3.1. Bolt Spacing Considerations

When considering the limitations for the five bolt spacing dimensions selected for analysis, the prying forces were computed for an applied force of 100 kips. Table 3.1-1 shows the results for the selected bolt spacing, applied loads, and resulting prying forces. Complete calculations are shown in Appendix B.

Table 3.1-1: Prying Forces for Tributary Length Limit.

AISC 14th Edition Provisions						
Bolt Spacing (in)		Max 2b p ≤ s (in)	$0 \leq \alpha \leq 1$	Prying Force (kips)	Bolt Force T (kips)	Applied Force (kips)
1.5b	5.25	5.25	1.000	9.848	34.848	25
2.0b	7.00	7.00	0.991	13.616	38.616	25
2.5b	8.75	7.00	0.991	13.616	38.616	25
3.0b	10.50	7.00	0.991	13.616	38.616	25
4.0b	14.00	7.00	0.991	13.616	38.616	25

The results indicate that when the bolt spacing exceeds 2b the prying force, q, had no change in magnitude. Table 3.1-2 shows the prying force, q, beyond the limitation of 2b, where the actual tributary length was used. The resulting prying forces diminish as the bolt spacing increased beyond 2b due to the increased tributary length.

Table 3.1-2: Prying Forces for Actual Tributary Length.

Tributary Length Used - AISC 14th Edition Provisions						
Bolt Spacing (in)		p (in)	$0 \leq \alpha \leq 1$	Prying Force (kips)	Bolt Force T (kips)	Applied Force (kips)
1.5b	5.25	6.13	1.000	11.79	36.79	25
2.0b	7.00	7.00	0.991	13.616	38.616	25
2.5b	8.75	7.88	0.745	11.674	36.674	25
3.0b	10.50	8.75	0.552	9.732	34.732	25
4.0b	14.00	10.50	0.272	5.848	30.848	25

Based on the values presented in Table 3.1-1 and Table 3.1-2, it is reasonable to expect the prying forces to diminish slightly as the bolt spacing increases due to an increase in tributary length.

Prying action forces are based on the WT shape's flange deformation starting between the gage distances and continuing towards the flange tip, which results in flexure

within the flange. As the bolt spacing increases, the WT shape's flange may exhibit

deformation along its length between the bolts. In other words, the WT shape would

have deformation along its cross-section and length simultaneously. With the

deformation of the WT shape along its length, additional prying forces may occur. Since

the b' distance, with regards to the WT shape's length, would be expanding with bolt

spacing, the additional prying force may be relatively low. From combined cross-

sectional and orthogonal flange deformation, the resulting prying forces will fall between

the AISC [3] values when using the bolt spacing limitations and the AISC [3] values

when using the actual tributary length. Table 3.1-3 shows the range of prying forces as

tributary length varies.

Table 3.1-3: Prying Forces along Cross-Section and Orthogonal Length.

WT Flange Deformation along Cross-Section and Orthogonal Length					
Bolt Spacing (in)	Max 2b $p \le s$ (in)	p (in)	Prying Force (kips) Limit	Prying Force (kips) No-Limit	Prying Force Range (kips)
1.5b	5.25	6.13	9.848	11.79	$9.848 \le q \le 11.79$
2.0b	7.00	7.00	13.616	13.616	$13.616 \le q \le 13.616$
2.5b	7.00	7.88	13.616	11.674	$11.674 \le q \le 13.616$
3.0b	7.00	8.75	13.616	9.732	$9.732 \le q \le 13.616$
4.0b	7.00	10.50	13.616	5.848	$5.848 \le q \le 13.616$

3.2. Alpha, α, Considerations

If the calculated value of α is greater than 1.0, and that value is used in the solution for the prying force in Equation (8), the resulting magnitude of the prying force would exceed the limit of $0 \leq \alpha \leq 1$. When using those same provisions to calculate α values for this research, it was found that when the bolt spacing equals 1.5b, α results in a value of 1.777 as shown in Table 3.2-1.

Table 3.2-1: Prying Forces for $0 \leq \alpha \leq 2$.

Limit $0 < \alpha < 2$ Used - AISC 14th Edition Provisions						
Bolt Spacing		Max 2b	$0 \leq \alpha$	Prying Force	Bolt Force	Applied Force
(in)		$p \leq s$ (in)		(kips)	T (kips)	(kips)
1.5b	5.25	5.25	1.777	17.499	42.499	25
2.0b	7.00	7.00	0.991	13.616	38.616	25
2.5b	8.75	7.00	0.991	13.616	38.616	25
3.0b	10.50	7.00	0.991	13.616	38.616	25
4.0b	14.00	7.00	0.991	13.616	38.616	25

The prying force magnitudes when the bolt spacing equals 1.5b were then compared between Table 3.1-1 and 3.2-1. The comparison showed prying forces of 11.79 kips and 17.499 kips, respectively. Based on the calculated values of α and corresponding prying forces, as well as the tested values from Swanson [5] which showed failure modes resulting with α values greater than 1.0, it would be reasonable to expect experimental prying forces to fall within the calculated ranges, $11.79 \text{ kips} \leq q_{exp} \leq 17.499$ kips, where $1.0 \leq \alpha_{exp} \leq 1.777$ because of the varying values of bolt force with respect to flange thickness for different values of α.

3.3. Combined Tributary Length and Alpha, α, Considerations

Even though the main focus of the research is to concentrate on the effects of prying action forces with regards to bolt spacing, a secondary consideration will be to see how the bolt spacing values relate to α. It was discussed previously that the bolt spacing has an effect on the amount of prying action force generated within the bolt. It was also shown how the prying force varies when using AISC [3] provisions for bolt spacing limits and using α > 1. To continue with the comparison, it would be valid to consider the prying forces generated with regards to both the bolt spacing limit and α limits being neglected for analysis purposes. The only change taken with regards to the AISC [3] provisions are using the actual tributary length and α. Table 3.3-1 shows the varying prying forces generated within the bolt based on that theory.

Table 3.3-1: Prying Forces for Actual Tributary Length and $0 \leq \alpha \leq 2$.

Tributary Length and $0 < \alpha < 2$ Used - AISC 14th Edition Provisions						
Bolt Spacing		p	$0 \leq \alpha$	Prying Force	Bolt Force	Applied Force
(in)		(in)		(kips)	T (kips)	(kips)
1.5b	5.25	6.13	1.3195	15.557	40.557	25
2.0b	7.00	7.00	0.991	13.616	38.616	25
2.5b	8.75	7.88	0.745	11.674	36.674	25
3.0b	10.50	8.75	0.552	9.732	34.732	25
4.0b	14.00	10.50	0.272	5.848	30.848	25

The only value for α greater than 1.0 in Table 3.3-1was the first bolt spacing, 1.5b, which had a tributary length of 6.13in and a value for α =1.3195. The remaining bolt spacing had values for α within the AISC [3] limits. In order to better study the effects of α > 1 the applied load would have to be increased. Table 3.3-2 shows the effects of the increased applied load.

Table 3.3-2: Prying Forces for Actual Tributary Length and $0 \leq \alpha \leq 2$.

Tributary Length and Limit $0 < \alpha < 2$ - AISC 14th Edition Provisions						
Bolt Spacing		p	$0 \leq \alpha$	Prying Force	Bolt Force	Applied Force
(in)		(in)		(kips)	T (kips)	(kips)
1.5b	5.25	6.13	1.715	20.222	49.222	29
2.0b	7.00	7.00	1.374	18.280	48.363	29.5
2.5b	8.75	7.88	1.15	18.087	48.587	30.5
3.0b	10.50	8.75	0.983	17.311	48.811	31.5
4.0b	14.00	10.50	0.733	15.759	49.259	33.5

With increasing the applied load up to the bolt limits, the first two bolt spacing, 1.5b and 2.0b, had values for $\alpha = 1.715$ and $\alpha = 1.374$, respectively. The bolt spacing beyond 2.0b had values for α fall within the AISC [3] limits. What is interesting about the analysis is that the two bolt spacing values which had $\alpha > 1$ were within the bolt spacing limits. By that observation, using the actual value for α would be more conservative than using the limit of $\alpha_{max} = 1$, which resulted in a less conservative value.

With the comparison done with regards to using the actual tributary length and α, the calculated results have shown some interesting effects. To see how the experimental data relate to that of Tables 3.3-1 and 3.3-2 may have a direct or indirect impact on how the limits for bolt spacing, tributary length, and α could be modified.

Chapter 4: Experimental Process

4.1. Introduction

Specimen testing was performed at the Construction Science and Engineering Center (CSEC) at the Milwaukee School of Engineering (MSOE) to determine the effects of prying forces on the connecting bolts of a WT shape's flange-to-base plate with regards to bolt spacing. The tested bolts were instrumented with strain gages. Three Linear Variable Displacement Transducer's (LVDT) were used to measure deformations at different locations. A tensile force was applied to the specimen and the bolt strains, member flange deformation, member bending deformation, and total axial deformation was recorded. One WT size was used with varying bolt spacing to provide a common comparison of tensile bolt forces.

4.2. Specimen Selection

The first step in the development of the experimental program was to select an appropriate shape for testing.

First, the connection limitations and calculations between the WT shape's web and actuator had to be checked so failure would not occur during testing. A total applied load of 100 kips was assumed. The following limit states apply to the connection from the WT shape's stem to the actuator: stem yielding, stem fracture, connecting bolt double shear failure, block shear within the stem, bearing of bolts within the stem. Yielding of the WT shape's stem at the connection governed and a minimum stem thickness of $t_w = 0.333$ in. resulted. The final check was the tensile failure of the connecting bolts of the WT shape flange-to-base plate. Complete calculations can be found in Appendix A.

With the minimum web thickness of the WT shape determined the next step was to select the shape. The WT shape was selected based on the AISC [3] provisions for prying action, with a minimum web thickness of $t_w = 0.333$ in. A WT6x32.5 was selected. The calculations for prying force can be found in Appendix B.

With the WT shape selected, the next step was to determine the bolt spacing to use for evaluation. The AISC [3] provision for prying force bolt spacing shown as Equation (2) was used in conjunction with prying force calculations to determine a reasonable spacing. Since the AISC [3] bolt spacing provision limits the spacing to a maximum of 2.0b, it was determined that the bolt spacing should be based on the 2.0b limitation. With that consideration, five bolt spacings were considered: 1.5b, 2.0b, 2.5b, 3.0b, and 4.0b. Appendix C shows the shop drawings of each specimen. It is expected that the bolt spacing being based on a factor of 2.0b will bring about a favorable comparison to calculated capacities, since the AISC [3] provision is limited to 2.0b. The prying action analysis was re-calculated with the different bolt spacing to validate applicability. The calculations of the various bolt spacing can be found in Appendix B. With the WT shape specimen and bolt spacing determined, the next step is to describe the experimental setup.

4.3. Experimental Setup

The test setup used is illustrated in Figure 4.3-1. The column frame is capable of resisting axial forces in excess of 100 kips. The frame consists of two wide flange columns with holes drilled in the flanges to accommodate various testing setups. The

horizontal components of the test frame consisted of two sets of channels, also shown in
Figure 4.3-1.
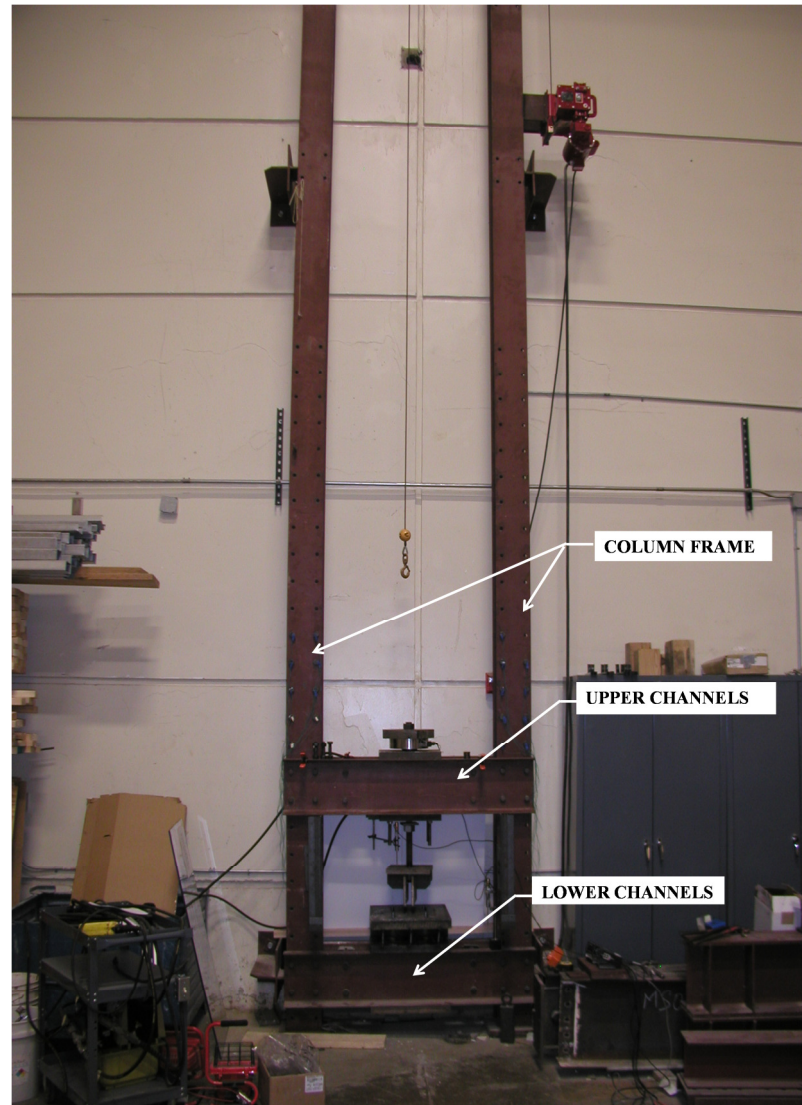
Figure 4.3-1: Column Test Frame System.

An actuator capable of producing an applied load in excess of 100 kips was
placed between the upper two back-to-back channels. An upper and lower plate was
connected to hold the actuator between the two channels and was connected using four
threaded rods as illustrated in Figure 4.3-2. A load cell capable of recording up to 100

kips was located on the top of the actuator above the upper channels. A large steel plate

was placed on the top side of the load cell and a 1 ¼ in threaded rod ran through the

center of the actuator and load cell which was then connected on the very top of the upper

steel plate as seen in Figure 4.3-3. Figure 4.3-4 shows the lower portion of the actuator

connecting plate.
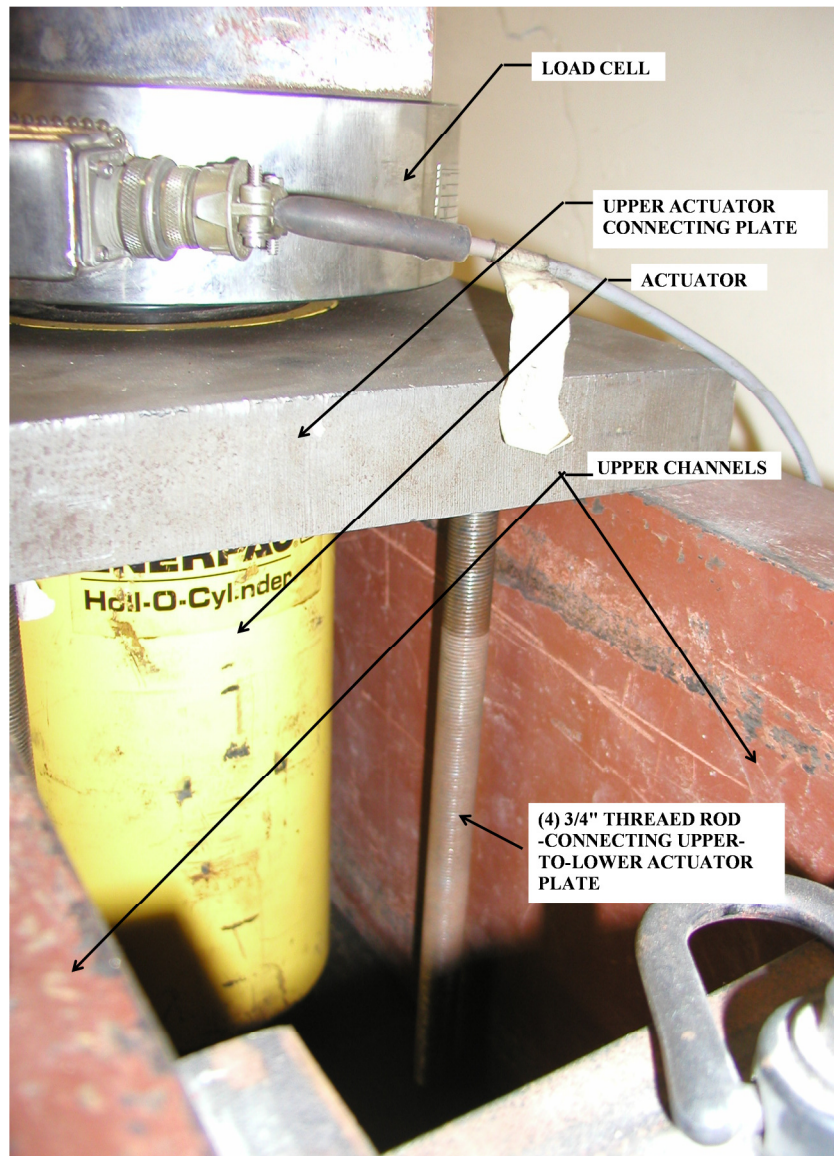
Figure 4.3-2: Actuator Location.
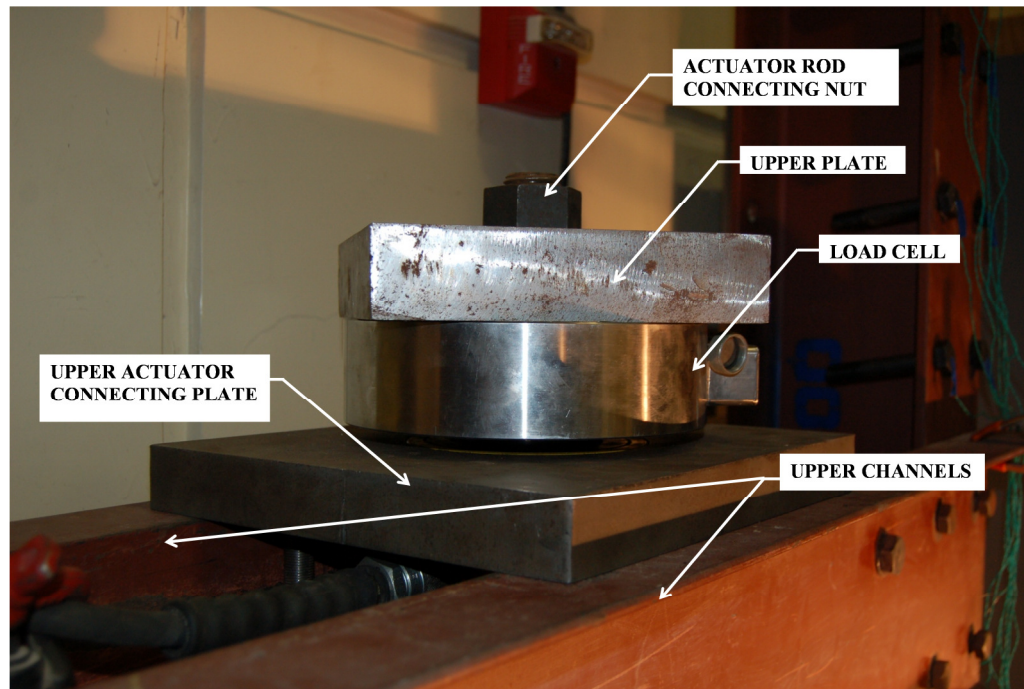
Figure 4.3-3: Upper Connection of Load Cell and Actuator.
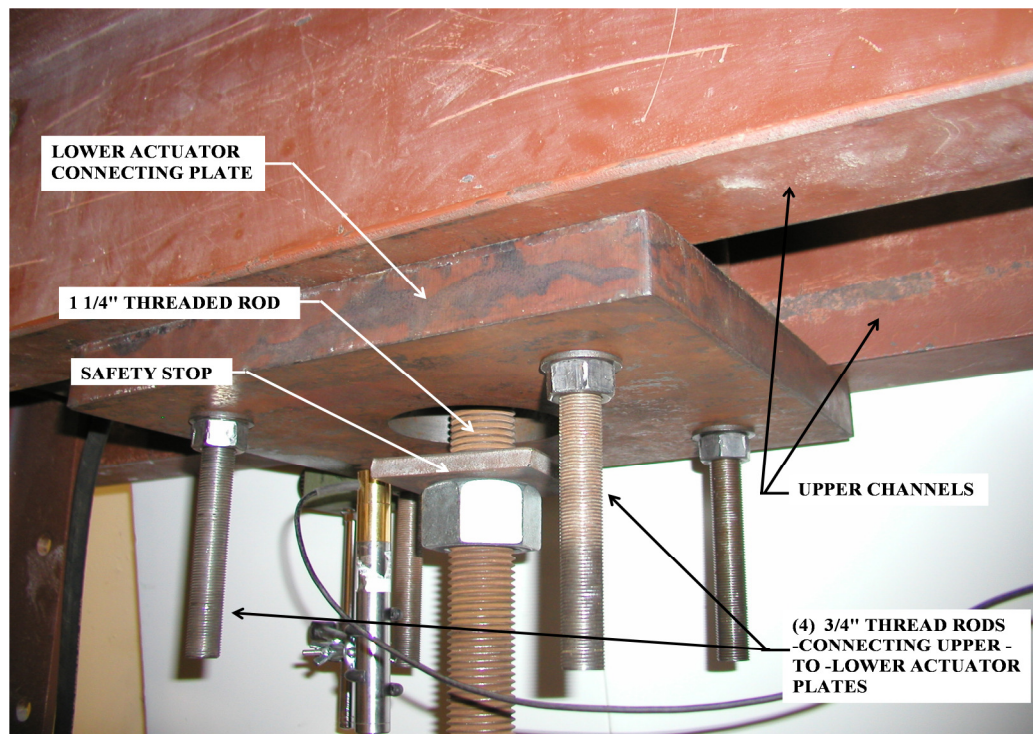
Figure 4.3-4: Lower Connection of Load Cell and Actuator.
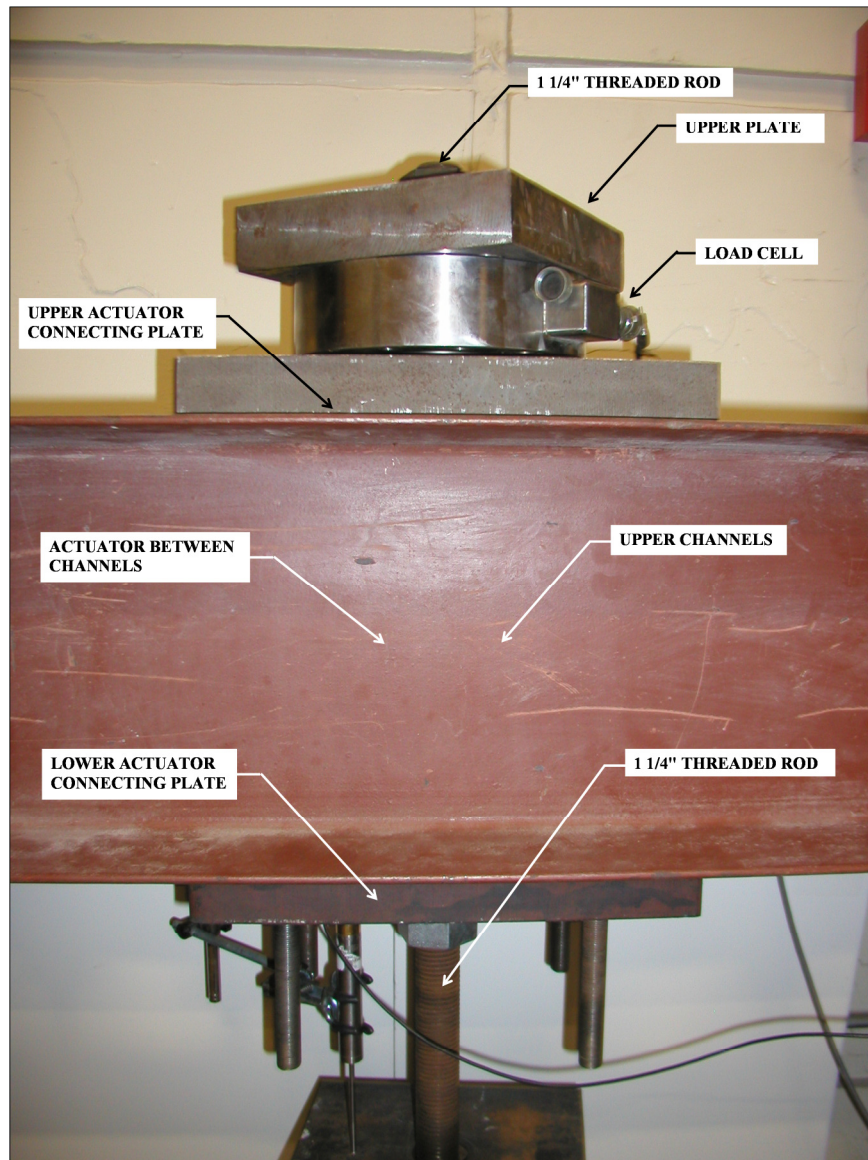
Figure 4.3-5: Full Assembly of Actuator and Load Cell.

The lower portion of the threaded rod was connected to a steel connection assembly, is capable of transferring forces in excess of 100 kips.

The base plate was designed to withstand loading in excess of 100 kips and was intentionally designed to be very stiff in order to minimize deformation. The base plate was located on the lower channels. The base plate sat on the top portion of the lower channels and a bottom steel plate was located on the bottom side of the lower channels.

The two plates were connected by four threaded rods. Figure 4.3-6 shows the base plate assembly and the steel connection assembly transferring force from the actuator.
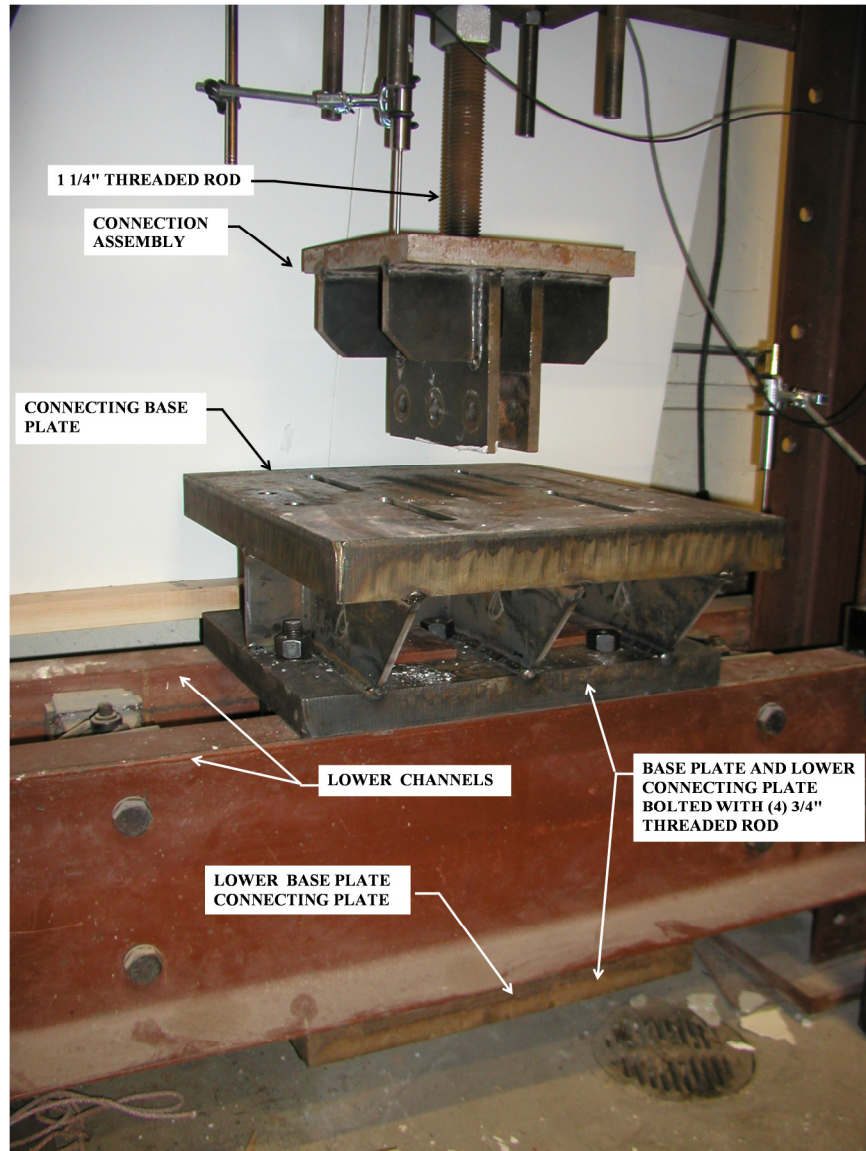
Figure 4.3-6: Base Plate Assembly and Connection Assembly.

The WT6x32.5 was placed on the base plate and centered. The web of the WT6x32.5 was connected to the connection assembly which was located on the lower portion of the 1 ¼ in threaded rod. Three A490X shear bolts were used to make that connection. Figure 4.3-7 shows how that connection was prepared.

When the WT6x32.5 was centered on the base plate, four A490X bolts were used to connect the WT shape to the base plate. Two of the four bolts were instrumented with strain gages to measure the strain in the bolts during testing. The fully bolted assembly of the WT shape to the base plate and actuator rod can be seen in Figure 4.3-7.
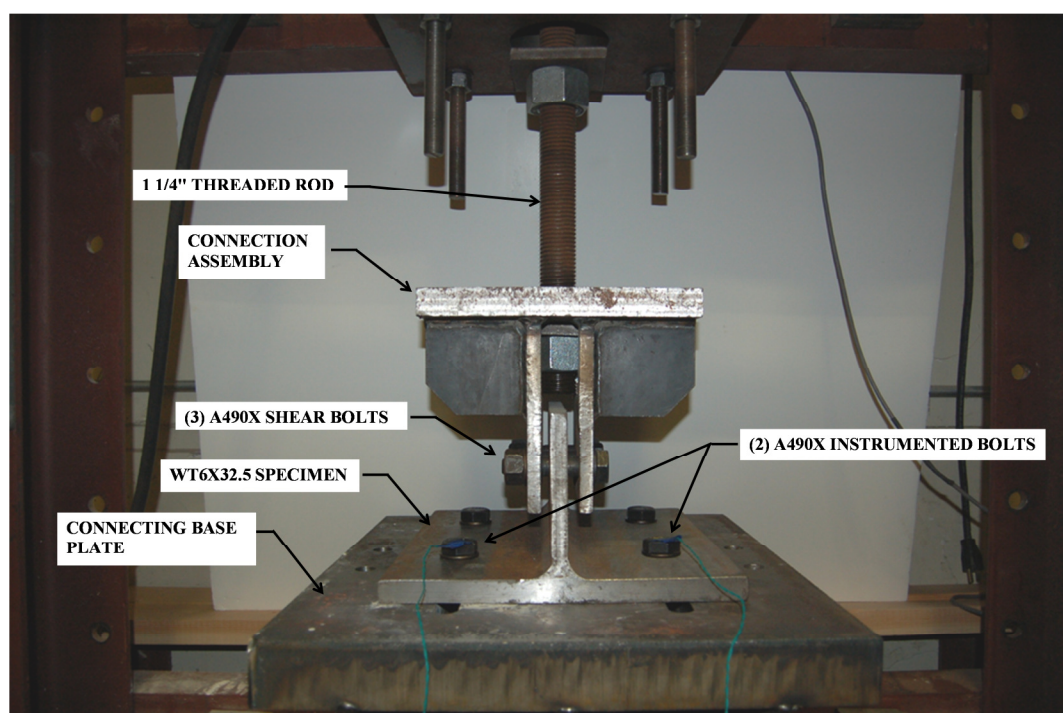
Figure 4.3-7: Fully Bolted Assembly of WT6x32.5.

The purpose of measuring the strains in the connecting bolts was to determine the experimental stresses which could then be converted into bolt forces. When comparing the bolt forces to the applied load, the prying force could then be determined and a comparison of the five specimens could be performed.

In order to instrument the bolts, the A490X bolts were placed into a lathe and a 5/64 in drill bit was used to drill a hole 1 ¾ in. deep into the center of the bolt. The bottom of the strain gage was placed at a depth of 1 ½ in. A high strength adhesive was

used to secure the strain gage in the A490X bolts. Appendix D shows the installation

procedure which was provided with the strain gages. Figure 4.3-8 illustrates an

instrumented bolt.
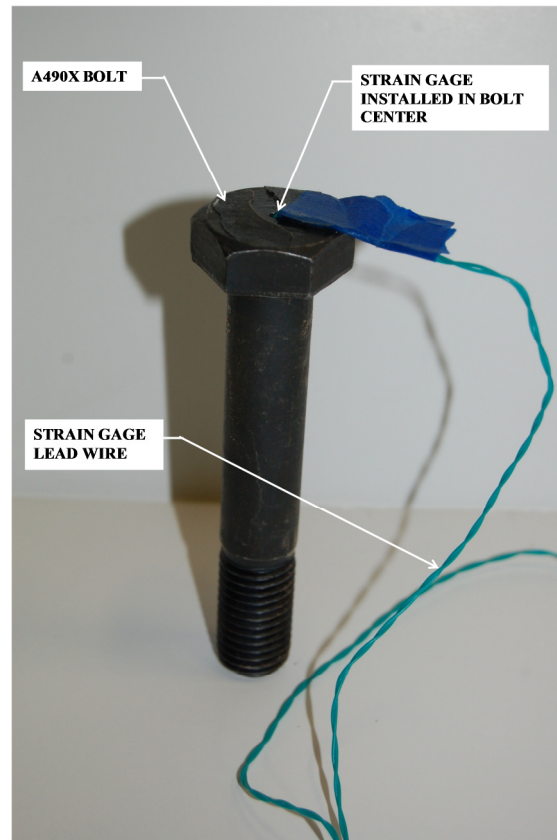
Figure 4.3-8: Instrumented Bolt.

In addition to the instrumented bolts, the other data of which to consider

measuring during the experiment was the deformation of various points of the specimen

during loading.

Utilizing LVDT's, three locations of consideration were chosen to measure. The

first location measured the total deflection of the actuator during testing and was noted as

"Top LVDT." The second was to measure the deflection of the WT6x32.5 stem, which

gave the deformation of the WT6x32.5 flange due to prying action effects during the

experiment and was noted as "Stem LVDT." The third location was centered between the bolt spacing, which gave the WT6x32.5 flange deflection in the WT6x32.5 center and was noted as "Flange LVDT." Figure 4.3-9 shows the complete experimental setup prior to testing. Plaster of Paris was applied on a few specimens to show stress patterns in the flange. Schematic drawings of the experimental setup can be found in Appendix E.
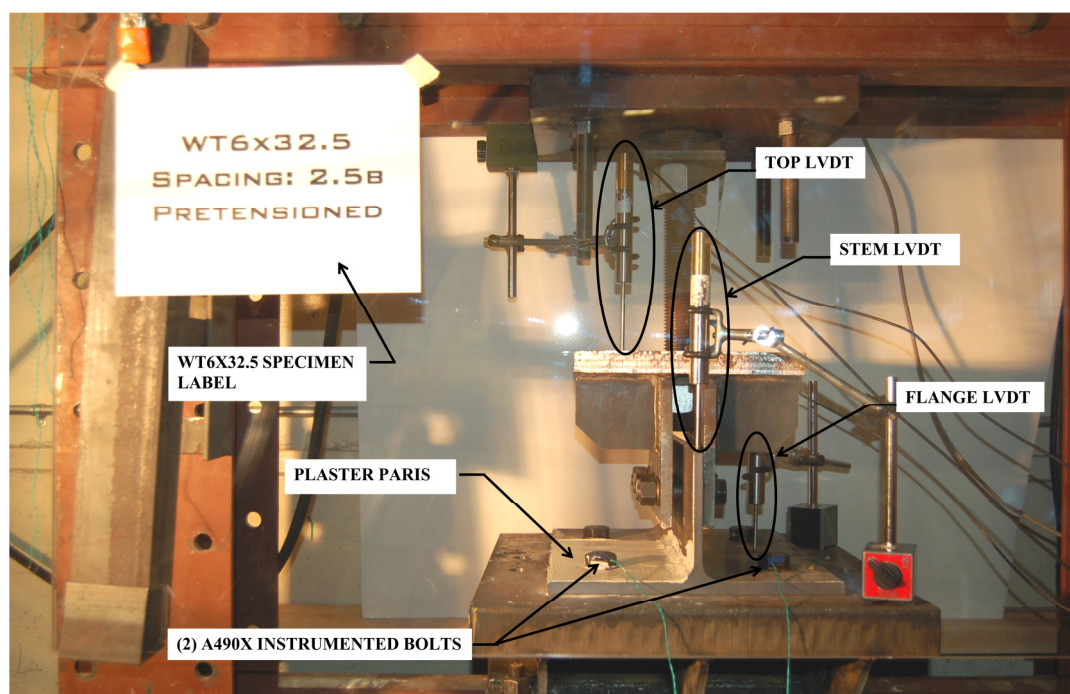
Figure 4.3-9: WT6x32.5 Complete Setup.

4.4. Experimental Procedure

After the experimental setup was complete, a check list was used to confirm consistency between specimens and helped eliminate errors within each experimental test. Appendix F shows the checklist that was used before each experiment was performed. Before the experiment began, the experimental setup portion of the testing protocol checklist was verified. Once everything was checked, the procedure went as follows.

LabVIEW software was used to collect the data during the experiment. The two strain gages, three LVDT's, and load cell were all connected to the computer which was running LabVIEW. The strain gages had gage factors which were entered into LabVIEW prior to testing. The three LVDT's used for the experiment were also calibrated prior to testing. Once LabVIEW was running appropriately the experiment was set to move forward.

The first step of the procedure was to maintain accuracy among each test. In order to achieve that, the instrumented bolts were pre-tensioned. With LabVIEW running, the two instrumented bolts were tightened until their corresponding strains were approximately 300 to 350 microstrain, which was approximately 3.8 kips to 4.4 kips. Since two of the four bolts were not instrumented, the non-instrumented bolts were tightened approximately the same as the instrumented bolts, which was judged by the turn of the nut by the student tightening each bolt. Those data were collected and will be discussed in Chapter 5.

In order to run consistent tests between each specimen, three lab personnel were used for each experiment, Richard DeSimone, Austin Meier, and Dr. Christopher Raebel. The operator of the hydraulic pump pressed the "up" button which initiated the actuator and began increasing the load on the system. The load was applied slowly per the judgment of the operator. The amount of load being applied was observed and instrumentation readings were verified. Connections were verified and photographs were taken during testing. When the applied load reached approximately 10 kips, the applied load was held for about ten seconds to confirm everything was going to protocol and all

instruments were reading properly. For the range up to 15 kips, what was noted as a system engagement period was occurring.

The system engagement period was when the upper and lower back-to-back channels were engaging themselves at their bolted connections to the column frame. Since the column frame bolt holes were slightly larger than that of the actual bolts, there was some initial movement in the connection. The system quickly engaged itself with the applied load. The effects of the system engagement period are mentioned in Chapter 5 and further consideration of the system engagement effects is addressed.

From that point, the applied load was slowly increased until an applied load of 100 kips was reached. The load cell's capacity is limited to 100 kips; therefore the tests were limited to 100 kips of force. If at any time during the experiment a failure would occur, the actuator would be disengaged as quickly as possible, to prevent any personnel injury or equipment damage. As the actuator reached 100 kips, pictures were taken to capture the maximum deformed shape. Once the actuator was disengaged, the deformed shape rebounded and lost a majority of its deformation magnitude. At that point the actuator was disengaged and was fully retracted so the test specimen could be removed and observed.

To finish up the experimental procedure, the specimen was removed from the testing frame and stress patterns were observed and photographed. The data collected using LabVIEW were exported into a Microsoft Excel file for further data analysis. The process was repeated for all five specimens and separate data files for each were collected and analyzed.

Chapter 5: Data Results and Discussion

5.1. Introduction

From each performed experiment, two sets of data were collected, the pre-tensioning and testing data, which could then be analyzed. With the collected data, a variety of graphs, graph comparisons, and photographs could be used to discuss the results, accuracy of the data, possible errors, and how the hypothesis compared to the resulting conclusion. In addition, all the plots of the experimental data are compared with AISC [3] provisions, AISC [3] provisions but substituting tributary length provision for the actual tributary length, and AISC [3] provision but using the actual value of α.

The microstrain for the instrumented bolts will be used to determine the stress in each bolt during the experiment and is calculated using

$$(\mu\varepsilon)E = \sigma, \tag{22}$$

where $\mu\varepsilon$ is the measured strain during the experiment, E is the Modulus of Elasticity of the bolt, and σ is the resulting bolt stress.

From the bolt stress the bolt force can then be determined by equation (23),

$$A\sigma = T, \tag{23}$$

where A is the gross cross-sectional area of the bolt minus the drilled hole for the strain gage, and T is the bolt force in kips. With the calculated bolt force and recorded applied load, the prying force, q, can be determined as

$$q = T - \frac{Applied\ Load}{4}. \tag{24}$$

The applied load is divided by four assuming equal distribution to all bolts.

Since the goal of this thesis is to determine the effects of prying force with regards to bolt spacing, the next logical setup would be to determine the experimental tributary length, since the tributary length is the basis for the bolt spacing limitations found in the AISC [3] provisions. Equation (25) is used to calculate the experimental tributary length as

$$p = \frac{[T\rho - q]4b'}{\rho F u t^2}. \tag{25}$$

From the tributary length equation, a secondary consideration discussed in previous chapters with regards to the ratio of moment at the bolt line to the moment at the stem edge, also known as α, can be calculated as

$$\alpha = \frac{q}{\left[(p-d')\rho\frac{Fut^2}{4b'}\right]}. \tag{26}$$

The derivations of Equations (25) and (26) can be found in Appendix G.

The data collected from the LVDT's are in inches and the resulting values are shown in plots of each specimen shown in Section 5.2.

5.2. Results

5.2.1. WT6x32.5 at Bolt Spacing 1.5b

As the experiment for specimen 1.5b was performed, the noticeable flange deformation was observed and photographed. Figure 5.2.1-1 shows the deformed shape at the point of 100 kip applied load.
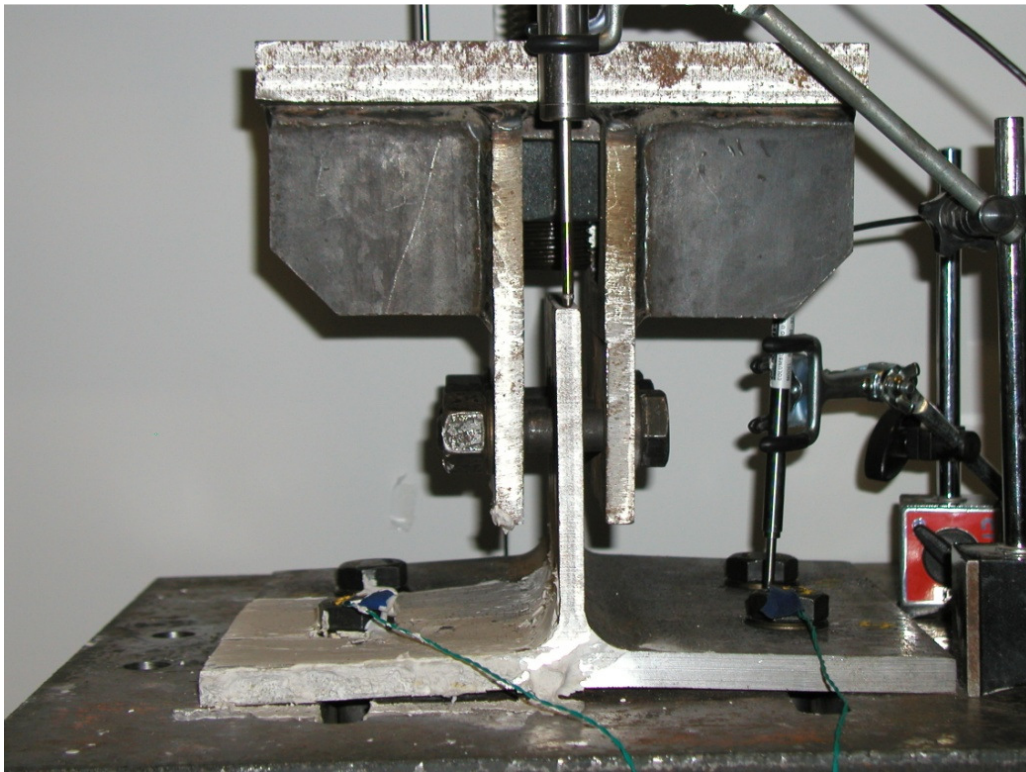
Figure 5.2.1-1: Deformed Shape for Specimen 1.5b at 100 kips Applied Load.

Figure 5.2.1-2 shows the Specimen's deformed shape after being removed from the experimental testing frame. The noticeable stress patterns are illustrated in Figure 5.2.1-3.
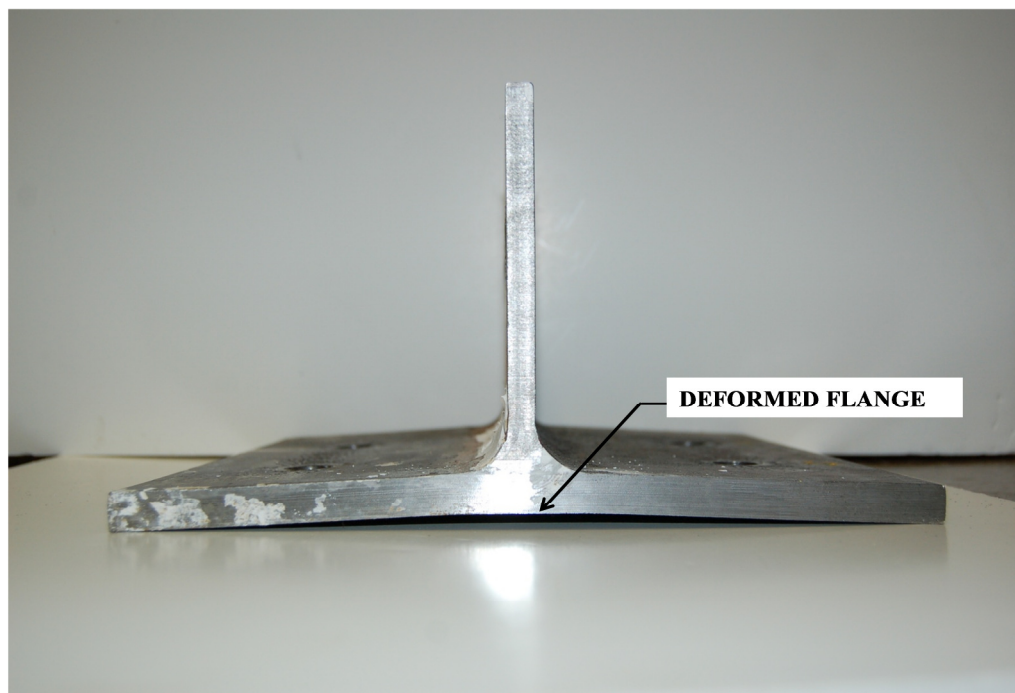
Figure 5.2.1-2: Deformed Shape for Specimen 1.5b Post-Testing.
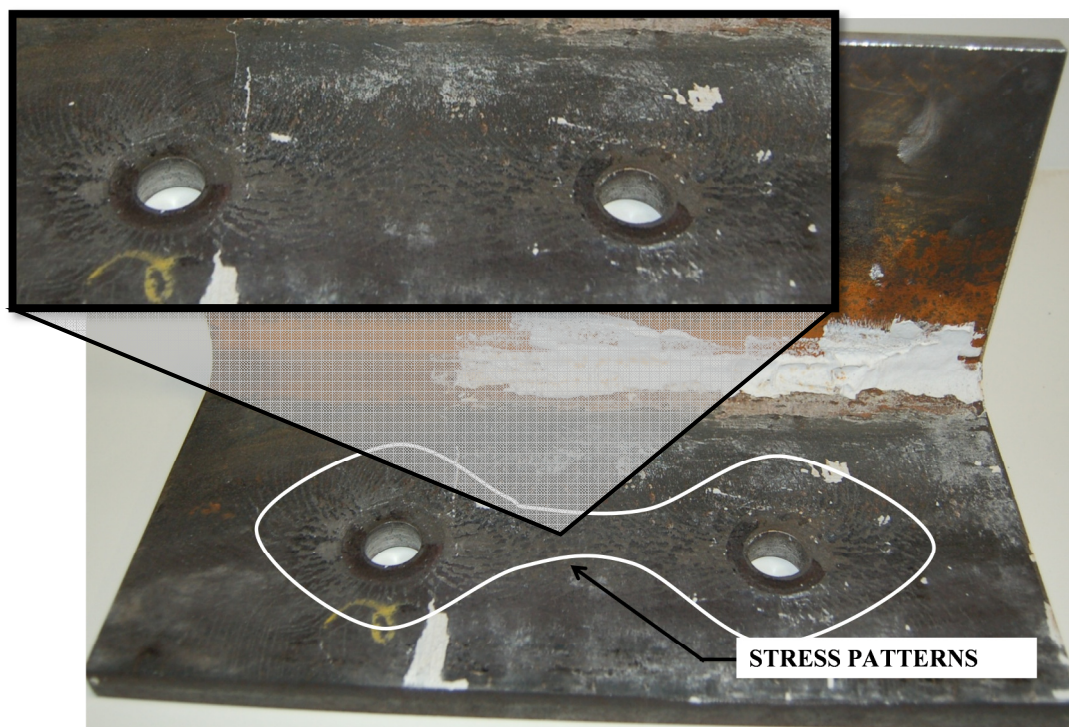
Figure 5.2.1-3: Stress Patterns for Specimen 1.5b.

The stress patterns indicated in Figure 5.2.1-3 illustrate how relatively small bolt spacing interact with each other when prying forces are generated in the system.

There is a noticeable increase in bolt force due to prying action and Figure 5.2.1-4 shows a plot of applied load versus bolt force. Additional plots show the applied load versus prying force as well as the bolt force versus prying force. These plots can be found in Figures 5.2.1-4 and 5.2.1-5, respectively.
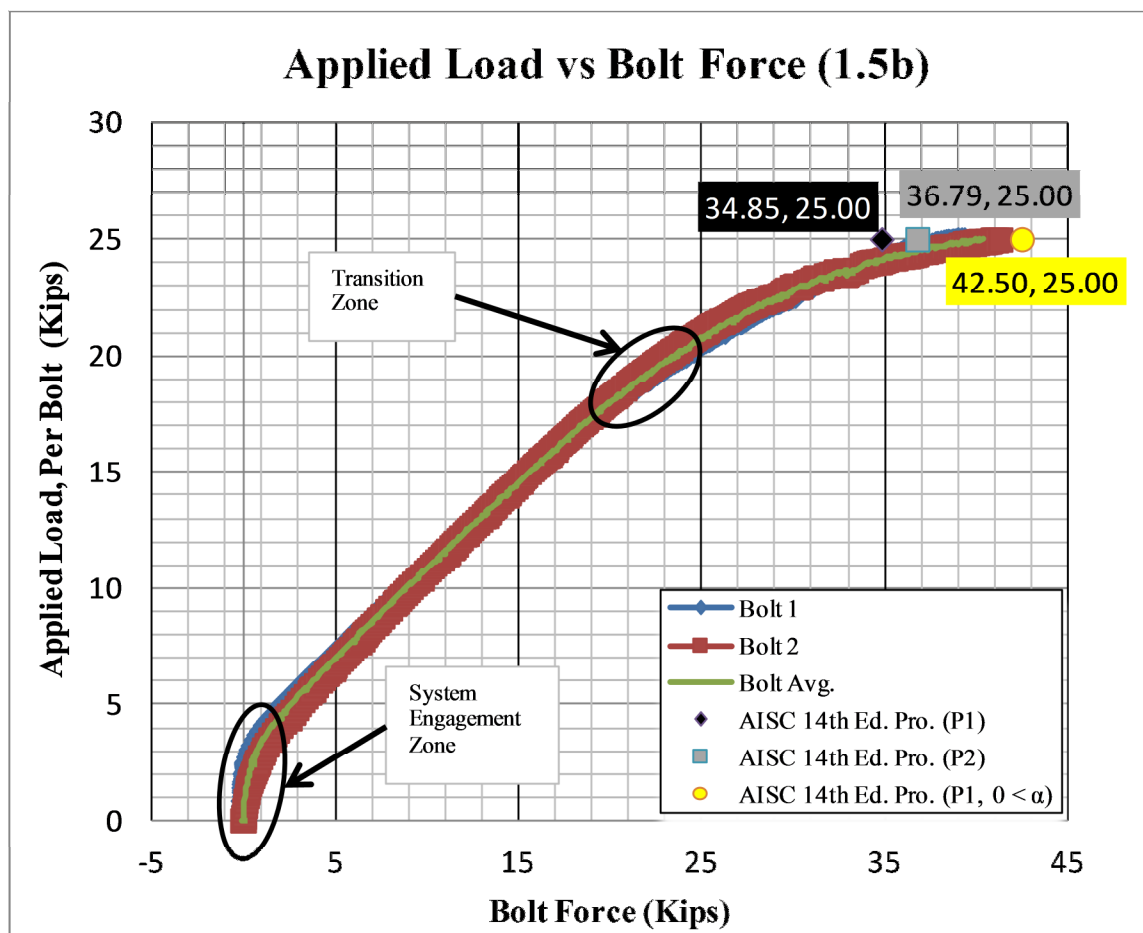
Figure 5.2.1-4: Applied Load versus Bolt Force.
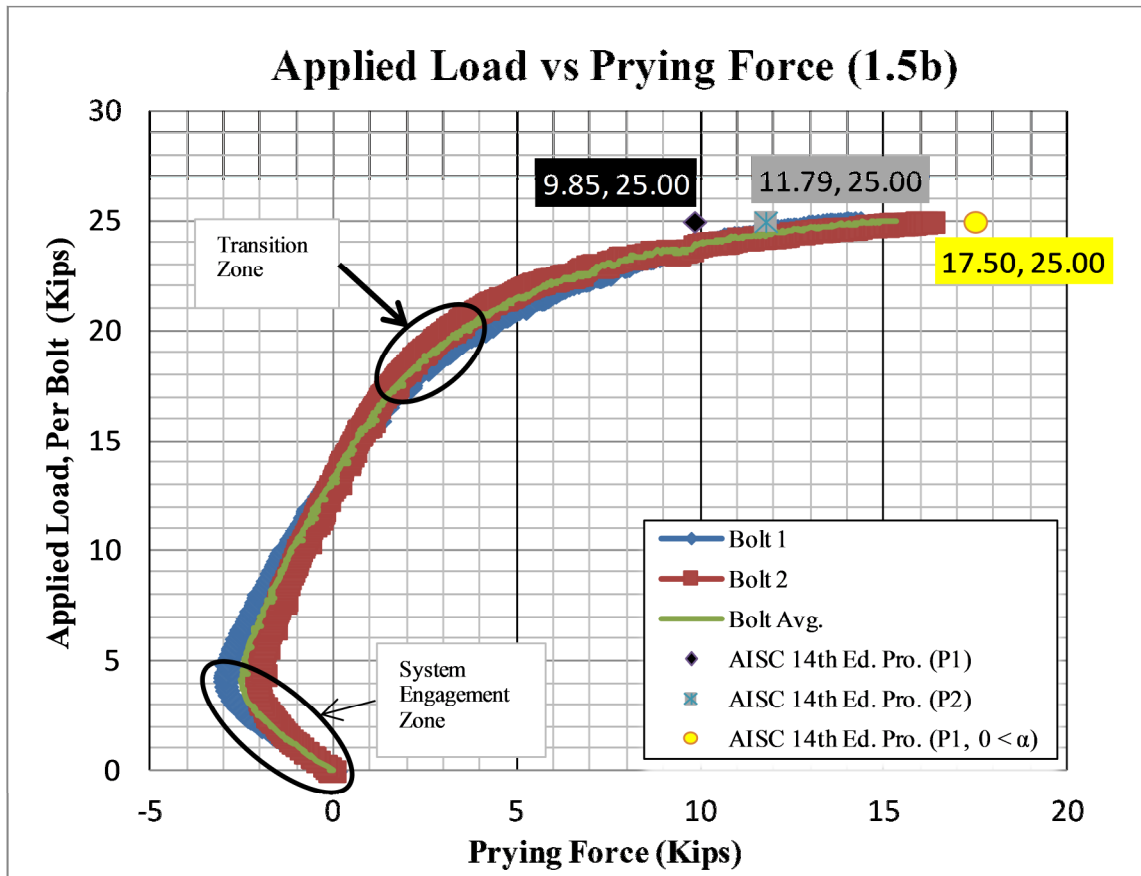
Figure 5.2.1-5: Applied Load versus Prying Force.

Bolt Force vs Prying Force (1.5b)
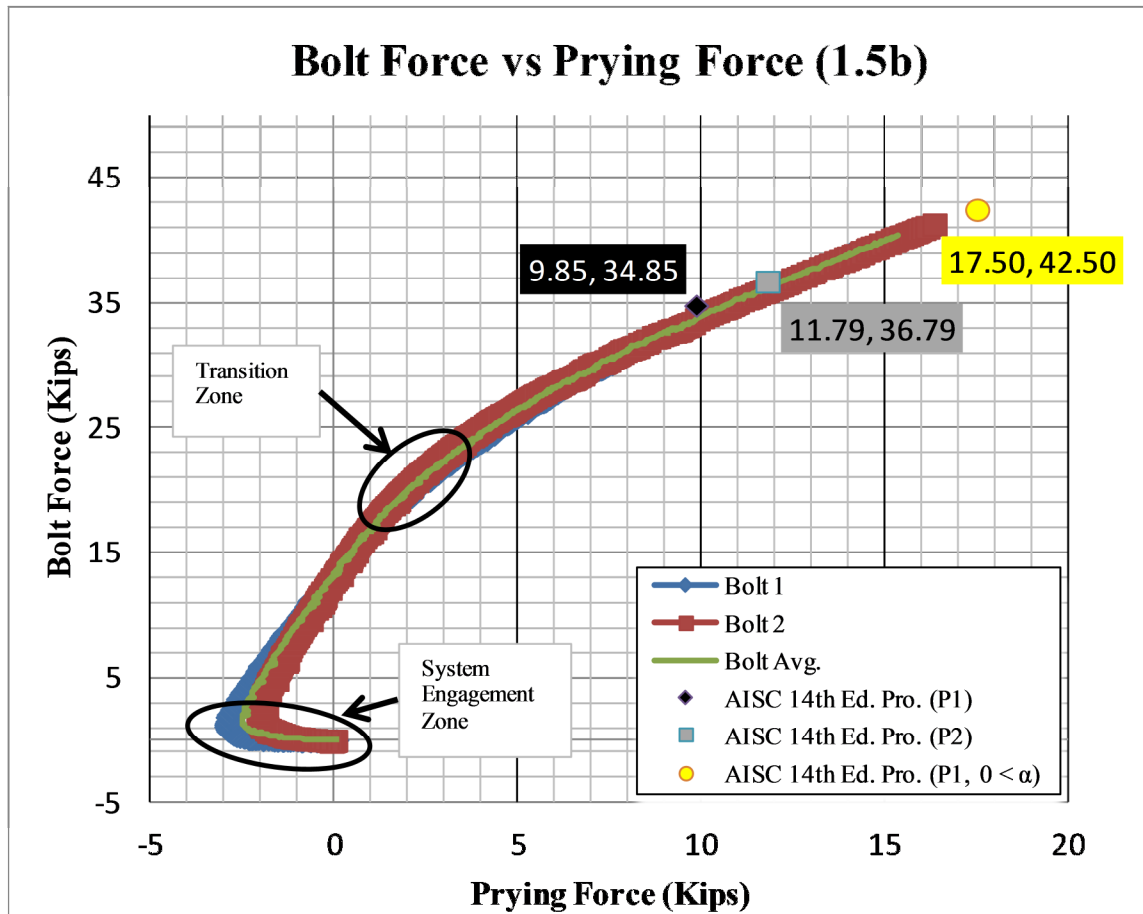
Figure 5.2.1-6: Bolt Force versus Prying Force.

The plots are isolating the engagement zone of the testing frame, as mentioned in

the experimental procedure portion of the thesis, and the noticeable transition zone from

linear to non-linear portion of the plot. The transition zone is also indicating when flange

yielding begins to occur. Since the engagement zone is the portion of the experiment

where the connecting elements of the test frame are engaging on each other, such as the

connecting frame bolts engaging against the bolt holes, a slight deviation is noticeable in

many of the experimental plots. After further consideration, the engagement zone could

also be representing the effects of pre-tensioned connecting bolts. Even though the bolts

were pre-tensioned prior to each experimental run, followed by zeroing the strain gages,

the pretension forces are still in the system which could have also resulted in the plot deviation. Since the prying forces were calculated using simple statics, a negative prying force has resulted within the engagement zone. The amount of force in the engagement zone is approximately the same value as that of the pre-tensioned force.

The effects of the deforming flange are occurring at the noted transition zones in Figures 5.2.1-4, 5.2.1-5, and 5.2.1-6. To complement the previous Figures, Figures 5.2.1-7 and 5.2.1-8 show the results of the effective length versus bolt force and the bolt force versus alpha, respectively. The effective length increases linearly with the increasing bolt force until the flange begins to yield. When the flange has fully yielded, the effective length begins to decrease. The effective length is the length of which the moment in the flange is being distributed; therefore, a larger effective length results in a smaller moment.
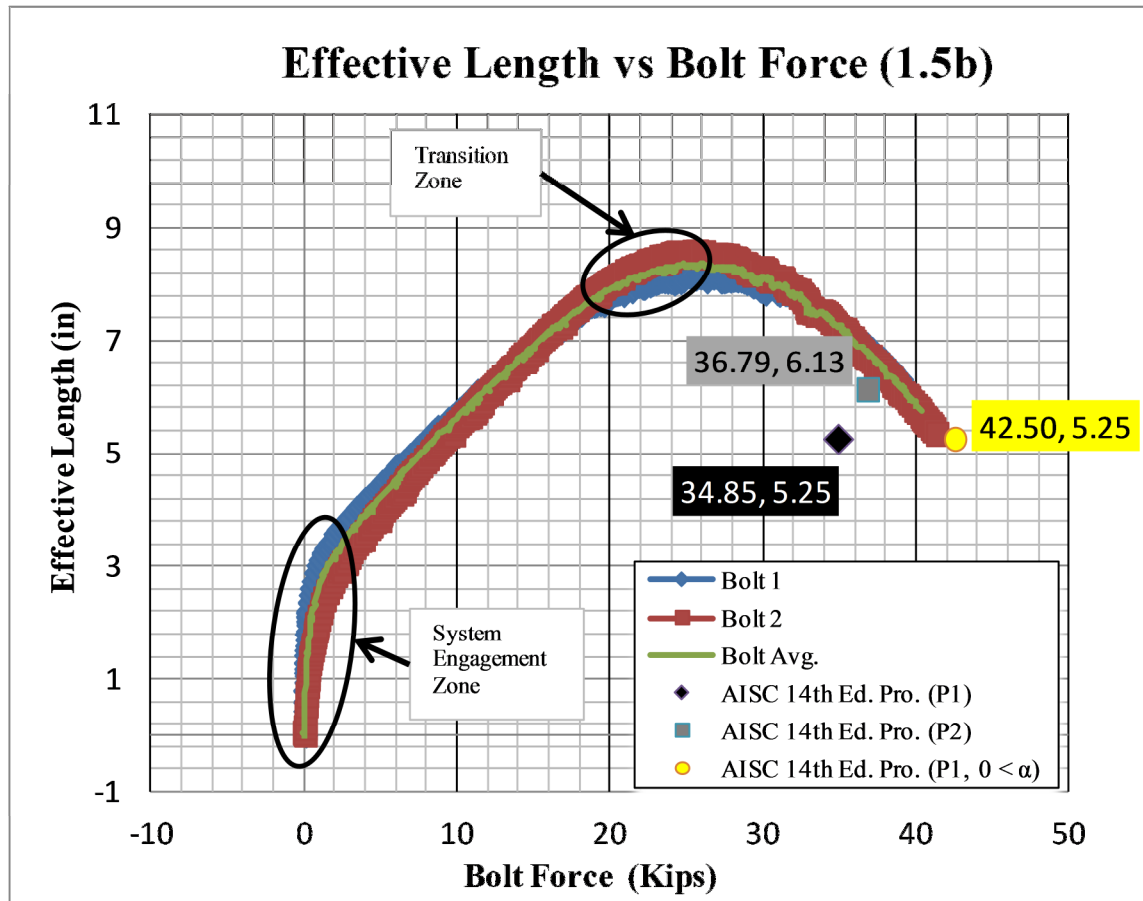
Figure 5.2.1-7: Effective Length versus Bolt Force.
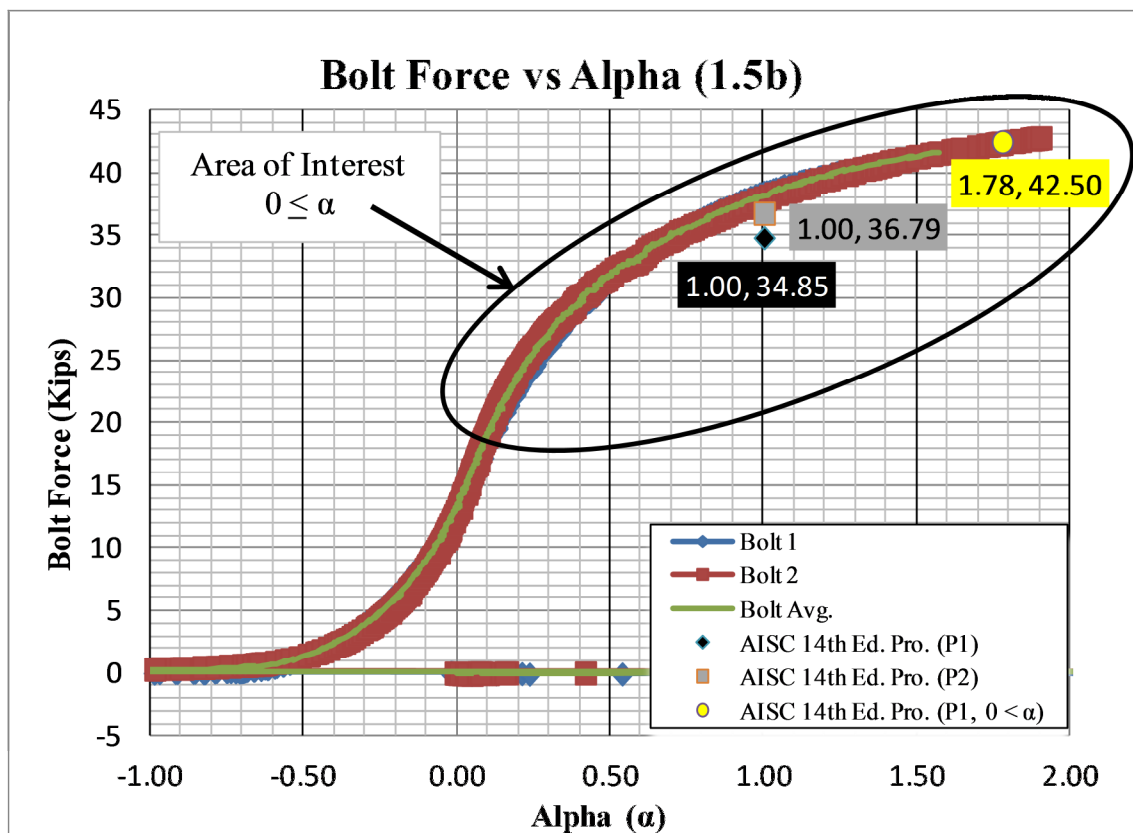
Figure 5.2.1-8: Bolt Force versus Alpha.

When comparing Figures 5.2.1-7 and 5.2.1-8, a noticeable transition zone occurs at approximately 20 kips of bolt force. The effective length appears to peak around 25 kips of bolt force and a tributary length of approximately 8.5 in. However, the maximum tributary length does not occur at the maximum bolt and prying forces. Appendix G-8 shows a plot of effective length versus prying force. The value of alpha, α, seems to be dramatically changing from beyond 25 kips of bolt force. This indicates that a fully yielded and/or hinge formation of the WT flange has occurred. The experimental value for alpha, α, peaks when the experiment is concluded at 100 kips of applied load. The resulting maximum bolt force average was measured at 41.383 kips and an average peak value for alpha of 1.398 was calculated.

When taking into account the engagement zone of the system, a varying value for the total prying force can be extracted. If the maximum measured and calculated value for prying force is not assumed to be the actual experimental maximum value for prying force, but consideration for the engagement zone is used, the correct approach would be to evaluate the total change from the lowest measured and calculated prying force to that of the highest measured and calculated prying force. By considering this, 3 kips would be added to the total prying force. This value is also indicated in Table 5.2.1-1 and is shown as q_{offset}.

In addition to the applied force, bolt force, and prying forces, deflection of various points of the specimens are also be considered. One of the key components that affect the amount of prying force generated during the experiment is the deformation of the specimen flange. The deformation of the specimen flange was captured by an LVDT which was placed on the top of the stem. See Figure 4.3-10 for the LVDT stem location. Prying forces increase with increased flange deformation. Figure 5.2.1-9 is a plot of the applied load versus deformation of the three LVDT's.
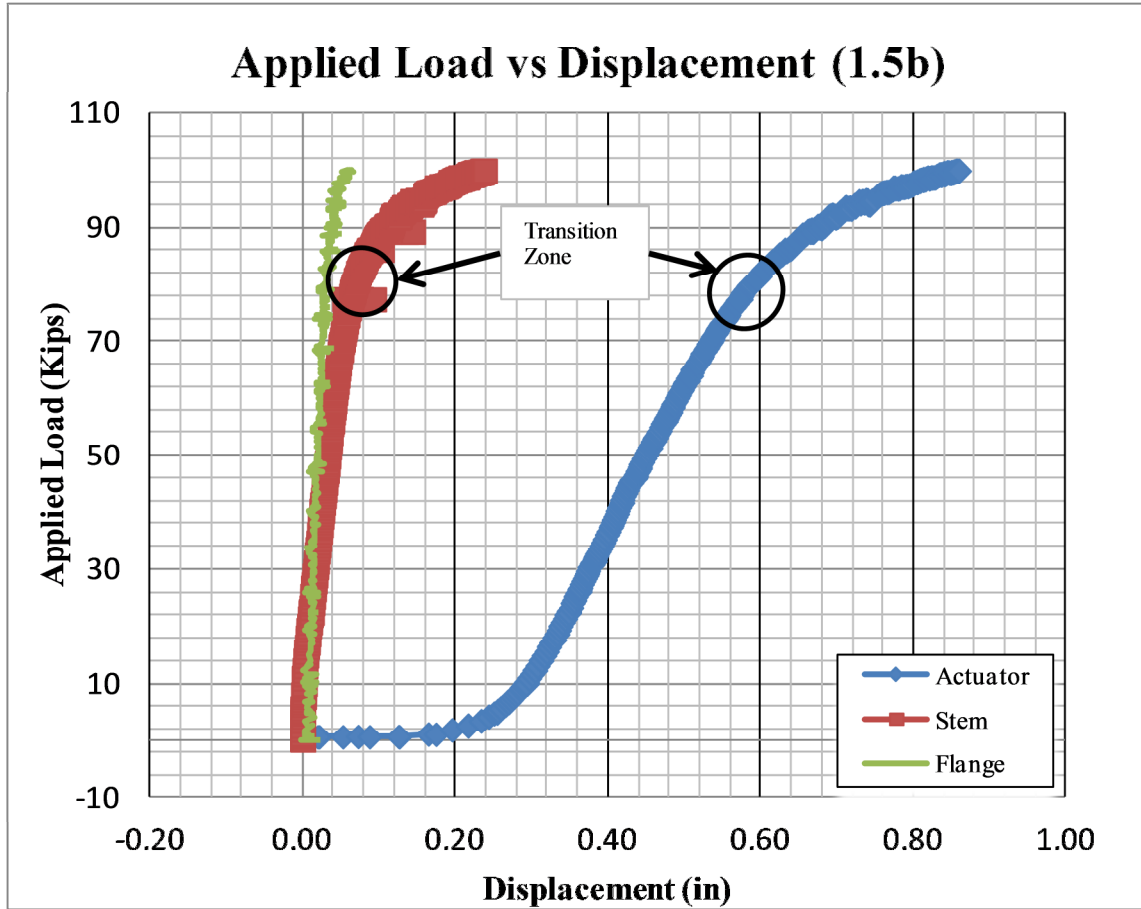
Figure 5.2.1-9: Applied Load versus Displacement.

With the AISC [3] provisions determined prior to testing, which were then

compared to that of the experimental data, some reasonable assumptions and conclusions

have resulted. The resulting measured bolt force was greater than that of the AISC [3]

provisions. To follow the increased bolt force, the resulting prying force was also greater

than that of the AISC [3] provisions. When determining the experimental tributary

length, it was found that the effective tributary length was much larger than that of the

AISC [3] provisions. The increased tributary length is not a cause for higher prying

forces since they do not occur at the same point on Figure 5.2.1-7. The secondary

consideration is that of alpha, α. Based on the calculations, the value for alpha, α, was

larger than that of the AISC [3] provisions. Based on the experiment, the resulting bolt

force was similar to that of the AISC [3] provisions if the actual value for alpha, α, was

used. Even though the experimental bolt forces were similar to the AISC [3] provisions

with the exact value for alpha, α, the experimental values for alpha were lower than the

initial calculations. This result is because the experimental value for tributary length was

much higher than that of the AISC [3] provisions. Table 5.2.1-1 shows a result summary

of the measured and calculated values for which is being analyzed and Appendix G

shows additional figures and plots for specimen 1.5b.

Table 5.2.1-1: Experimental Results Summary Specimen 1.5b.

Experimental Results Summary WT6x32.5_1.5b								
Bolt 1			**Bolt 2**			**Displacements**		
$\mu\varepsilon_{max}$	3144	μStrain	$\mu\varepsilon_{max}$	3301	μStrain	Actuator$_{max}$	0.860	in
σ_{max}	91.174	ksi	σ_{max}	95.731	ksi	Stem$_{max}$	0.239	in
T_{max}	39.360	kips	T_{max}	41.328	kips	Flange$_{max}$	0.067	in
q_{max}	14.373	kips	q_{max}	16.340	kips			
q_{offset}	17.373	kips	q_{offset}	18.340	kips			
p_{max}	8.174	in	p_{max}	8.578	in			
α_{max}	1.121	Ratio	α_{max}	1.506	Ratio			
PreTension			**PreTension**			**Applied Load**		
$\mu\varepsilon_{max}$	350.464	μStrain	$\mu\varepsilon_{max}$	347.206	μStrain	Applied Load$_{max}$	99.95	kips
σ_{max}	10.163	ksi	σ_{max}	10.069	ksi			
T_{max}	4.388	kips	T_{max}	4.347	kips			

NOTE: q_{offset} is the total change from the engagement zone to the
max recorded value. Taken from the Bolt Force vs. Prying Force
Graph.

5.2.2. *WT6x32.5 at Bolt Spacing 2.0b*

As the experiment for Specimen 2.0b was performed, the noticeable flange deformation was observed and photographed. Figure 5.2.2-1 shows the deformed shape at the point of 100 kip applied load.
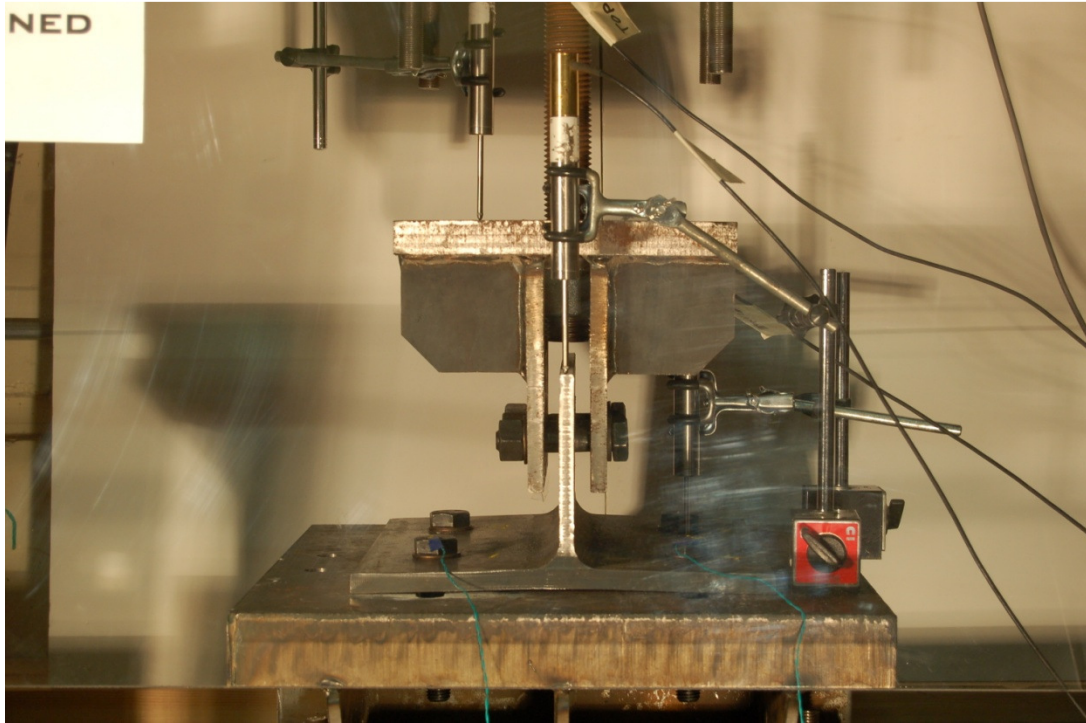
Figure 5.2.2-1: Deformed Shape for Specimen 2.0b at 100 kips Applied Load.

Figure 5.2.2-2 shows the specimen's deformed shape after being removed from the experimental testing frame. The noticeable stress patterns are illustrated in Figure 5.2.2-3.

Figure 5.2.2-2: Deformed Shape for Specimen 2.0b Post-Testing.
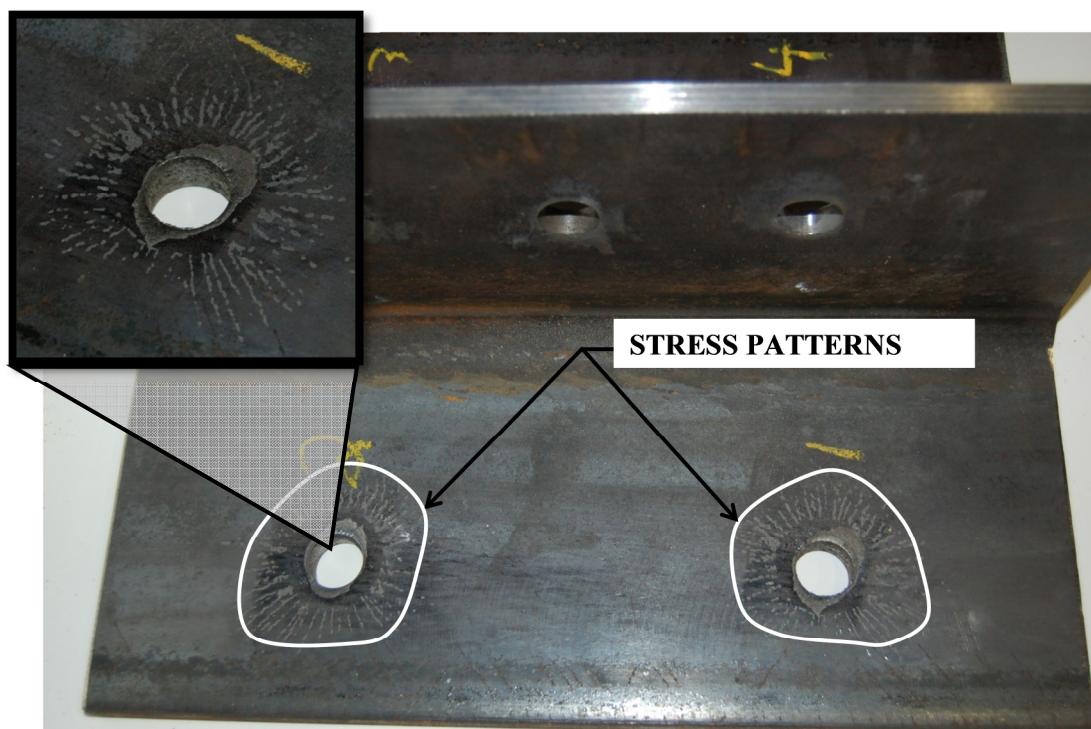
Figure 5.2.2-3: Stress Patterns for Specimen 2.0b.

The stress patterns indicated in Figure 5.2.2-3 illustrate how the stress patterns have become independent of each other, unlike that of specimen 1.5b. As mentioned in the earlier portions of the paper, 2.0b is the maximum allowable tributary length when calculating prying forces according to AISC [3].

There is a slight increase in bolt force due to prying action and Figure 5.2.2-4 shows a plot of the applied load versus bolt force. Additional plots show the applied load versus prying force as well as the bolt force versus prying force. These plots can be found in Figures 5.2.2-4 and 5.2.2-5, respectively.

Figure 5.2.2-4: Applied Load versus Bolt Force.

Figure 5.2.2-5: Applied Load versus Prying Force.

Figure 5.2.2-6: Bolt Force versus Prying Force.

When comparing the experimental results to that of the AISC [3] provisions, the experiment plots are indicating a lower value of prying force. This indicates that the AISC [3] provisions are relatively conservative.
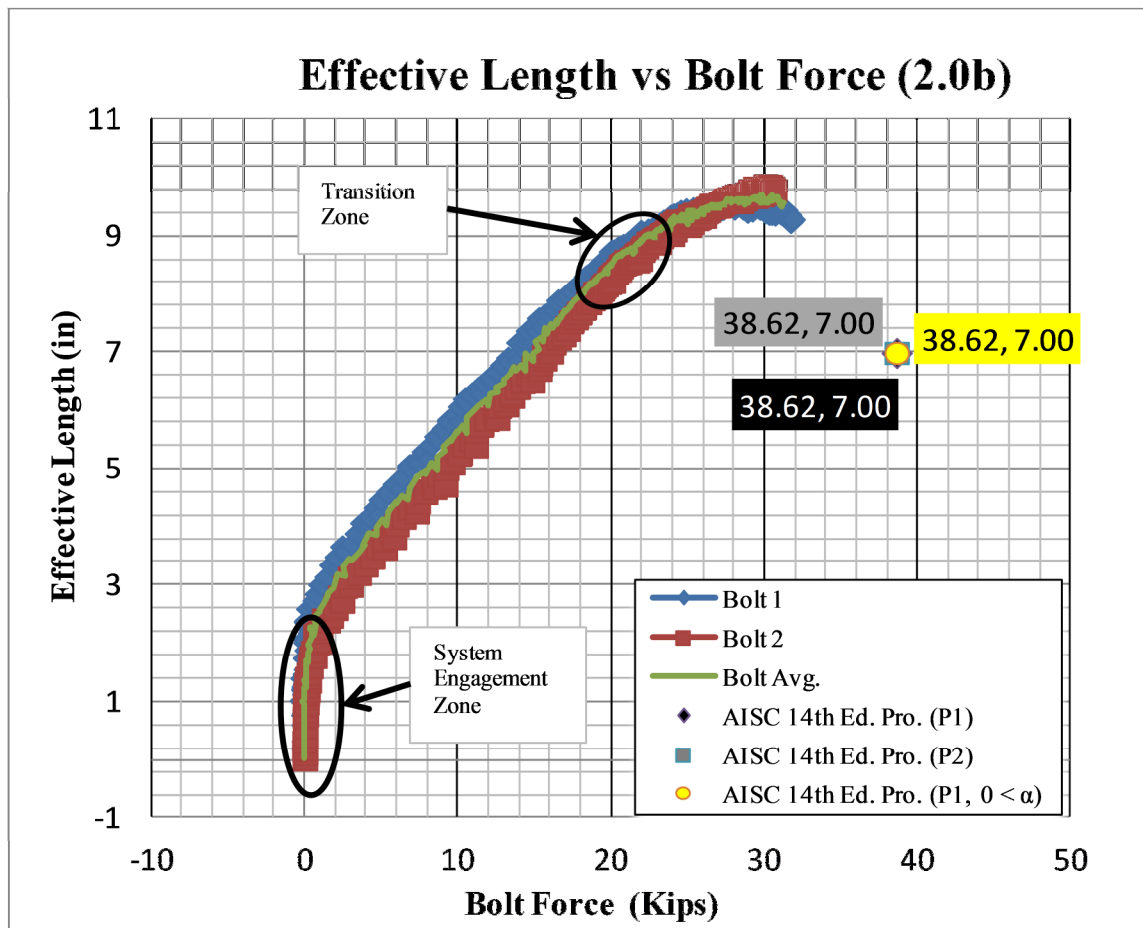
Figure 5.2.2-7: Effective Length versus Bolt Force.

Unlike specimen 1.5b, the maximum effective length correlates with the maximum bolt and prying force. The experimental results indicate a larger value of tributary length than that of the AISC [3] provisions, but the resulting prying force is lower than that of the AISC [3] provisions.
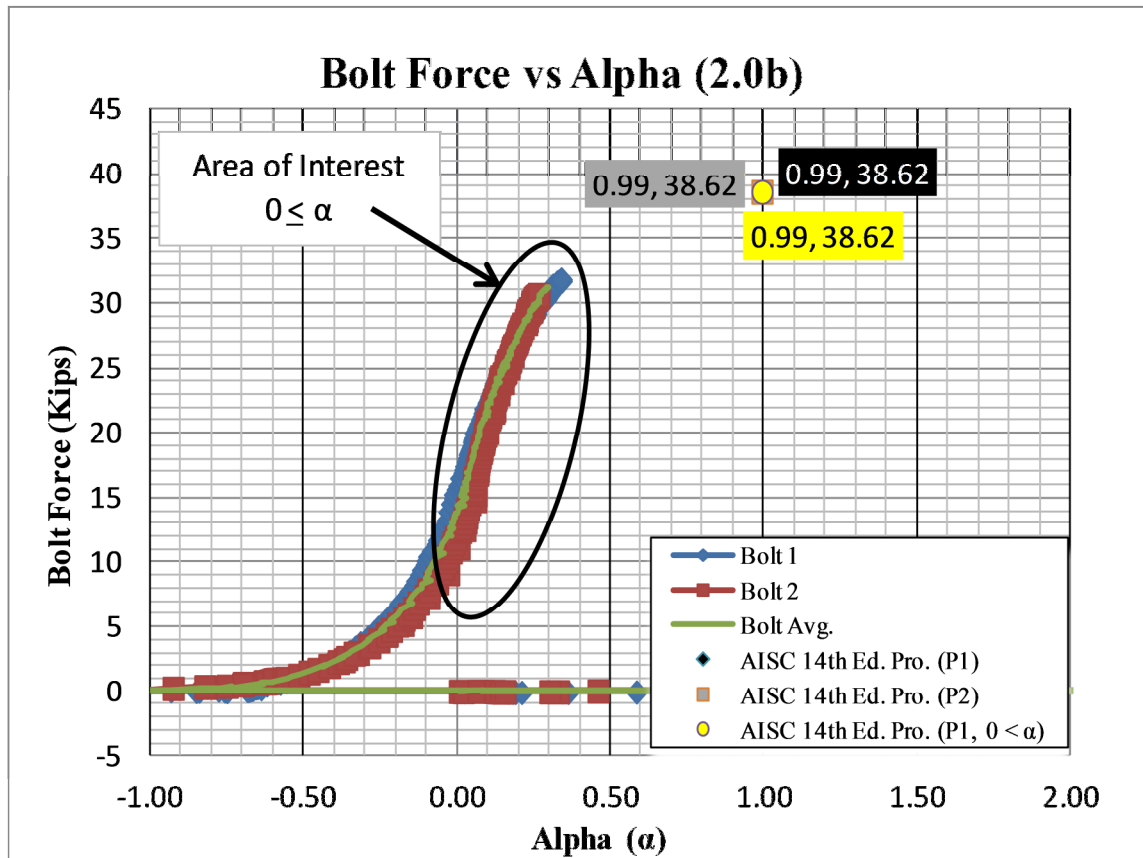
Figure 5.2.2-8: Bolt Force versus Alpha.

Similar to that of specimen 1.5b, the AISC [3] provisions indicate a value for alpha at approximately 1.0, therefore comparing the experimental value for α greater than one should be considered. After reviewing the experimental results, the maximum value for α was much lower than that of the AISC [3] provision value. Based on the amount of prying force when compared to the AISC [3] provisions, the results are consistent with one another. Since the remaining specimen showed α values much less than one, according to the AISC [3] provisions and the experimental results, a discussion comparing α to the AISC [3] provisions for specimens 2.5b, 3.0b, and 4.0b will not be included but their respective plots can be found in Appendix G.

Figure 5.2.2-9 shows a plot of the applied load versus deformation of the three

LVDT's. The plot illustrates the point of which flange yielding is beginning to occur.

Figure 5.2.2-9: Applied Load versus Deformation.

The results summary of the measured and calculated values for which is being

analyzed can be found in Table 5.2.2-1.

Table 5.2.2-1: Experimental Results Summary Specimen 2.0b.

Experimental Results Summary WT6x32.5_2.0b

Bolt 1			Bolt 2			Displacements		
$\mu\varepsilon_{max}$	2543	μStrain	$\mu\varepsilon_{max}$	2447	μStrain	Actuator$_{max}$	0.694	in
σ_{max}	73.741	ksi	σ_{max}	70.976	ksi	Stem$_{max}$	0.176	in
T_{max}	31.835	kips	T_{max}	30.641	kips	Flange$_{max}$	0.202	in
q_{max}	6.847	kips	q_{max}	5.656	kips			
q_{offset}	8.847	kips	q_{offset}	8.156	kips			
p_{max}	9.593	in	p_{max}	9.883	in			
α_{max}	0.337	Ratio	α_{max}	0.264	Ratio			
PreTension			PreTension			Applied Load		
$\mu\varepsilon_{max}$	385.210	μStrain	$\mu\varepsilon_{max}$	365.350	μStrain	Applied Load$_{max}$	99.95	kips
σ_{max}	11.171	ksi	σ_{max}	10.595	ksi			
T_{max}	4.823	kips	T_{max}	4.574	kips			

Note: q_{offset} is the total change from the engagement zone to the max recorded value. Taken from the Bolt Force vs. Prying Force Graph.

See Appendix G for additional plots for specimen 2.0b.

5.2.3. *WT6x32.5 at Bolt Spacing 2.5b*

Similar to specimens 1.5b and 2.0b, a photograph was taken at the conclusion of the experiment where the applied load is at 100 kips. Figure 5.2.3-1 shows the maximum deformed shape and Figure 5.2.4-1 shows the deformed shape post-experiment.
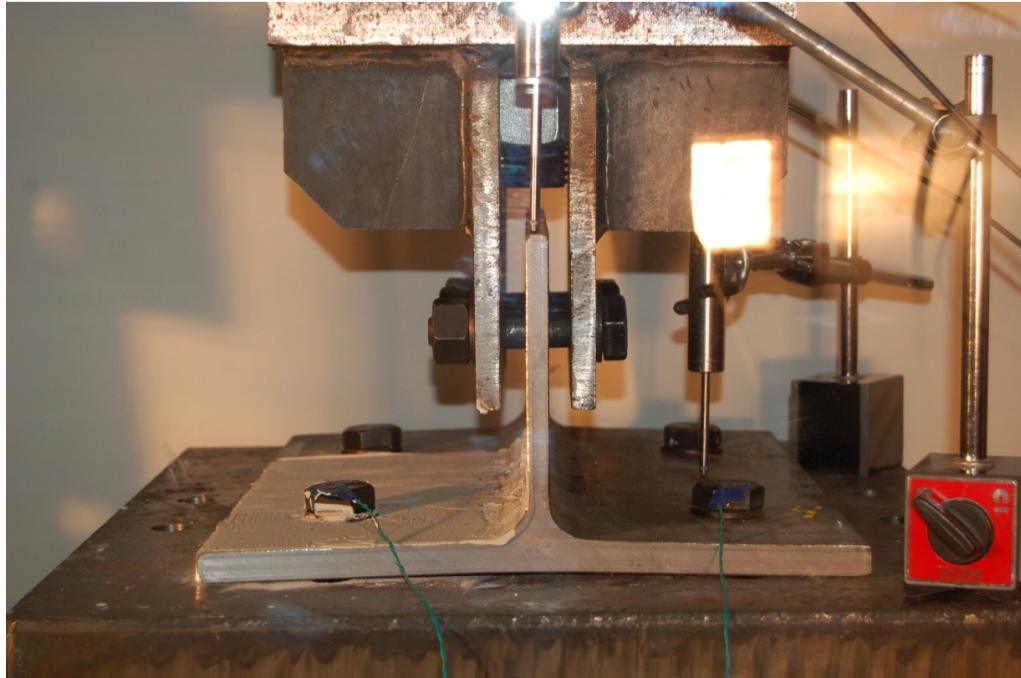
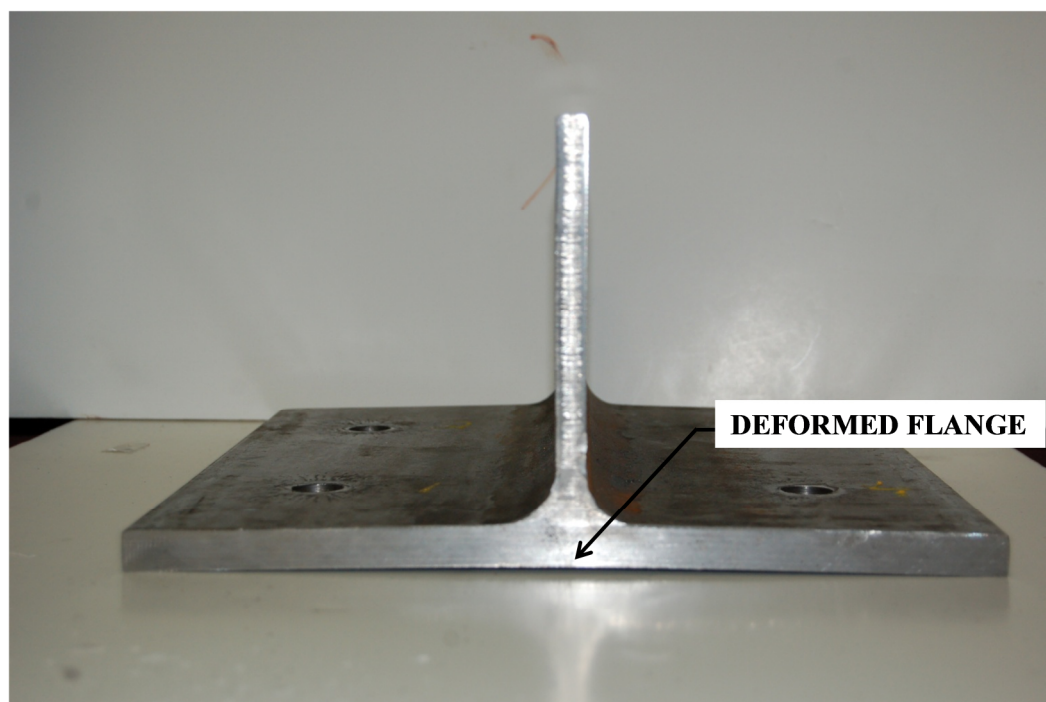**Figure 5.2.3-1: Deformed Shape for Specimen 2.5b at 100 kips Applied Load.**

Figure 5.2.3-2: Deformed Shape for Specimen 2.5b Post-Testing.
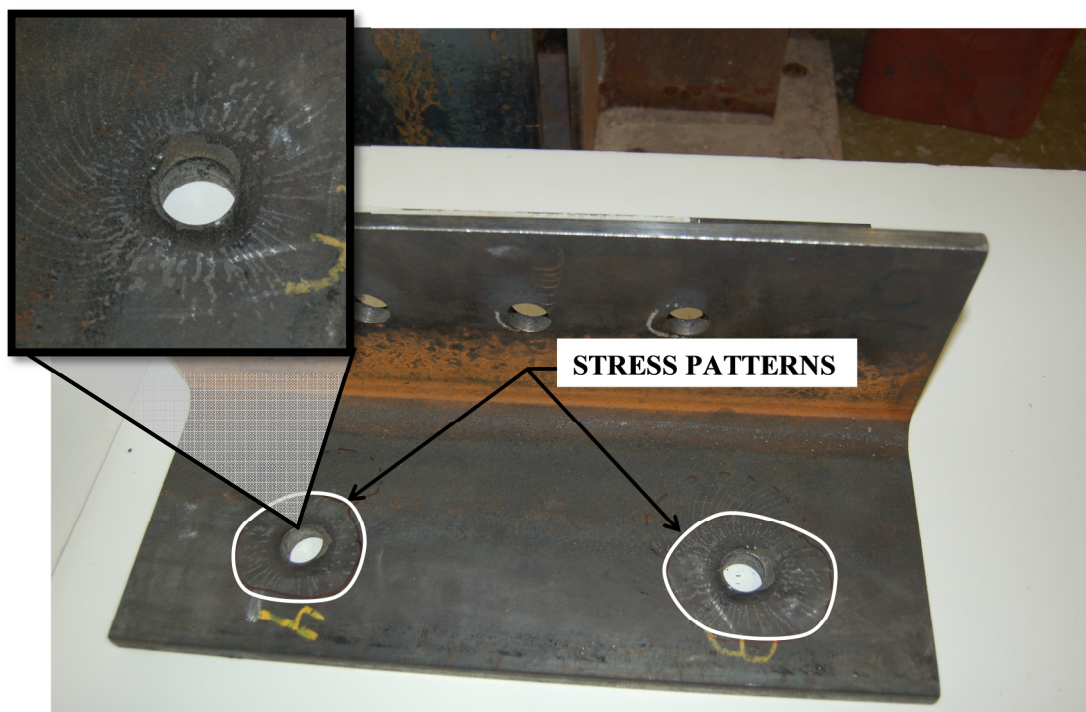
Figure 5.2.3-3: Stress Patterns for Specimen 2.5b.

The stress patterns for specimen 2.5b are similar to that of specimen 2.0b. The stress is concentrated between each bolt.

There was a slight increase in bolt force due to prying action and Figure 5.2.3-4 shows a plot of applied load versus bolt force. Additional plots show the applied load versus prying force as well as the bolt force versus prying force. These plots can be found in Figures 5.2.3-4 and 5.2.3-5, respectively.
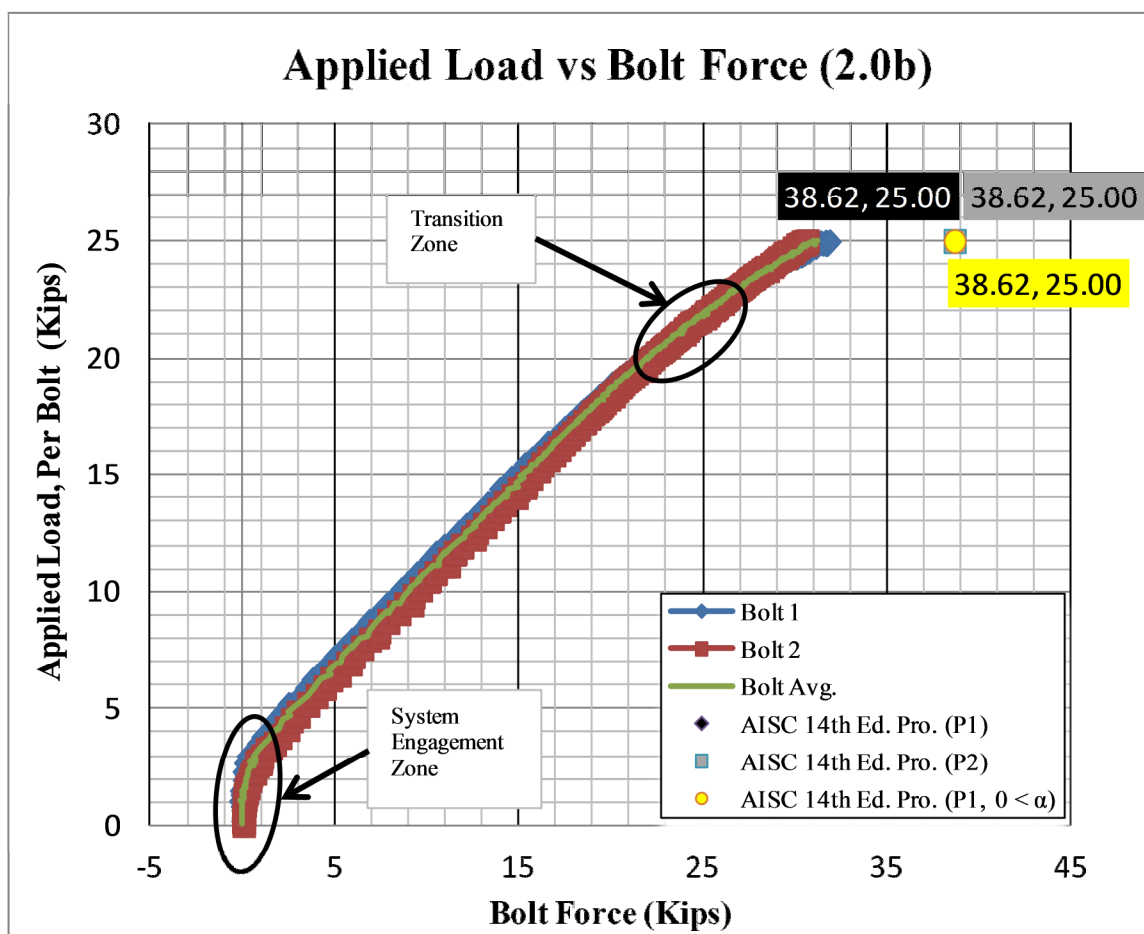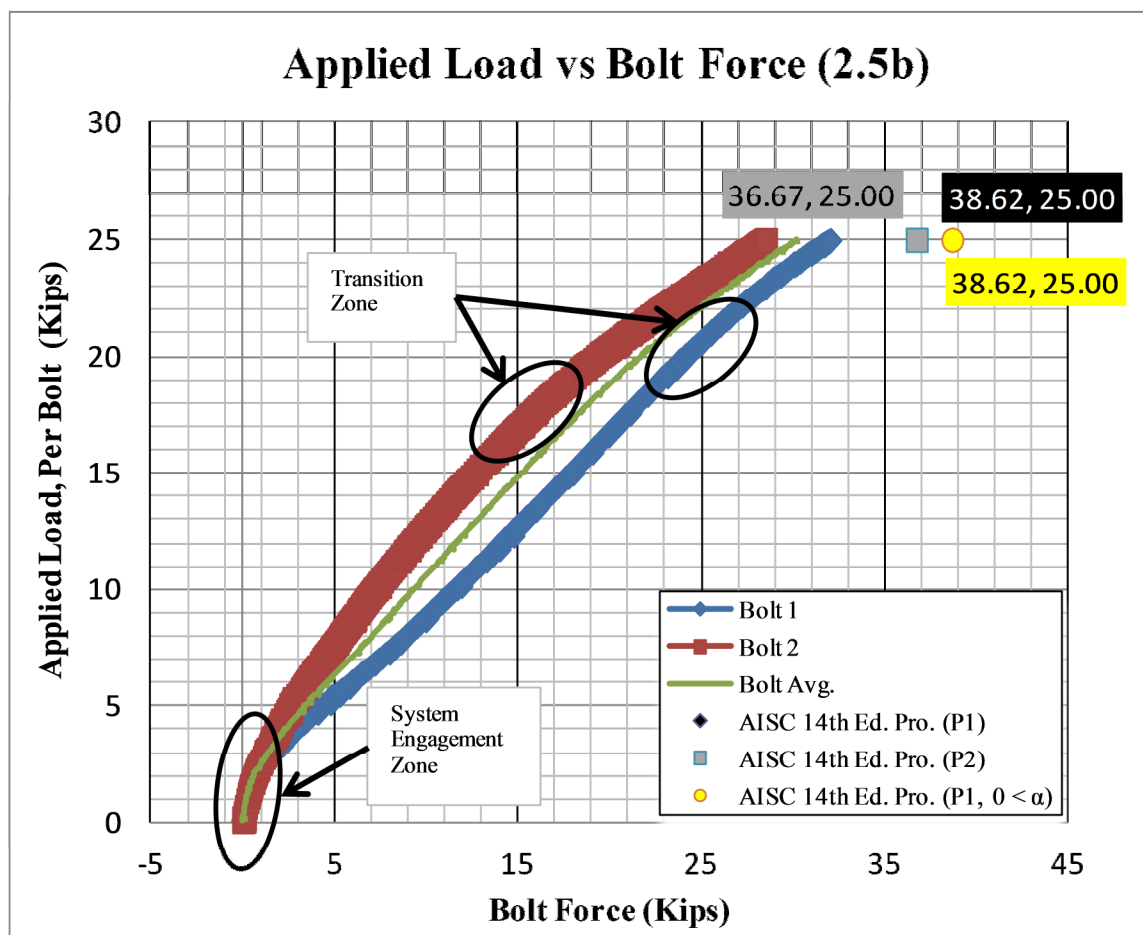

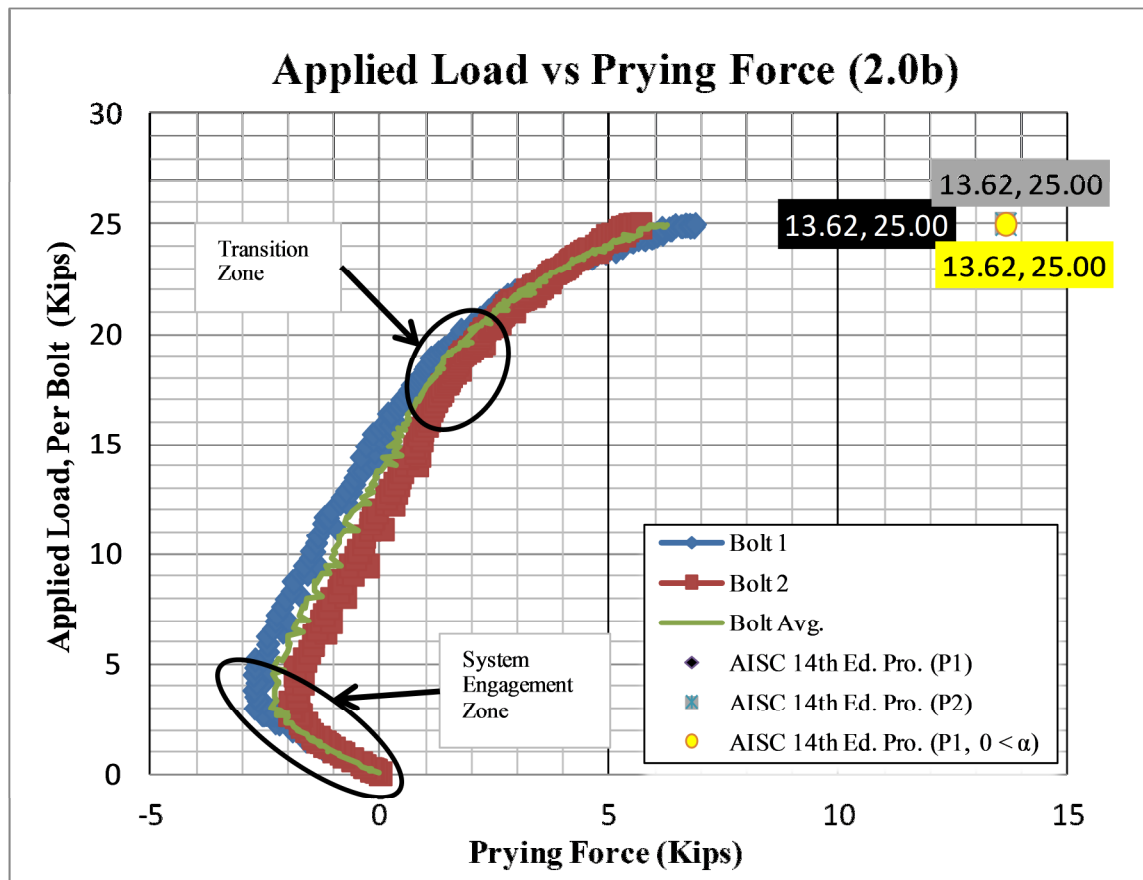**Figure 5.2.3-4: Applied Load versus Bolt Force.**
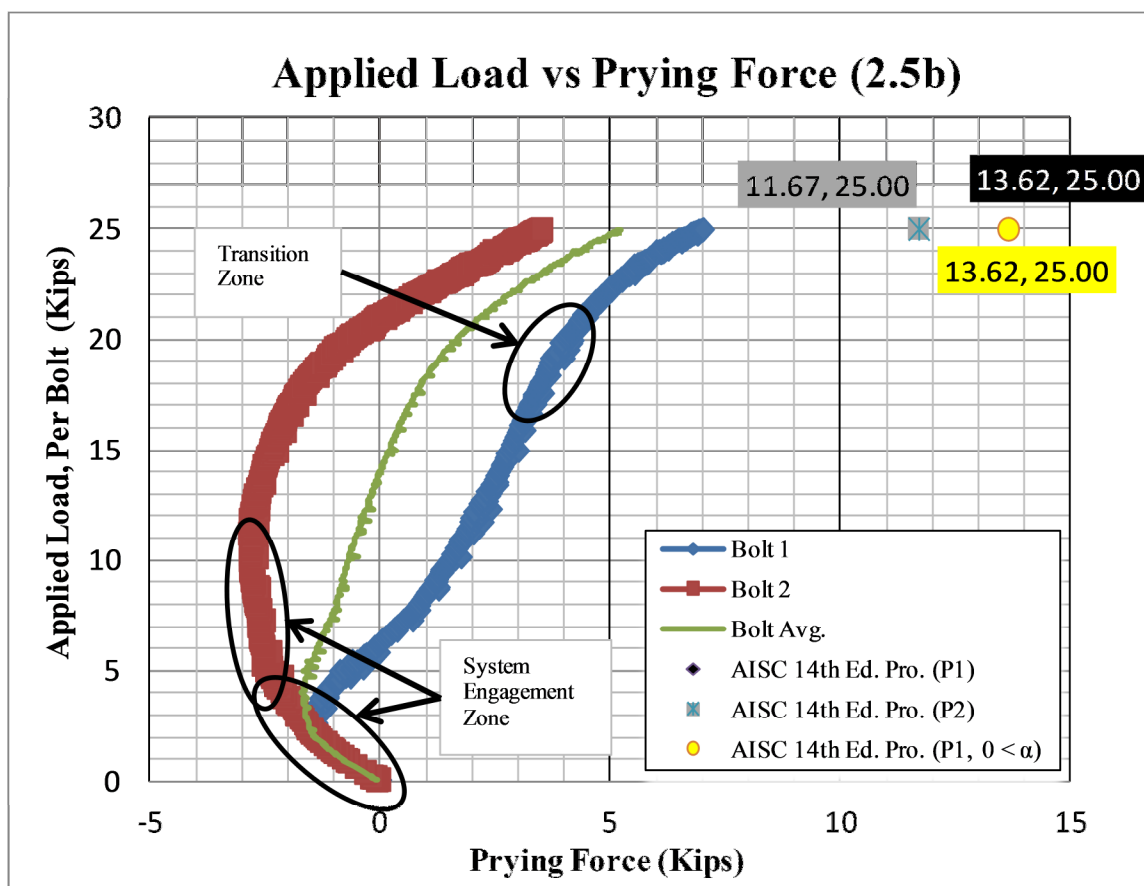
Figure 5.2.3-5: Applied Load versus Prying Force.
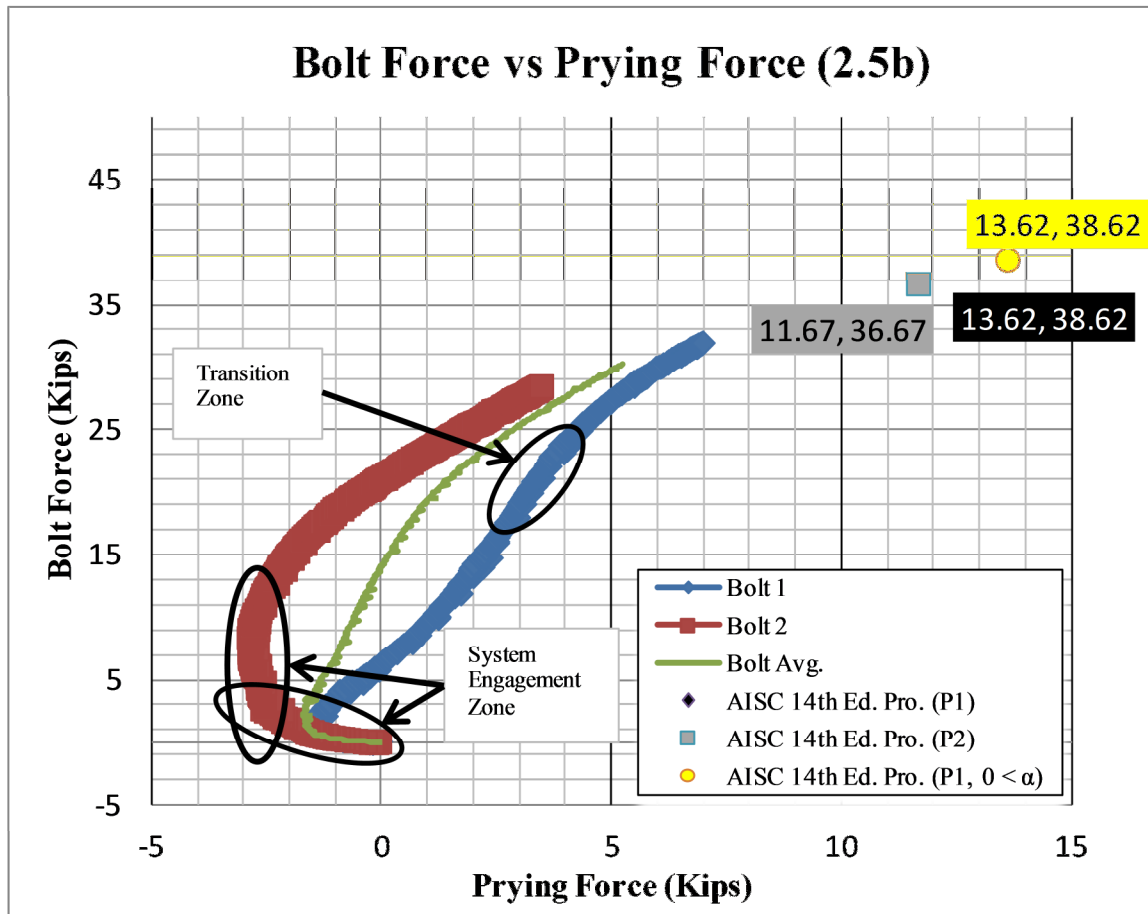
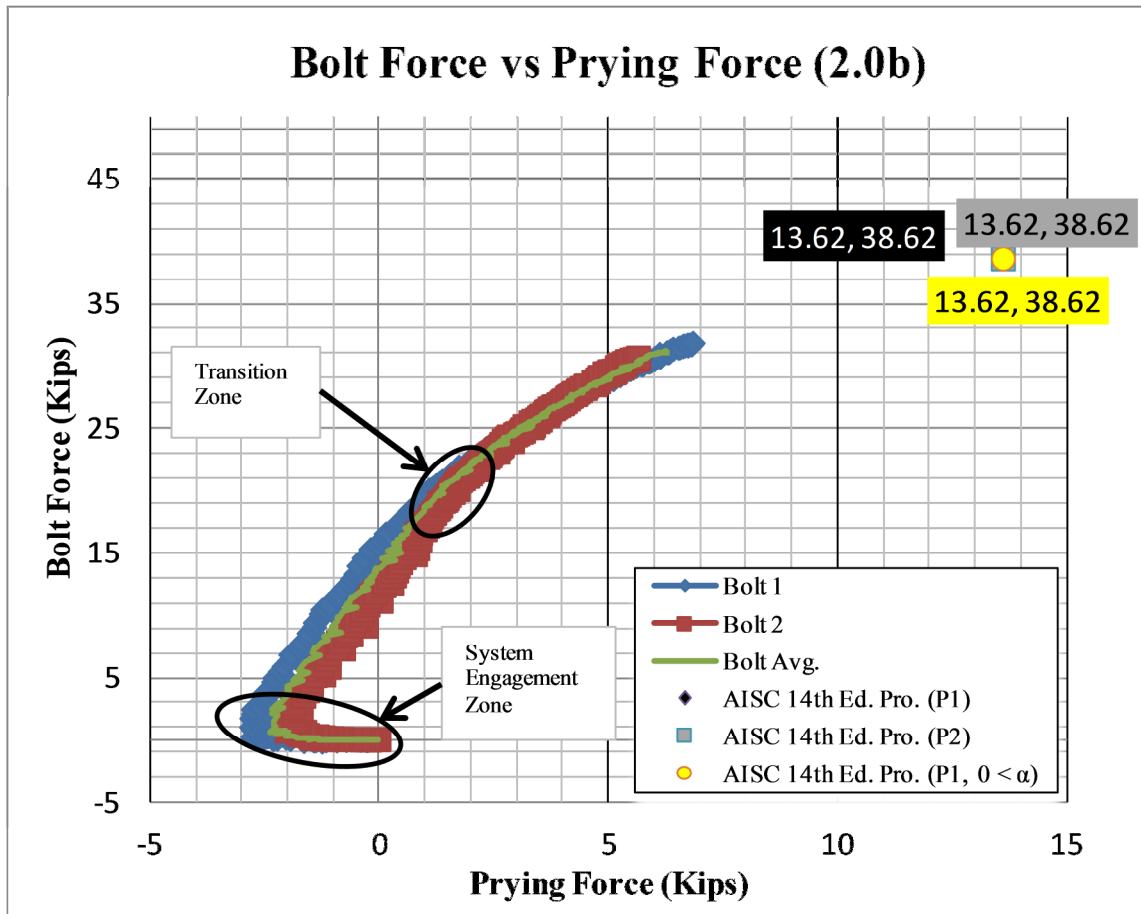**Figure 5.2.3-6: Bolt Force versus Prying Force.**

When comparing the experimental results to that of the AISC [3] provisions, results similar to that of specimen 2.0b have resulted. The experimental values of bolt and prying force are relatively lower than that of the AISC [3] provisions. Figure 5.2.3-6 shows some discrepancy between forces in bolts one and two.
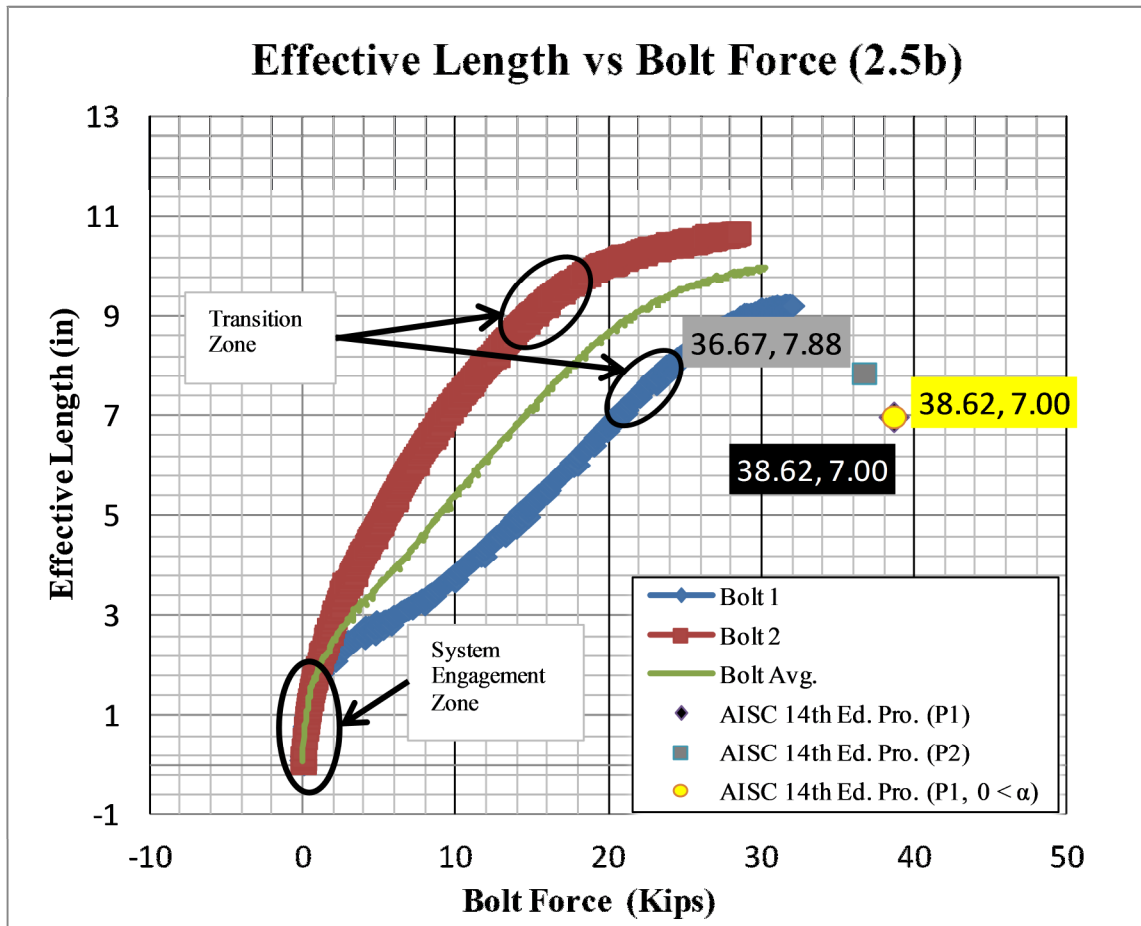
Figure 5.2.3-7: Effective Length versus Bolt Force.

The experimental results indicate a larger value of tributary length than that of the AISC [3] provisions, but the resulting prying force is lower than that of the AISC [3] provisions. The maximum bolt force occurs at approximately the same point as the maximum tributary length.

When observing Figure 5.2.3-9, the point of transition, or flange yielding, can be seen, but indicates a relatively minor transition. That would be consistent with the amount of prying force generated.
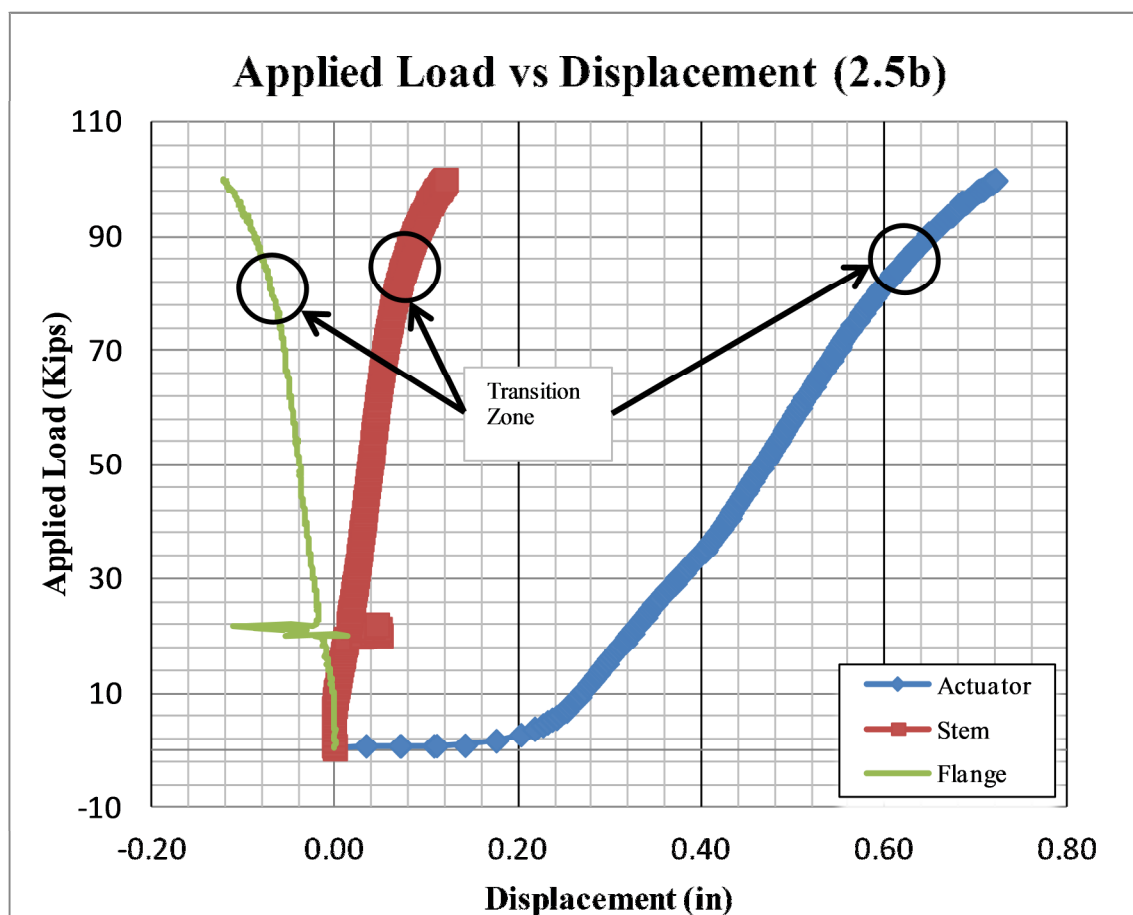
Figure 5.2.3-8: Applied Load versus Deformation.

The results summary of the measured and calculated values for which was being analyzed for specimen 2.5b can be found in Table 5.2.3-1.

Table 5.2.3-1: Experimental Results Summary Specimen 2.5b.

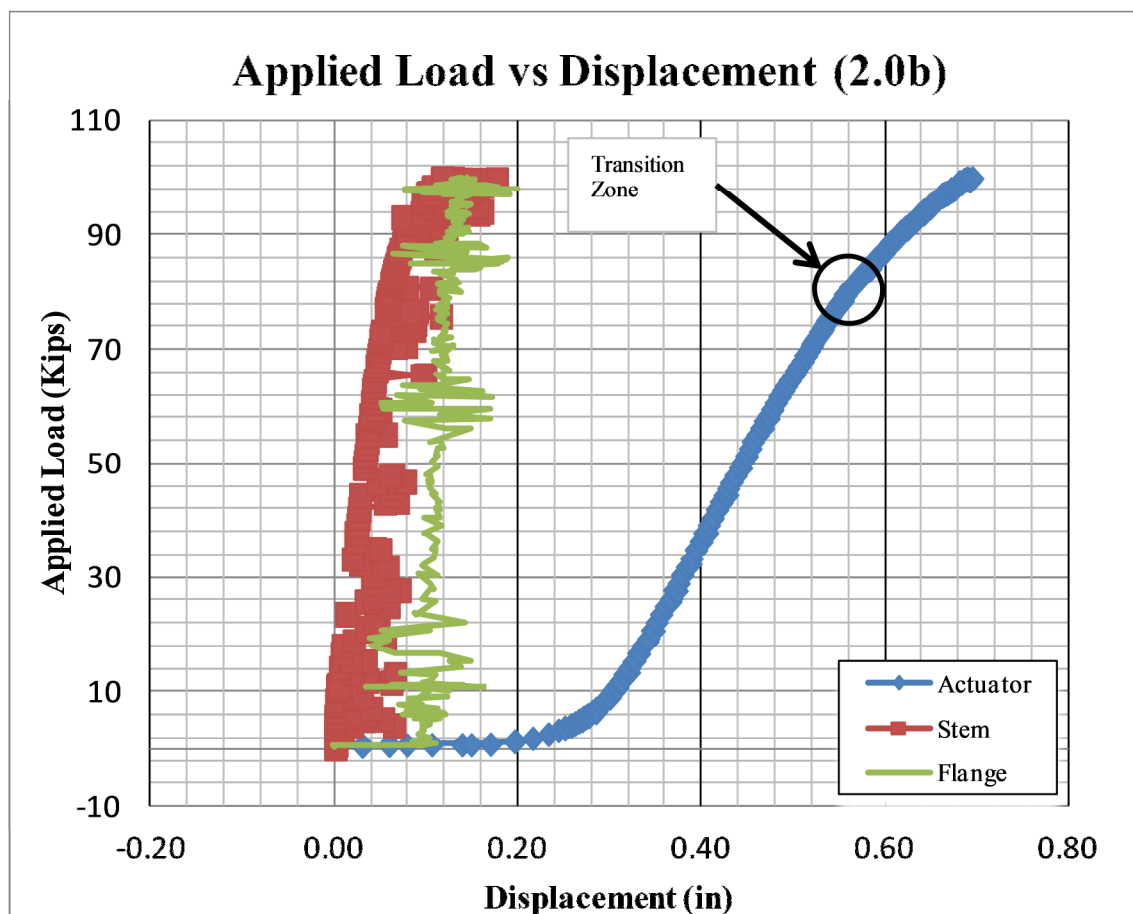| Experimental Results Summary WT6x32.5_2.5b								
Bolt 1			**Bolt 2**			**Displacements**		
$\mu\varepsilon_{max}$	2551.01	μStrain	$\mu\varepsilon_{max}$	2270.75	μStrain	Actuator$_{max}$	0.721	in
σ_{max}	73.177	ksi	σ_{max}	65.136	ksi	Stem$_{max}$	0.122	in
T_{max}	31.978	kips	T_{max}	28.464	kips	Flange$_{max}$	0.136	in
q_{max}	6.990	kips	q_{max}	3.477	kips			
q_{offset}	7.990	kips	q_{offset}	5.977	kips			
p_{max}	9.250	in	p_{max}	10.707	in			
α_{max}	0.346	Ratio	α_{max}	0.147	Ratio			
PreTension			**PreTension**			**Applied Load**		
$\mu\varepsilon_{max}$	350.464	μStrain	$\mu\varepsilon_{max}$	347.206	μStrain	Applied Load$_{max}$	99.95	kips
σ_{max}	10.1635	ksi	σ_{max}	10.069	ksi			
T_{max}	4.44136	kips	T_{max}	4.40007	kips			

Note: q_{offset} is the total change from the engagement zone to the max recorded value. Taken from the Bolt Force vs. Prying Force Graph.

See Appendix G for additional plots for specimen 2.5b.

5.2.4. *WT6x32.5 at Bolt Spacing 3.0b, 4.0b*

Specimens 3.0b and 4.0b had experimental results very similar to one another. Therefore, all plots will consist of specimens 3.0b and 4.0b. The photograph taken at the conclusion of the experiment where the applied load is at 100 kips shows very little flange deformation. Figure 5.2.4-1 shows the maximum deformed shape and Figure 5.2.4-2 shows the deformed shape post experiment.
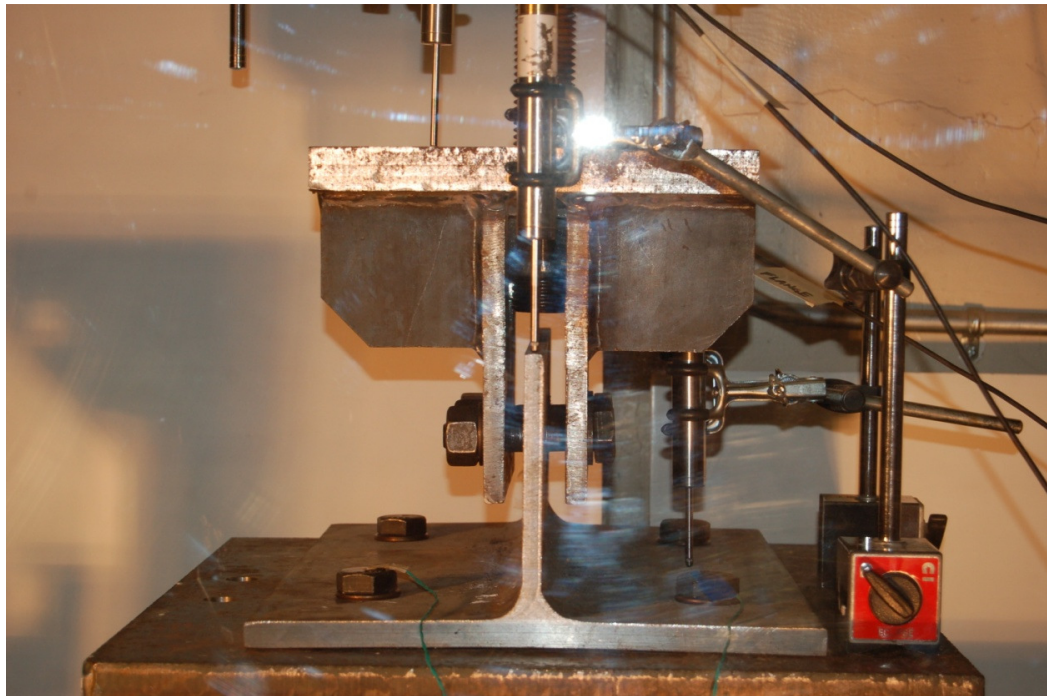
Figure 5.2.4-1: Deformed Shape for Specimen 3.0b at 100 kips Applied Load.
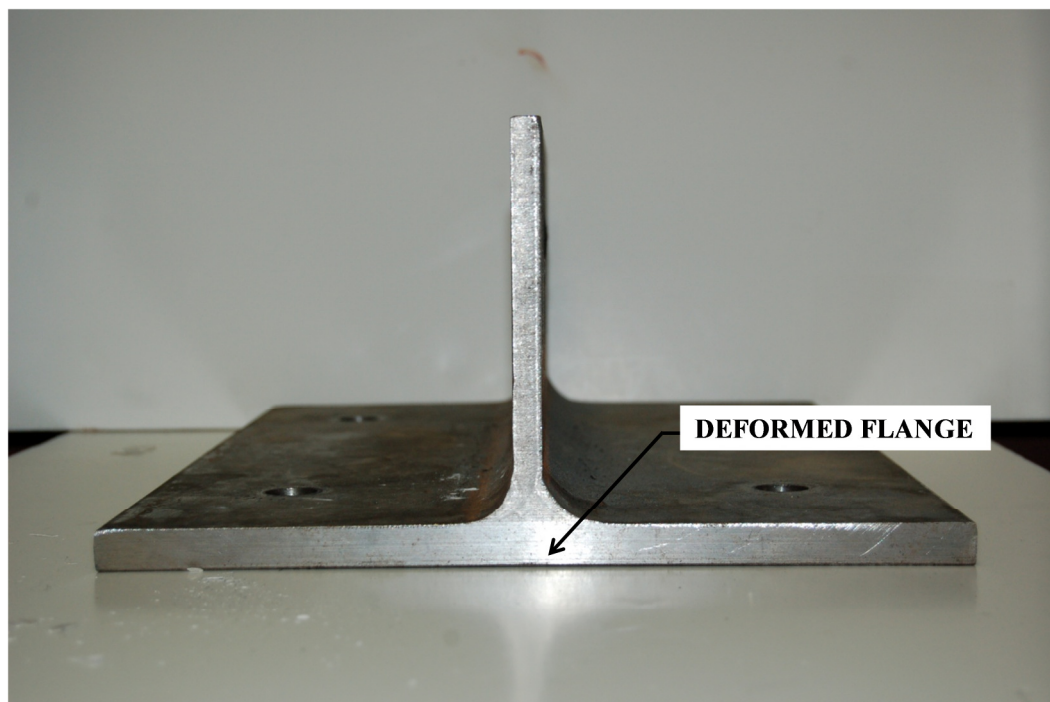
Figure 5.2.4-2: Deformed Shape for Specimen 3.0b Post-Testing.
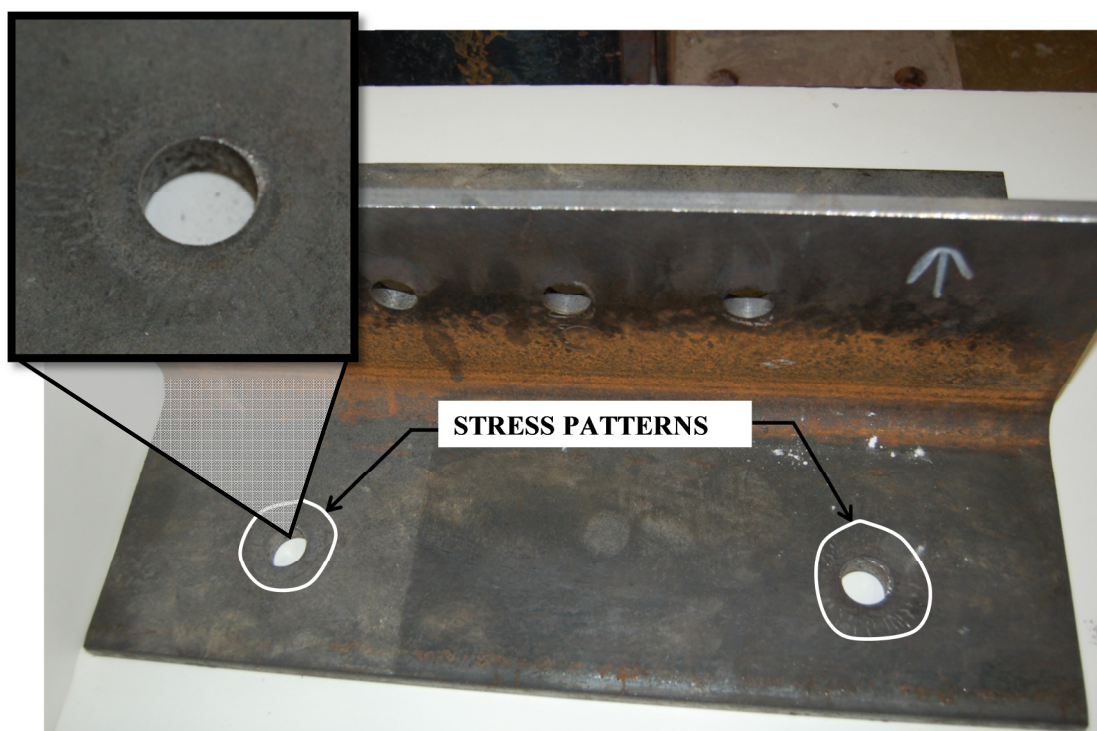
Figure 5.2.4-3: Stress Patterns for Specimen 3.0b.

The post-testing flange deformation and stress patterns were almost identical when comparing specimens 3.0b and 4.0b. Only one of the two specimens were shown due to their similarities.

There was very little increase in bolt force due to prying action and Figure 5.2.4-4 illustrates this. Additional plots show the applied load versus prying force as well as the bolt force versus prying force. These plots can be found in Figures 5.2.4-5 and 5.2.4-6, respectively.
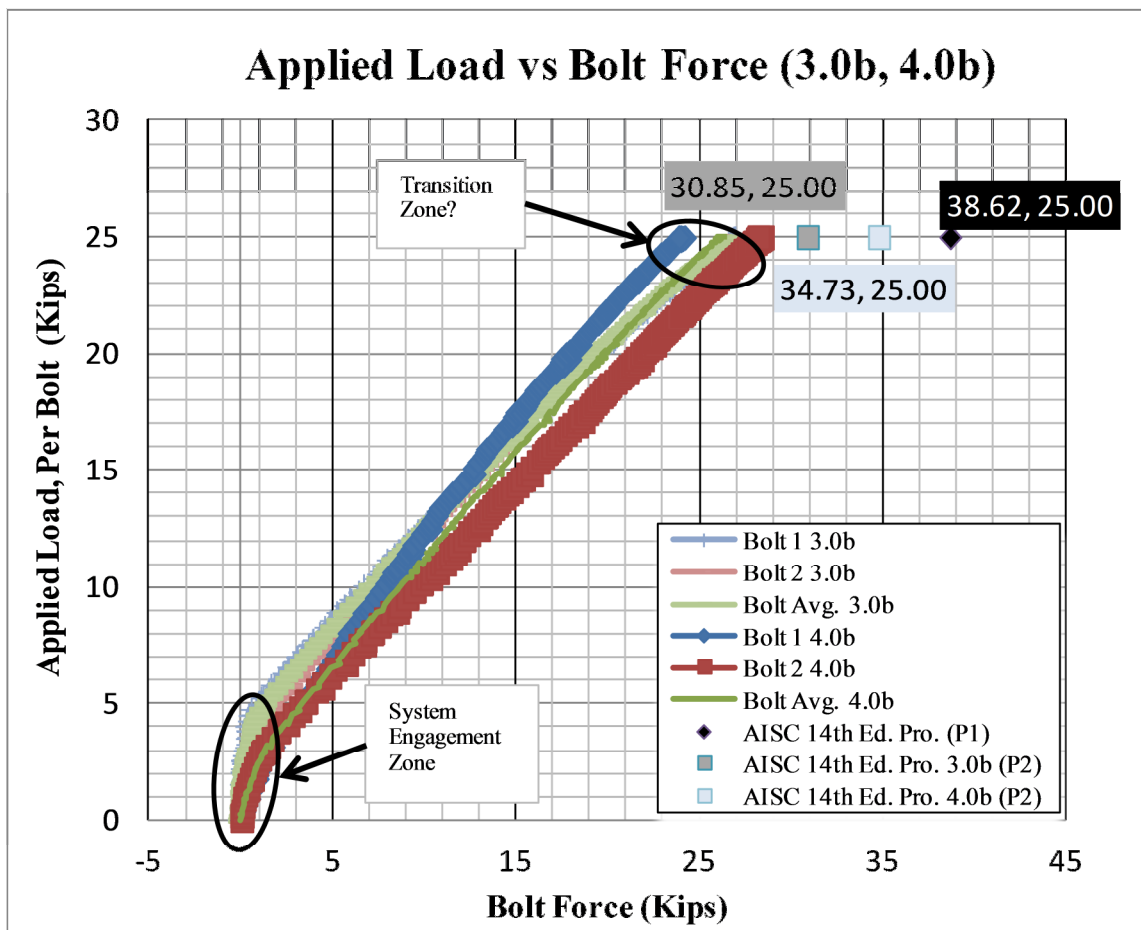
Figure 5.2.4-4: Applied Load versus Bolt Force 3.0b, 4.0b.
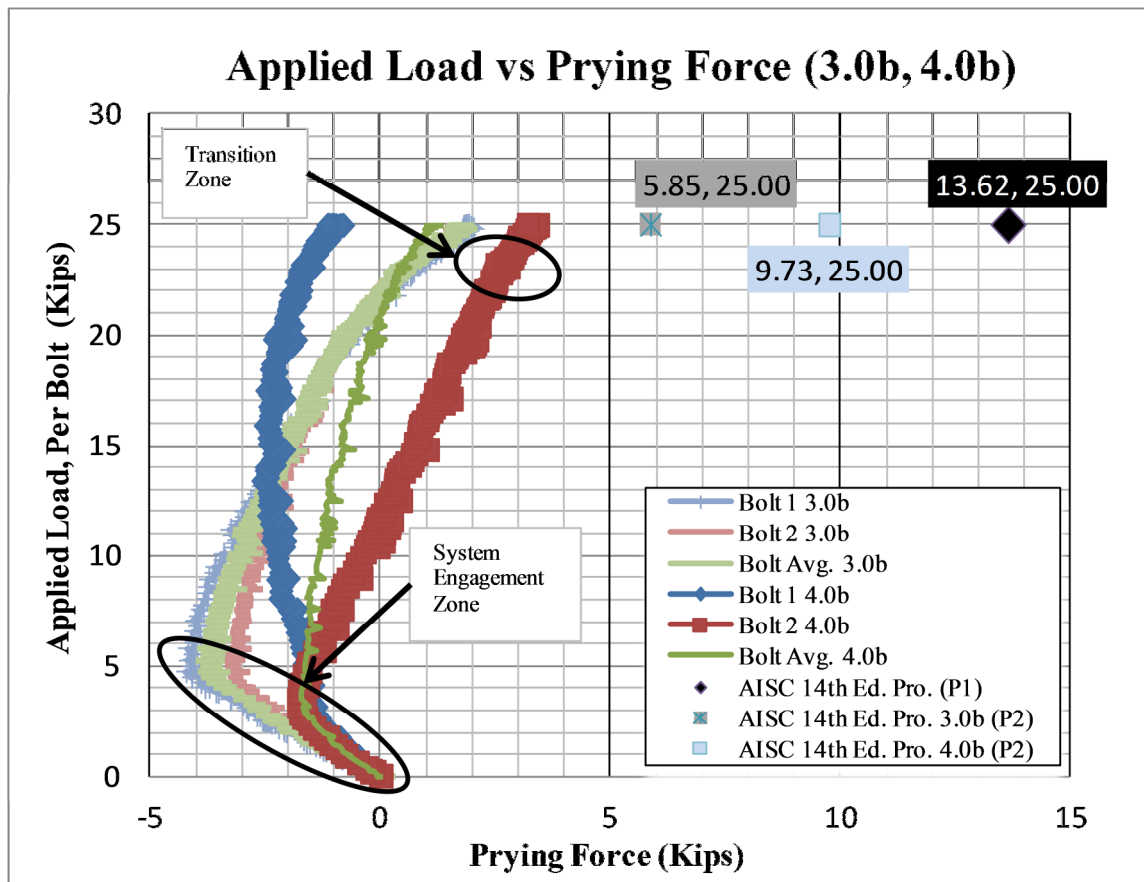
Figure 5.2.4-5: Applied Load versus Prying Force 3.0b, 4.0b.
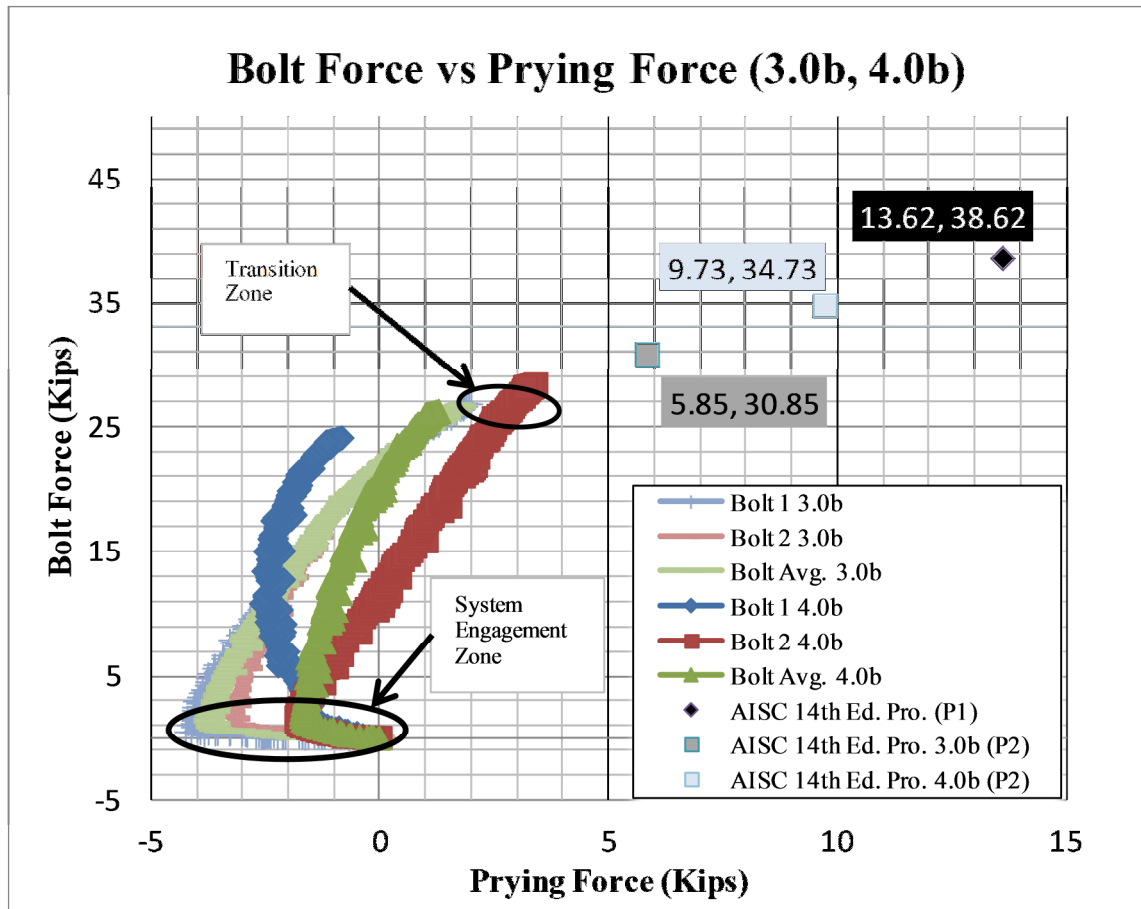
Figure 5.2.4-6: Bolt Force versus Prying Force 3.0b, 4.0b.

When comparing the experimental results to that of the AISC [3] provisions, the experimental values for bolt and prying force were much lower.   The very little prying force is consistent with that of the noticeable stress patterns and minimal flange deformation. The same type of bolt inconsistency between bolts one and two is observed for specimens 3.0b and 4.0b, similar to that of specimen 2.5b.
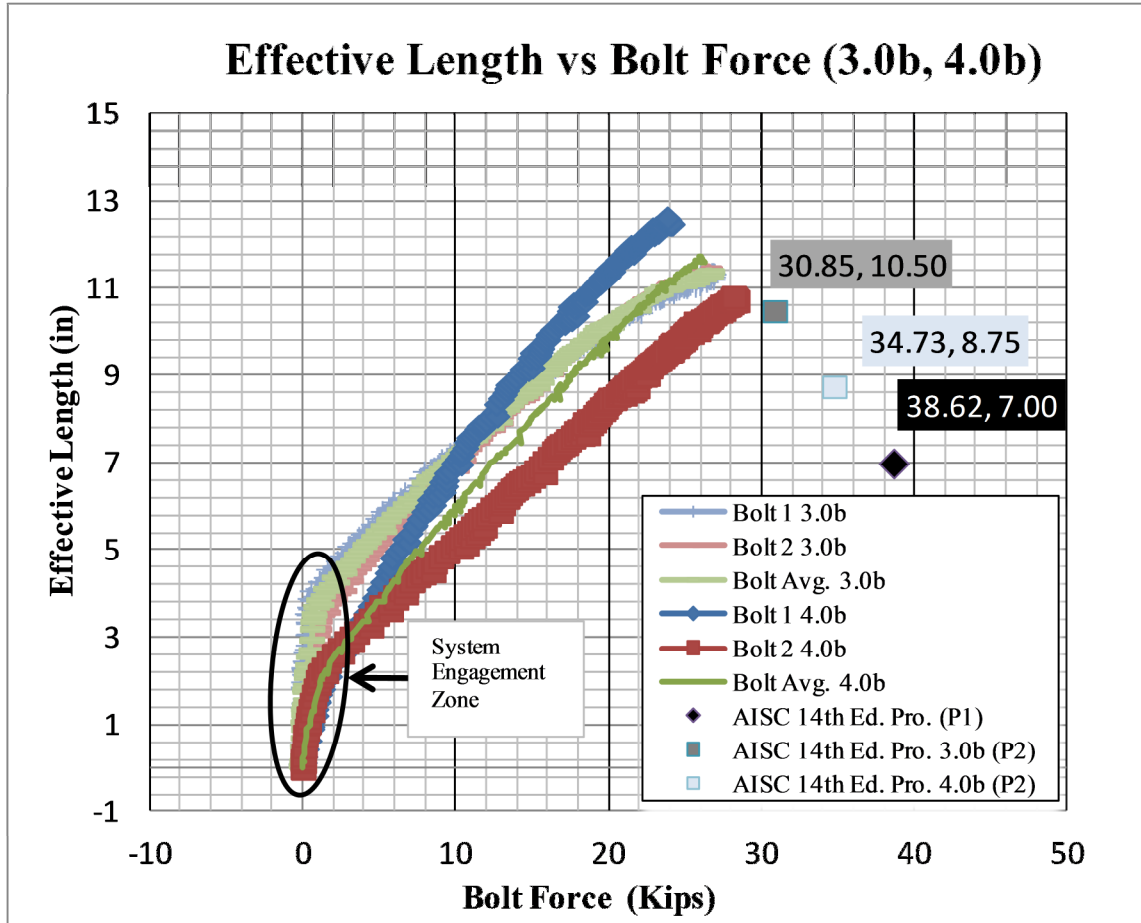
Figure 5.2.4-7: Effective Length versus Bolt Force.

As in all the specimens, the experimental tributary length was determined to be much larger than that of the theoretical, and the resulting bolt and prying force were relatively lower.

The plots of load versus displacement have resulted in scattered data for the stem and flange LVDT, the data seem to be rather irregular. This is likely due to the displacement magnitudes being so small and approaching the limits of the LVDT measurement capabilities.
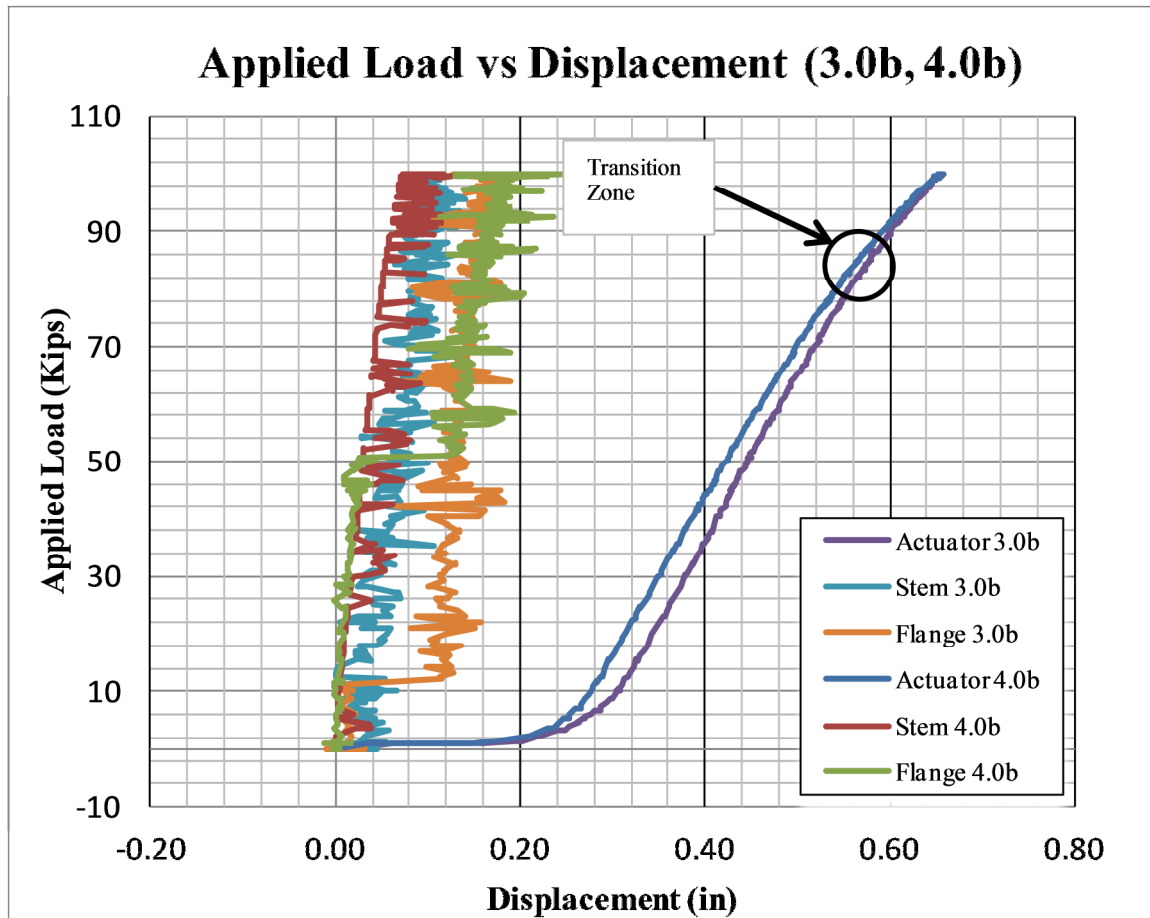
Figure 5.2.4-8: Applied Load versus Deformation.

Tables 5.2.4-1 and 5.2.4-2 show the experimental results summary for specimens 3.0b and 4.0b, respectively. In addition to the results summary, Appendix G shows additional plots for specimen 3.0b and 4.0b individually.

Table 5.2.4-1: Experimental Results Summary Specimen 3.0b.

Experimental Results Summary WT6x32.5_3.0b

Bolt 1			Bolt 2			Displacements		
$\mu\varepsilon_{max}$	2147	µStrain	$\mu\varepsilon_{max}$	2124	µStrain	Actuator$_{max}$	0.655	in
σ_{max}	62.273	ksi	σ_{max}	61.601	ksi	Stem$_{max}$	0.142	in
T_{max}	26.884	kips	T_{max}	26.594	kips	Flange$_{max}$	0.210	in
q_{max}	1.999	kips	q_{max}	1.658	kips			
q_{offset}	4.999	kips	q_{offset}	5.658	kips			
p_{max}	11.381	in	p_{max}	11.504	in			
α_{max}	0.080	Ratio	α_{max}	0.065	Ratio			
PreTension			PreTension			Applied Load		
$\mu\varepsilon_{max}$	389.519	µStrain	$\mu\varepsilon_{max}$	449.598	µStrain	Applied Load$_{max}$	99.95	kips
σ_{max}	11.296	ksi	σ_{max}	13.038	ksi			
T_{max}	4.877	kips	T_{max}	5.629	kips			

Note: q_{offset} is the total change from the engagement zone to the max recorded value. Taken from the Bolt Force vs. Prying Force Graph.

Table 5.2.4-2: Experimental Results Summary Specimen 4.0b.

Experimental Results Summary WT6x32.5_4.0b								
Bolt 1			**Bolt 2**			**Displacements**		
$\mu\varepsilon_{max}$	1929.05	μStrain	$\mu\varepsilon_{max}$	2268.09	μStrain	Actuator$_{max}$	0.658	in
σ_{max}	55.942	ksi	σ_{max}	65.775	ksi	Stem$_{max}$	0.126	in
T_{max}	24.151	kips	T_{max}	28.395	kips	Flange$_{max}$	0.258	in
q_{max}	-0.002	kips	q_{max}	3.408	kips			
q_{offset}	1.498	kips	q_{offset}	4.908	kips			
p_{max}	12.642	in	p_{max}	10.827	in			
α_{max}	-0.030	Ratio	α_{max}	0.143	Ratio			
PreTension			**PreTension**			**Applied Load**		
$\mu\varepsilon_{max}$	387.695	μStrain	$\mu\varepsilon_{max}$	355.769	μStrain	Applied Load$_{max}$	99.95	kips
σ_{max}	11.2432	ksi	σ_{max}	10.3173	ksi			
T_{max}	4.85375	kips	T_{max}	4.45405	kips			

Note: q_{offset} is the total change from the engagement zone to the max recorded value. Taken from the Bolt Force vs. Prying Force Graph.

5.2.5. WT6x32.5 Specimen Comparison

With the experimental analysis and calculations performed on each individual specimen a comparison of the specimens to each other will provide a better illustration of the behavior of prying forces with regards to bolt spacing.

Table 5.2.5-1 shows the maximum experimental bolt force and prying force. The table also shows consideration for the offset of prying force which can be seen on the bolt force versus prying force graphs for each specimen.

Table 5.2.5-1: Experimental Results Summary WT6x32.5.

Experimental Results Summary WT6x32.5					
Specimen	Bolt	Max Bolt Force	Max Prying Force	Prying Force Offset	Prying Force with Offset
1.5b	Bolt 1	39.36	14.37	-3	17.37
	Bolt 2	41.33	16.34	-3	19.34
	Bolt Avg.	40.34	15.36	-3	18.36
2.0b	Bolt 1	31.83	6.85	-2	8.85
	Bolt 2	30.64	5.66	-2.5	8.16
	Bolt Avg.	31.24	6.25	-2.25	8.50
2.5b	Bolt 1	31.98	6.99	-1	7.99
	Bolt 2	28.46	3.48	-2.5	5.98
	Bolt Avg.	30.22	5.23	-1.75	6.98
3.0b	Bolt 1	26.88	2.00	-3	5.00
	Bolt 2	26.59	1.66	-4	5.66
	Bolt Avg.	26.74	1.83	-3.5	5.33
4.0b	Bolt 1	24.15	0.00	-1.5	1.50
	Bolt 2	28.40	3.41	-1.5	4.91
	Bolt Avg.	26.27	1.70	-1.5	3.20

Figures 5.2.5-1, 5.2.5-2, and 5.2.5-3 show the variations of applied load, bolt force, and prying force of the five Specimens. The prying force offset values are values taken from the plots of prying force, bolt force and applied load. If these values are considered, the resulting prying force would be slightly larger than that measured and calculated experimentally.
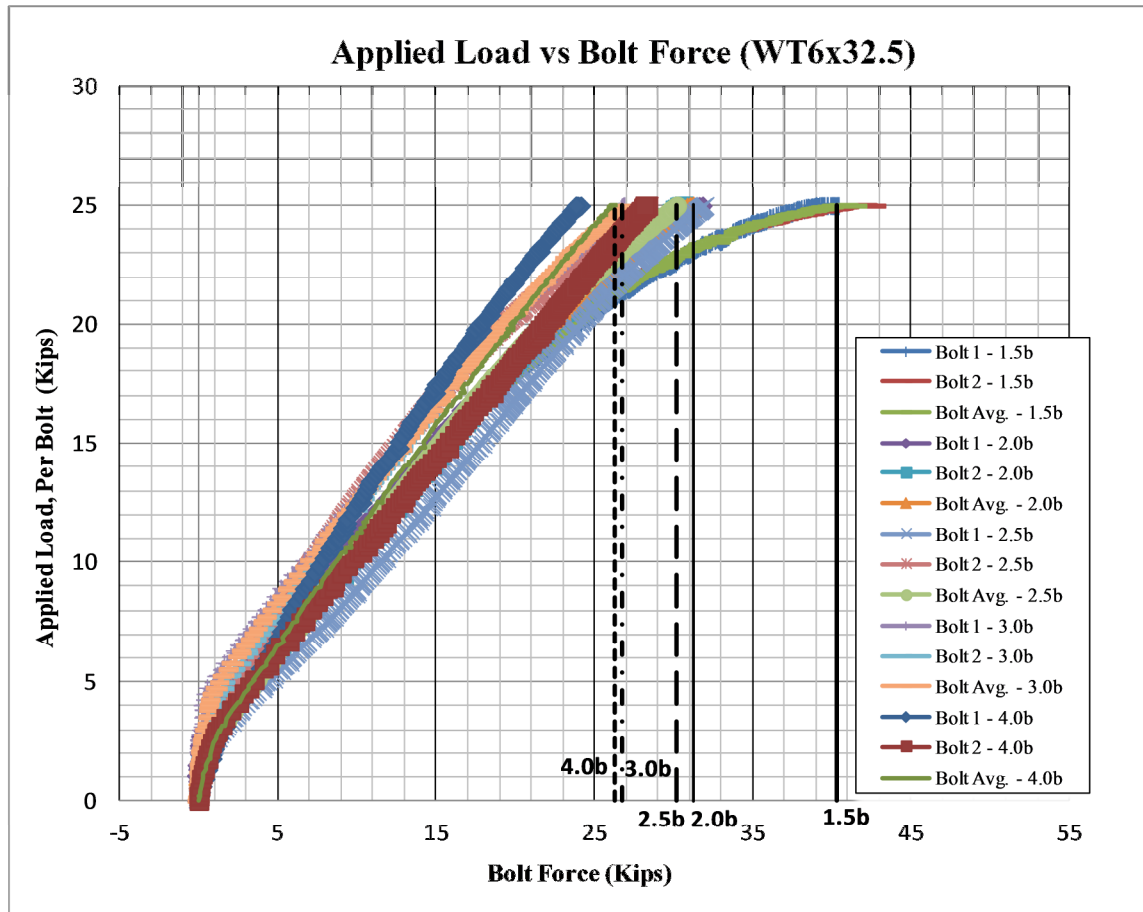
Figure 5.2.5-1: Applied Load versus Bolt Force of All Specimens.

By observing Figure 5.2.5-1, specimen 1.5b experienced a larger amount of prying force.

Specimens 2.0b and 2.5b experienced magnitude of prying, and specimens 3.0b and 4.0b

experienced almost exactly the same amount of prying force. Figure 5.2.5-2 reinforces

this observation.
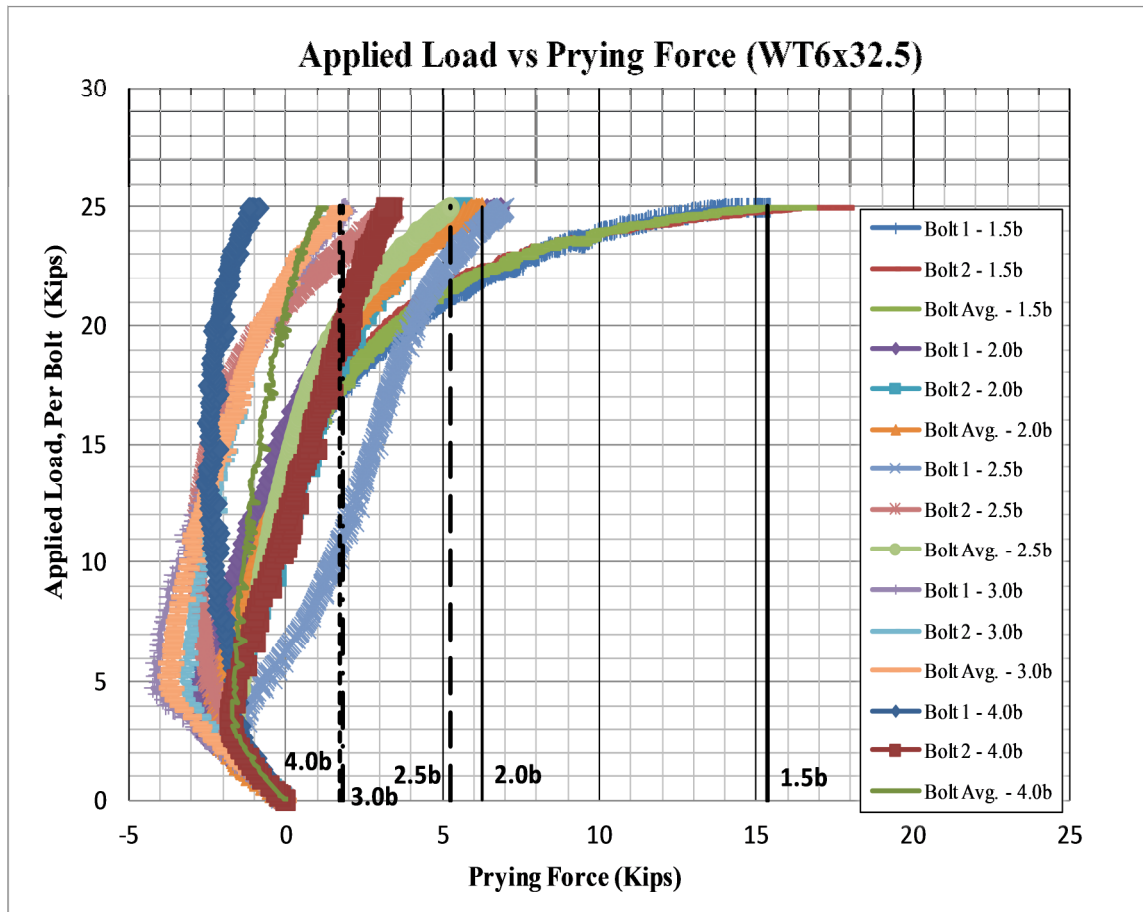
Figure 5.2.5-2: Applied Load versus Prying Force of All Specimens.
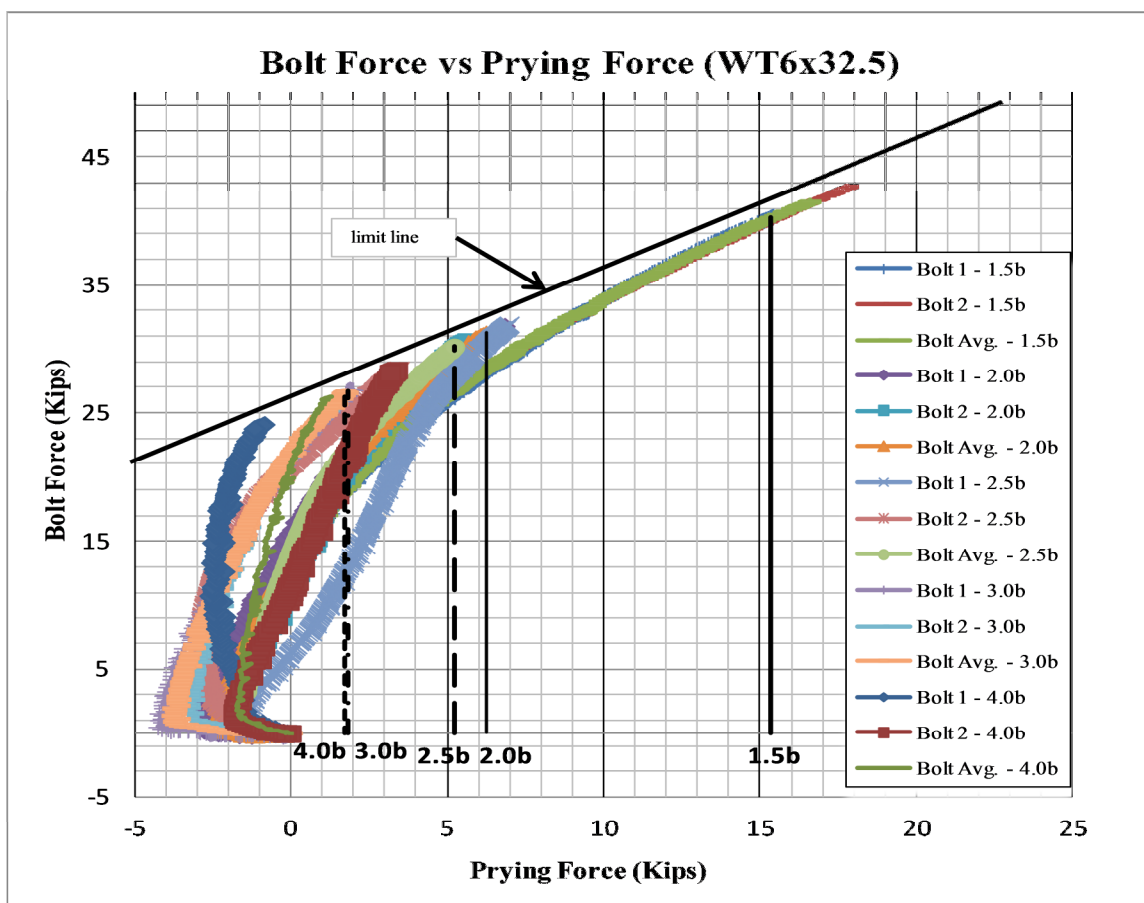
Figure 5.2.5-3: Bolt Force versus Prying Force of All Specimens.

Figure 5.2.5-3 has the best illustration of comparing the five specimens. The figure indicates a consistent drop in prying force as the bolt spacing was increased. The limit of each specimen is illustrated by the "limit line" as shown Figure 5.2.5-3.

Each of the three previous figures shows the average maximum point of prying and bolt force of each specimen. This helps illustrate the amount of force generated within the experiment between each specimen. A common occurrence between the three figures is that specimen 1.5b has a significantly higher magnitude of prying force than that of specimens 2.0b, 2.5b, 3.0b, and 4.0b. Specimens 3.0b and 4.0b have

approximately the same magnitudes of prying force, and specimens 2.0b and 2.5b have nearly identical magnitudes of prying force.

Figures 5.2.5-4 and 5.2.5-5 show plots of specimen 1.5b and 2.0b, respectively, versus the AISC [3] provisions. The comparison of these two specimens is ideal because specimen 1.5b shows some additional interest with the possibility of alpha greater than one, and specimen 2.0b is the bolt spacing at which AISC [3] limits the prying force calculations.
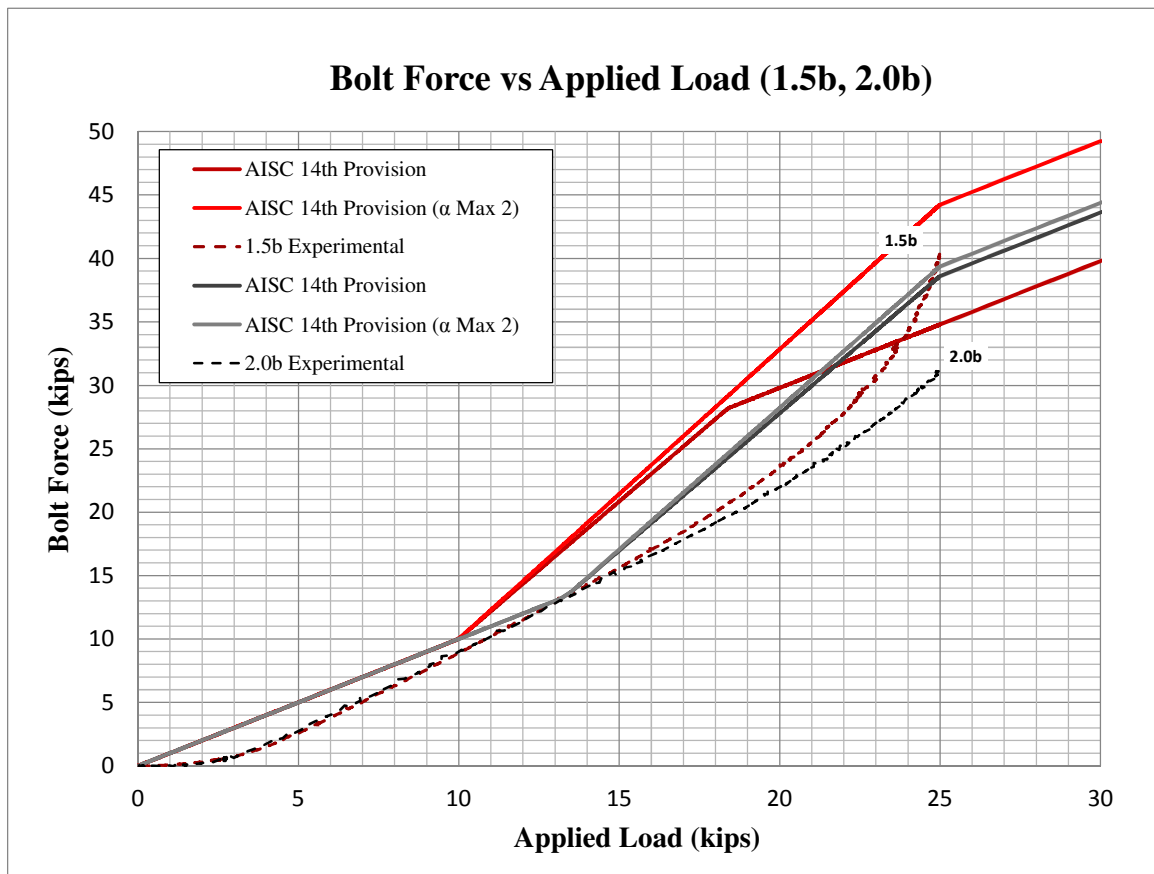
Figure 5.2.5-4: Bolt Force versus Applied Load (1.5, 2.0b) with AISC [3].
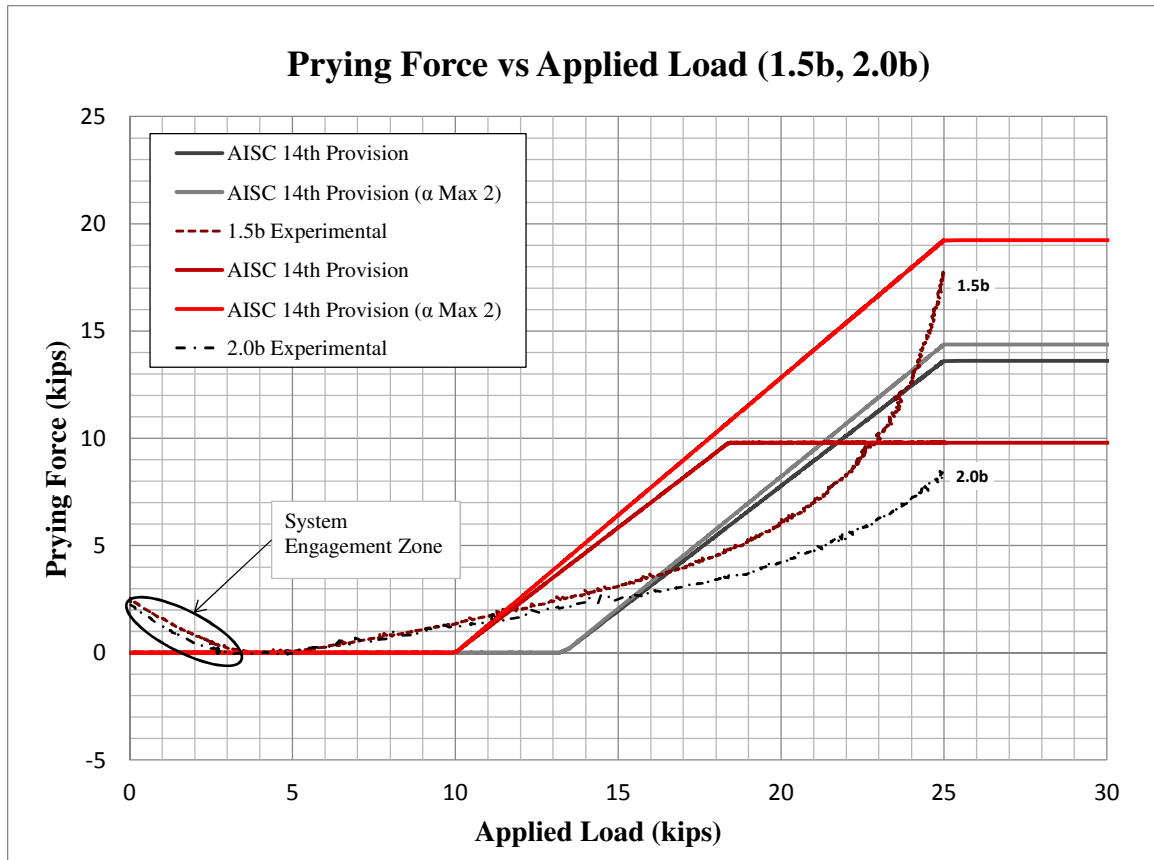
Figure 5.2.5-5: Prying Force versus Applied Load (1.5b, 2.0b) with AISC [3].

There is a noticeable difference between the AISC [3] provisions for specimens 1.5b and 2.0b. The experimental results for specimen 1.5b shows some validity of alpha values greater than one. As for specimen 2.0b, the AISC [3] provisions showed a value of alpha near 1.0 but experimentally the value of alpha experienced was much lower than one.

Figures 5.2.5-6 and 5.2.5-7 show a similar comparison, but with specimens 2.5b, 3.0b and 4.0b. Because the limit for the tributary length is reached, the three specimens can be compared on the same plot.
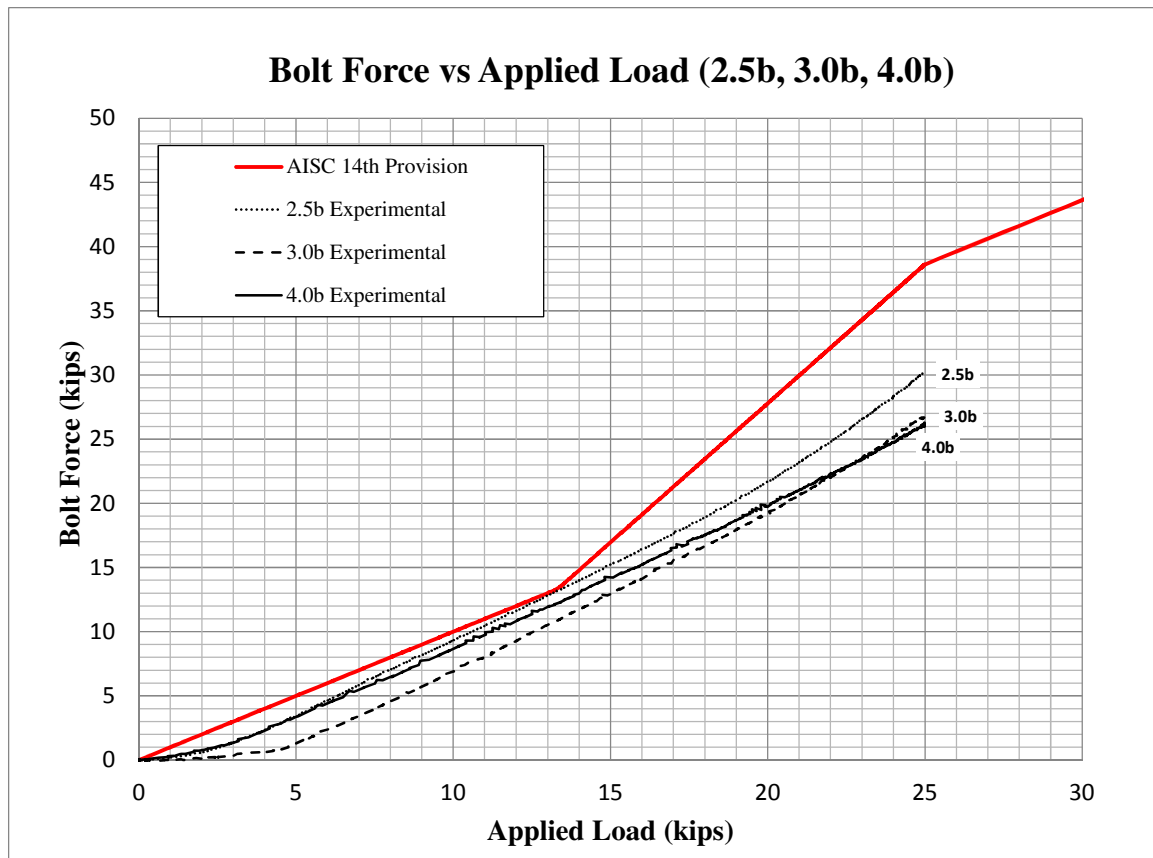
Figure 5.2.5-6: Bolt Force versus Applied Load (2.5b, 3.0b, 4.0b) with AISC [3].

Prying Force vs Applied Load (2.5b, 3.0b, 4.0b)
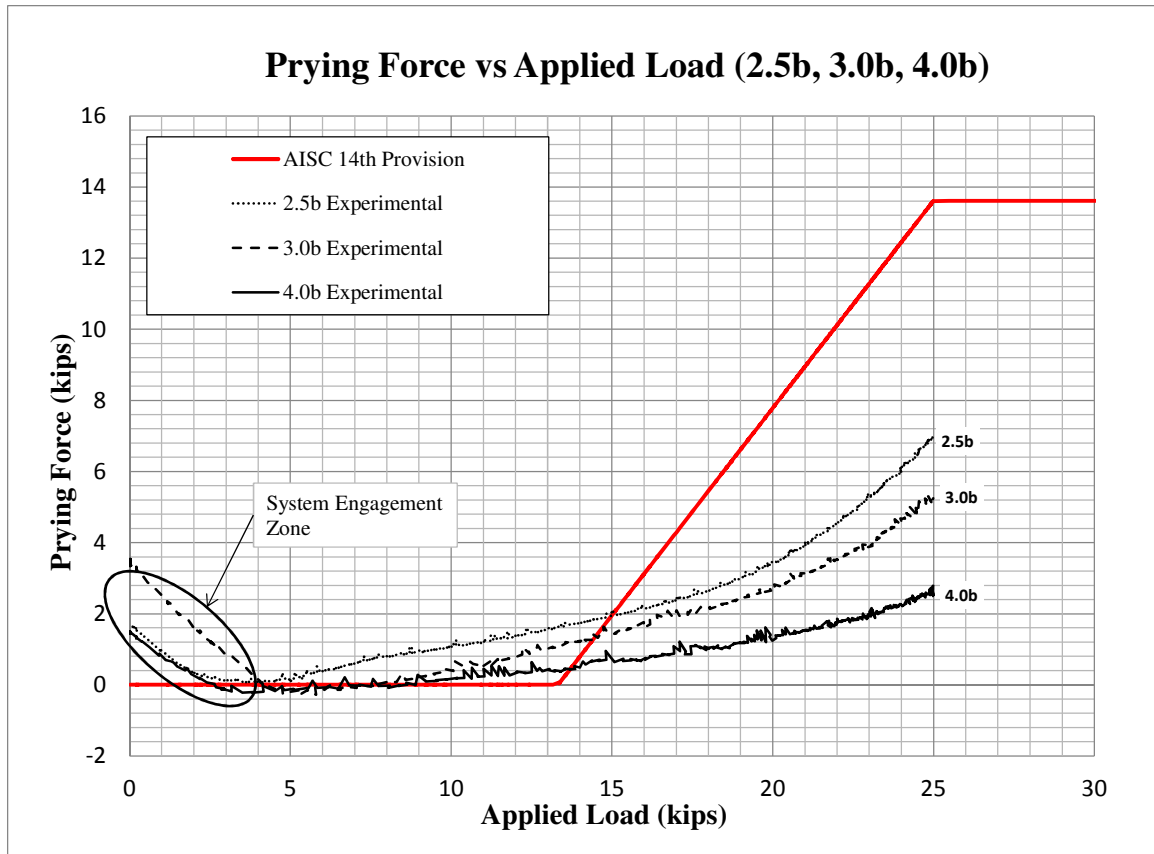
Figure 5.2.5-7: Prying Force versus Applied Load (2.5b, 3.0b, 4.0b) with AISC [3].

From Figure 5.2.5-6, it is apparent that specimen 2.5b experienced slightly more bolt force than specimens 3.0b and 4.0b. Figure 5.2.5-7 shows a slight decline in prying force from specimen 2.5b to 3.0b to 4.0b, but they are relatively close. Even though the range of prying force is approximately 4 kips, the system engagement zone has shown greater effects than that of specimens 1.5b and 2.0b.

5.3. Material Properties Test

A WT shape is formed from ASTM A992 hot rolled steel, which has a minimum yield stress of 50 ksi and minimum ultimate stress of 65 ksi. To accurately determine the

experimental prying forces, a uniaxial tension test generally conforming to ASTM E8-04

[19] was conducted to determine yield and ultimate stress.

One dogbone-shaped Specimen was cut out of a WT6x32.5 web and flange. The

web and flange of the WT6x32.5 was first separated from each other using a band saw.

A computer model of the dogbone-shape specimens was inputted into a computerized

CNC machine which cut out the shape. The two dogbone-shaped specimens are shown

in Figure 5.3-1.

Figure 5.3-1: Dogbone-Shaped Specimens for WT6x32.5.

These two dogbone-shaped specimens were then tested in a Tinius-Olson tension

testing machine. A stress versus strain plot was generated during testing and can be

found in Appendix H. Table 5.3-1 shows the results of the dogbone uniaxial tension tests

compared to the minimum A992 yield and ultimate stress.

Table 5.3-1: Results from Tension Testing ASTM E8-04 for WT6x32.5.

Tensile Test Results of WT6x32.5		
Specimen	Yield Strength (ksi)	Ultimate Strength (ksi)
Flange	53.40	68.98
Web	61.01	71.45
Average	57.20	70.21
Analysis of Tensile Test Results of WT6x32.5		
Specimen	Yield Strength	Ultimate Strength
vs. A992 (Flange)	1.068	1.06
vs. A992 (Web)	1.220	1.10

The results indicated that the WT6x32.5 web had a slightly higher ultimate strength than that of the AISC [3], which uses 65 ksi for ultimate strength for A992 material. Compared to the WT6x32.5 flange, the average ultimate strength was used for the analysis, and the results were using 70.21 ksi in place of AISC's [3] 65 ksi.

To complement the tensile test, an instrumented bolt was also tested. The goal was to determine the validity of the strain gage by measuring strain versus applied load. From that, the modulus of elasticity was determined. Figure 5.3-2 shows the stress versus strain curve and the modulus of elasticity was calculated at approximately 28,800 ksi. Calculations used 29,000 ksi, so the experimental value validates the theoretical value.
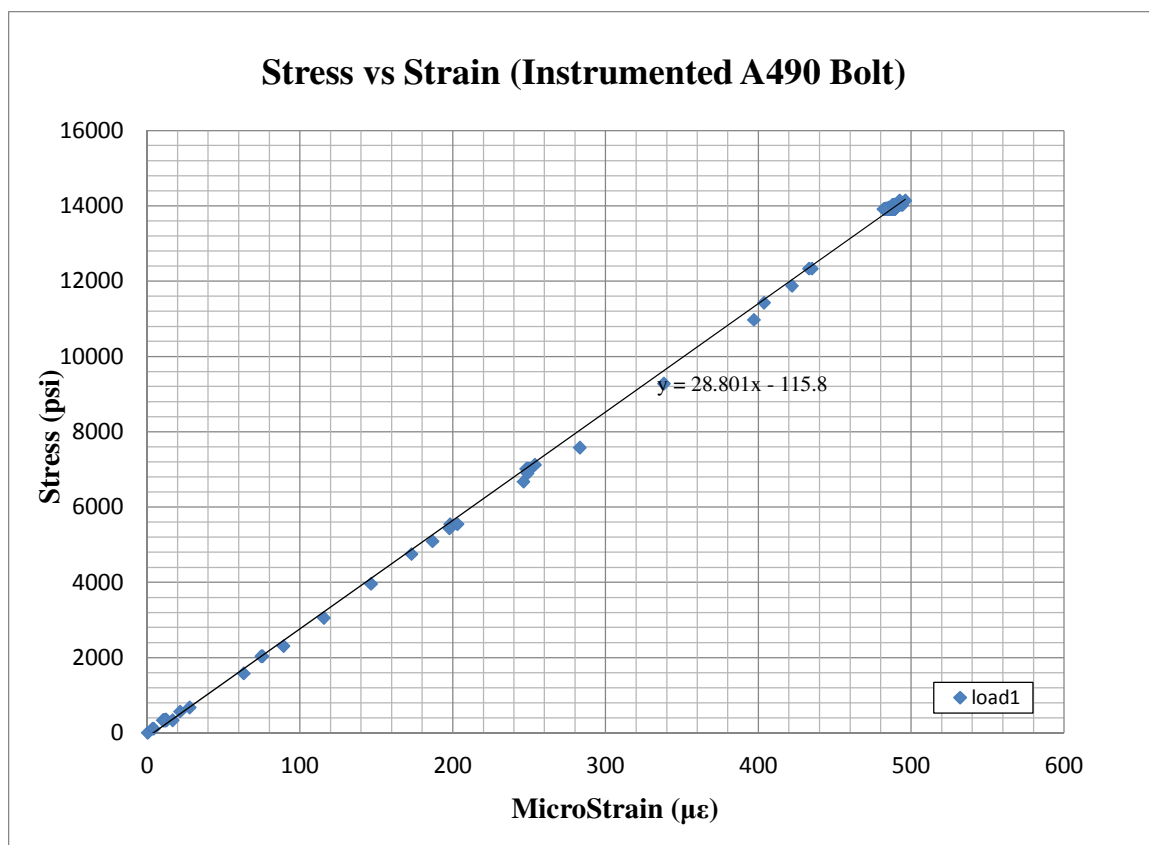
Figure 5.3-2: Stress Strain Plot of Instrumented A490 Bolt.

Chapter 6:   Conclusion and Recommendations

The phenomenon of prying action has been studied for many years. With every new test performed, new information was learned, some of which was incorporated into the AISC design provisions. The objective of this research was to determine the effects of prying forces on selected specimens while varying the bolt spacing along the length of the member. The effects of bolt spacing on the prying force provisions in AISC [3] is not directly included into the prying force calculations, but is used to determine a tributary length. The tributary length is the amount of length of which the flange moment is distributed along and is used to determine prying forces. By comparing the test results of bolt and prying forces of each of the five specimens, recommendations on the effects bolt spacing has on prying forces can be developed. In addition to bolt spacing, a secondary consideration of the variable alpha and its magnitude was considered.

If a large enough prying force is achieved in a connection which than causes flange yielding to occur, the ratio of moment at the bolt line to that of the web face should be analyzed. The ratio is limited between zero and one and is noted as alpha (α). Because using the actual value for alpha would result in a larger prying force than that of limiting alpha to 1.0, determining the value for alpha experimentally was also considered.

6.1. Prying Force Comparison

After all the experimental data were collected and analyzed for specimens 1.5b, 2.0b, 2.5b, 3.0b, and 4.0, the data were then compared to that of the AISC [3] provisions. The following conclusions were determined based on the findings.

Specimen 1.5b experienced bolt forces of 39.174 kips and 41.328 kips, respectively, and when compared to that of the AISC [3] provision bolt force, which was 34.85 kips, the experimental forces were reasonably larger. The complementary prying forces for specimen 1.5b was 14.37 kips and 16.34 kips experimentally and 9.85 kips according to AISC [3]. As noted in Table 5.2.1-1, when the prying force offset was considered, the experimental prying forces were 17.373 kips and 19.340 kips for bolts 1 and 2, respectively. By comparison, the experimental values for prying force are larger than that of AISC [3]. When the actual value for alpha was used to calculate the prying forces per AISC [3], the values for bolt and prying forces are 42.50 kips and 17.5 kips respectively. The average experimental values for bolt and prying force offset was 43.34 kips and 18.36 kips, respectively, which was similar to that of AISC [3] when using the actual calculated alpha value.

Based on the findings it was reasonable to state that specimen 1.5b experienced a value for alpha greater than one. Based on the experimental analysis, a value for alpha of 1.121 and 1.506 for bolts 1 and 2, respectively, as shown in Table 5.2.1-1, resulted. When analyzing Figure 5.2.1-7, the transition zone indicated the point of yielding but it also indicated the point of plastic hinging beginning to occur. The sudden drop in effective length due to hinging correlated with the value of alpha increasing above 1.0. Thus, it is reasonable to say that limiting the value of alpha to 1.0 is somewhat conservative and due to the effects of flange yielding, which could result in flange plastic hinging, the actual value of alpha should be considered for determining the actual bolt and prying forces.

Specimen 2.0b had a bolt spacing which matched the maximum allowable tributary length from AISC [3]. When comparing the bolt and prying forces to that of AISC [3] provisions, the average experimental forces were 31.24 kips and 6.25 kips, respectively, with a prying force offset of 8.50 kips. When using AISC [3] provisions, a bolt and prying force of 38.62 kips and 13.62 kips, respectively, was determined, which resulted in a difference in bolt force of approximately 7.4 kips. The difference between the experimental and AISC [3] values were approximately 7.4 kips or 5.1 kips with prying force offset. Specimen 2.0b still experienced flange yielding but the amount of yielding was not enough to create plastic hinging within the flange. Therefore, alpha was not a factor in the experimental values for prying force. When comparing alpha from AISC [3], a value of 0.91 resulted; therefore, the limit of 1.0 did not play a role, which correlated with the experimental data. Since the experimental effective length was much larger than that of the AISC [3] provision, a lower prying force had resulted. Based on that comparison, it was reasonable to state that AISC [3] provisions were somewhat conservative to that of the experimental data.

Specimens 2.5b, 3.0b, and 4.0b were specimens which had bolt spacing larger than that of the AISC [3] provision limitations. Essentially, determining the prying force using AISC [3] provisions for specimens 2.0b, 2.5b, 3.0b, and 4.0b all resulted in the same values. Clearly the experimental data did not correlate with AISC [3]. From Figure 5.2.6-1, a noticeable drop in bolt force had occurred from Specimen 1.5b to 4.0b. Specimen 3.0b and 4.0b seemed to have experienced approximately the same amount of bolt force. The same observation was seen in Figures 5.2.6-2 and 5.2.6-3. There was a large difference between specimens 1.5b and 2.0b, as well as a smaller gap between

specimens 2.5b and 3.0b with regards to bolt and prying forces. Figure 5.2.6-3 showed a limit line for illustration purposes only, but illustrates a boundary which the bolt forces never surpassed during the testing. A fourth order polynomial was determined from a trend line of Figure 5.2.6-3. As with the bolt force, Figure 5.2.6-2 showed a noticeable drop in prying force between specimens 1.5b to 4.0b.

6.2. Conclusions

Based on the results presented, one can conclude that prying forces drop as the bolt spacing increases. There was also a noticeable flange deformation along each specimen's cross-section. From experimental observations and the flange LVDT, the orthogonal deformation was rather small, virtually unnoticeable, which resulted in no orthogonal prying forces. The plots of all specimens clearly indicated a drop in prying force as the bolt spacing was increased. The reason for the drop in prying forces is from the increased effective length of which the specimens experienced.

Based on the results presented for specimens with bolt spacing less than that of the AISC [3] limitations the actual value for alpha should be considered since it compares better with the experimental results. For specimens beyond the AISC [3] limitations, an increase of tributary length should be considered since the experimental results show a much larger tributary length than that of AISC [3].

6.3. Experimental and Data Accuracy

Even though the experimental data show promising results, like most experiments, errors could exist within the experimental setup, procedure, and/or analysis. The first cause of error could be from the actual instrumented bolts. Even though a bolt

was tested to confirm the Modulus of Elasticity of 29,000 ksi, there was no guarantee that all the bolts had a Modulus of Elasticity of 29,000 ksi. In order to eliminate that possible error, bolt testing of each instrumented bolt could have been done to determine the Modulus of Elasticity for each individual bolt and use their corresponding Modulus of Elasticity when determining the experimental bolt stresses. However, even with a variance of the Modulus of Elasticity of the individual bolts, the resulting bolt and prying forces would have minimal change. This is not expected to be a significant source of error.

When observing some of the plotted bolt and prying forces, such as in Figure 5.4.2-6, one bolt seemed to show a curve in the plot while the other had a fairly linear plot. An explanation for that is as the applied load was increased on the system there was some eccentricity being generated on the bolts causing the slight variance in the bolt and prying forces. The setup was centered as accurately as possible before initiating testing in order to minimize the effect of any eccentricity.

The system engagement zone indicated on the experimental plots may not necessarily be a source of error, but understanding what was happening within the engagement zone should be considered. Specifically, the prying force graphs showed a negative trend as the applied load was increased to about ten to fifteen kips. From that point the plots showed a linear increase of prying force. The reason for the negative trend was from the testing frame engaging as well as the pre-tensioning in the bolts. To better understand the effects of the engagement zone the experimental data should have been collected from pre-tensioning through the final applied load, without zeroing the strain gages.

6.4. Future Research

The results presented show validity but additional testing should be considered. To complement the experimental data, additional specimens should be tested. It would be of good comparison to use the same WT shape, WT6x32.5, and test a larger variety of bolt spacing. Test specimens for recommendation could be of three or four specimens between 1.5b and 2.0b, as well as adding some intermediate bolt spacing between the remaining specimens tested. In addition to the bolt spacing additions, the total applied load should be increased. The recommendation there would be to determine an applied load of which will bring the connecting bolts and/or WT shape near their failure point. One reason for doing so would be to ensure flange yielding among all testing specimens. The flange yielding would be complimented by increased prying forces which could result in a better comparison of bolt and prying forces between the specimens. In addition to the bolt spacing effects, ensuring flange yielding would help better understand the effects of alpha between various specimens and not limited to one specimen. It would be important to yield a specimen because the inelastic range is the most difficult range to test and understand, but given robustness and/or inelastic behavior in building connection design, it would be the most beneficial. If the data concluded promising results, then the experiment could be extended to multiple WT shapes, using the same bolt spacing.

Another consideration would be to use the same bolt spacing and WT shapes, but have the variable be the hole distance from flange edge, and repeat all other experimental protocols. With a total comparison of data for a specific WT shape with varying bolt spacing and location, a complete understanding of the prying effects could result.

References

[1]   Kulak, G. L., Fisher, J. W., and Struik, J. H. A. 1987. *Guide to Design Criteria for Bolted and Riveted Joint*s. John Wiley & Sons, Inc.

[2]   Nair, R.S., Birkemoe, P.C., Munse, W.H. 1969. "Behavior of Bolts in Tee-Connections Subject to Prying Action." *Department of Civil Engineering.* Structural Research Series No. 353. Technical Report. [Internet, WWW, PDF], *Available*: Available from; Address: http://www.ideals.illinois.edu/bitstream/handle/2142/14290/SRS-353.pdf. [Accessed; 09 September 2011].

[3]   AISC. 2011. *Steel Construction Manual.* 14th ed. Chicago, IL: American Institute of Steel Construction.

[4]   Thornton, W. A. 1985. "Prying Action - A General Treatment," *Engineering Journal*: *American Institute of Steel Construction* Volume 22 (2), pp. 67-76.

[5]   Swanson, James A. 2002. "Ultimate Strength Prying Models for Bolted T-stub Connections." *Engineering Journal: American Institute of Steel Construction* Volume 39 (3), pp.136-147.

[6]   Swanson, J.A., Gao, X. 2000. "Strength Determination of Heavy Clip-Angle Connection Components" *University of Cincinnati Department of Civil & Environmental Engineering*. Fourth International Workshop. Roanoke, VA., pp. 234-243.

[7]   Swanson, J. A. and Leon, R. T. 2001. "Stiffness Modeling of Bolted T-stub Connection Components," *Journal of Structural Engineering: American Society of Civil Engineers.* Volume 127 (5), pp. 498-505.

[8]   Zoetmeijer, P. 1974. "A Design Method for the Tension Side of Statically Loaded, Bolted Beam-to-Column Connections," *Heron,* Volume 20 (1), pp.1-59.

[9]   Nair, R.S., Birkemoe, P.C., Munse, W.H. 1974. "High Strength Bolts Subject to Tension and Prying." *Journal of Structural Engineering: American Society of Civil Engineers* Volume 100 (2), pp. 351-372.

[10]   Dowswell, B. 2011. "A Yield Line Component Method for Bolted Flange Connections," *Engineering Journal, American Institute of Steel Construction* Volume 48 (2), pp. 93-116.

[11]   Wheeler, A.T., Clarke, M.J., Hancock, G.J. Murray, T.M. 1998. "Design Model for Bolted Moment End Plate Connections Joining Rectangular Hollow Sections." *Journal of Structural Engineering: American Society of Civil Engineers.* Volume 124 (2), pp. 164-173.

[12]   Willibald, S., Packer, J.A., Puthli, R.S. 2002. "Experimental Study of Bolted HSS Flange-Plate Connections in Axial Tension." *Journal of Structural Engineering: American Society of Civil Engineers* Volume 128 (3), pp. 328-336.

[13]   Douty, R. T. and McGuire, W. April 1965. "High Strength Bolted Moment Connections," *Journal of the Structural Division, ASCE*, Vol. 91, ST2, pp.101-128.

[14]   Swanson, J. A., Leon, R. T. 2000. "Bolted Steel Connections: Tests on T-stub Components," *Journal of Structural Engineering: American Society of Civil Engineers*. Volume 126 (1), pp. 50-56.

[15]   *High Strength Bolts: A Primer for Structural Engineers*. 2002. Chicago, IL: American Institute of Steel Construction.

[16]   Thornton, W.A., Kane, T. 1999. "Design of Connections for Axial Moment and Shear Forces," Ch. 2, *Handbook of Structural Steel Construction Design and Details,* Tamboli, A.R. Ed., McGraw-Hill, New York.

[17]   *Steel Construction Manual.* 13th ed. 2005. Chicago, IL: American Institute of Steel Construction.

[18]   Thornton, W. A. 1992. "Strength and Serviceability of Hanger Connections" *Engineering Journal: American Institute of Steel Construction* Volume 29 (4), pp. 145-149.

[19]   ASTM International. ASTM Committee E28 on Mechanical Testing. Subcommittee E28.04 on Uniaxial Testing. 1 April 2004. *Standard Test Methods for Tension Testing of Metallic Materials*. Designation E8-04. In annual Book of ASTM Standards. Volume 01.02. West Conshohocken, PA: ASTM International.

Bibliography

Chasten C.P., Lu, L., Driscoll, G. C. 1992. "Prying and Shear in End-Plate Connection Design." *Journal of Structural Engineering: American Society of Civil Engineers.* Volume 118 (5). pp. 1295-1311.

Coelho, A.M.G. Da Silva, L.S., Bijaard, F.S.K. 2006. "Finite-Element Modeling of the Nonlinear Behavior of Bolted T-Stub Connections." *Journal of Structural Engineering: American Society of Civil Engineers.* Volume 132 (6). pp. 918-928.

Estrada, H., Huang, J.L. 2006. "Rational Analysis of Prying Action in Tension Bolted Connections;" *The Architectural Engineering Institute of the American Society of Civil Engineers.* pp.1-6.

Kumalasari, C., Ding, Y., Madugula, M. 2006. "Prying Action in Bolted Steel Circular Flange Connections." *Canadian Journal of Civil Engineers* Volume 33 (4). pp. 497-500.

Appendix A: Connection Calculations

The following information shows the connection limit states and how the Specimen shape was determined. Figure A-1 shows the connection of which was being checked.
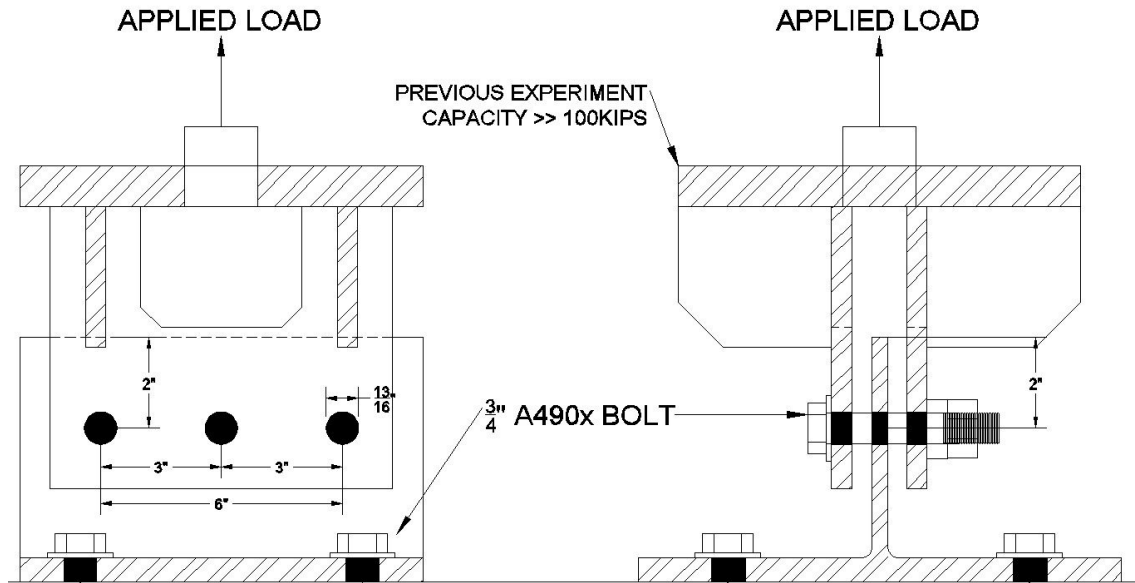
Figure A–1: Schematic Design of Connection.

The following six limit states were checked using AISC[1] provisions and are as follows:

1. *WT shape web yielding (Conservative Using 6", Assume ɸ = 1.0 for Experiment)*

$$\phi Rn \leq \phi AgFy \quad => \quad Ag = \frac{Pu}{\phi Fy}$$

$$t * 6" = \frac{100 kips}{1.0 * 50 ksi} \quad => \quad t = \mathbf{0.33"}$$

---

[1] AISC. 2011. *Steel Construction Manual.* 14th ed. Chicago, IL: American Institute of Steel Construction.

2. *WT shape web fracture (Assume ɸ = 1.0 for Experiment)*

$$\phi Rn \leq \phi AeFu \quad => \quad Ae = \frac{Pu}{\phi Fu}$$

$$t * 6" = \frac{100kips}{1.0 * 65ksi} \quad => \quad \boldsymbol{t = 0.256"}$$

3. *Connecting bolt double shear failure (Assume ɸ = 1.0 for Experiment)*

(3) A490x Bolt

$$\phi Rn \ (1) = \phi FnvAg$$

$$\phi Rn \ (3) = 113.9\text{ksi} * 0.442in^2 * 3 = 151.03kips$$

4. *Block shear within the WT shape web (Assume ɸ = 1.0 for Experiment)*

$$\phi Rn = 0.6 FuAnv + UbsFuAnt \ \leq 0.6 FyAgv + UbsFuAnt$$

$$Anv = \left(2" - \frac{0.75in}{2}\right) * 2t = 3.25t$$

$$Ant = \ (6" - \ 2 * 0.75in) * t = 4.5t$$

$$Agv = 4t$$

$$\phi Rn = 0.6 * 65ksi * 3.25t + 1 * 65ksi * 4.5t \ \leq 0.6 * 50ksi * 4t + 1 * 65ksi * 4.5t$$

$$100kips = 419.25t \leq 412.5t$$

$$t = \boldsymbol{0.318"}, 0.323"$$

5. *Bearing of bolts within WT shape web (Assume* ɸ *= 1.0 for Experiment)*

$$\phi Rn = 1.2 L_c t F_u \leq 2.4 dt F_u$$

$$100 kips = 3 * (1.2 * 2" * t * 65 ksi \leq 2.4 * 0.75 in * t * 65 ksi)$$

$$\frac{100 kips}{3} = 156t \leq 117t$$

$$t = \mathbf{0.285}", 0.38"$$

6. *Bolt WT shape flange-to-base plate Tensile Strength (Assume* ɸ *= 1.0 for*

   Experiment)

$$\phi Rn \leq \phi F_{nt} A_g \quad => \quad 0.75 * 85.7 ksi * 0.437" = 37.4 kips$$

$$Rn\ (1) = \frac{37.4 kips}{0.75} = 49.9 kips$$

Minimum Web Thickness t = 0.33"

Appendix B: Prying Force Calculations

Prying force calculations were performed using AISC[2] provisions and the following shows the step-by-step process of which was used. The WT6x32.5 and A490x bolt material properties, strengths, etc., were also obtained from AISC[3].

WT6x32.5 Properties/Strengths/Bolt Locations:

t_f = 0.605in t_w = 0.390in

Fu = 65ksi   Fy = 50ksi

b = 3.50in   a = 2.31in   b' = 3.13in   a' = 2.68in   db = 0.75

d' = 0.75in + 0.0625in = 0.8125in   g = 7.5in

Testing Parameters

T = 25kips

A490x Bolt Properties/Strengths:

Fu = 113ksi   Ru = FuAg = Fu(Ag – Drilled Hole)

$$Ru = B = 113\text{ksi}\left(\frac{\pi 0.75^{"2}}{4} - \frac{\pi 0.0781^{"2}}{4}\right) = 49.38\text{kips}$$

Prying Force Checks AISC 14th Ed.

Prying Action Calculations for WT6x32.5 @ Bolt Spacing of 1.5b:

Tributary Length for Specimens 1.5b

---

[2] AISC. 2011.
[3] AISC. 2011.

$p = \max 2b,$ but $\leq s, = \max(2.0 * 3.5\text{in}, 3.5\text{in} \leq 5.25\text{in}) = 5.25\text{in}$

$$t_{min} = \sqrt{\frac{4Tb'}{\phi p F_u}} = \sqrt{\frac{4 * 25\text{kips} * 3.13\text{in}}{1.0 * 5.25\text{in} * 65\text{ksi}}} = 0.957\text{in}$$

$$T \leq \frac{\phi F_u t^2 p}{2b} = \frac{1.0 * 65ksi * (0.605in)^2 * 5.25in}{2 * 3.5in} = 17.84\text{kips}$$

$$\delta = 1 - \frac{d'}{p} = 1 - \frac{0.8125in}{5.25in} = 0.845$$

$$\rho = \frac{b'}{a'} = \frac{3.13\text{in}}{2.68\text{in}} = 1.17$$

$$\beta = \frac{1}{\rho}\left(\frac{B}{T} - 1\right) = \frac{1}{1.17}\left(\frac{49.38\text{kips}}{25\text{kips}} - 1\right) = 0.82$$

$\alpha' = 1.0$ if $\beta \geq 1 =$ the lesser of 1 and $\frac{1}{\delta}\left(\frac{\beta}{1-\beta}\right)$ if $\beta < 1$

$$\alpha' = \min\left(1.0, \frac{1}{\delta}\left(\frac{\beta}{1-\beta}\right)\right) = \min\left(1.0, \frac{1}{0.845}\left(\frac{0.84}{1-0.84}\right)\right) = \min(1.0, 6.23)$$

$$\alpha' = 1.0$$

$$t_{min} = \sqrt{\frac{4Tb'}{\phi p F_u(1 + \delta\alpha')}} = \sqrt{\frac{4 * 25\text{kips} * 3.13\text{in}}{\phi * 5.25\text{in} * 65\text{ksi} * (1 + 0.845 * 1.0)}} = 0.704\text{in}$$

$$a' = \left(a + \frac{d_b}{2}\right) \leq \left(1.25b + \frac{d_b}{2}\right) = \left(2.31\text{in} + \frac{0.75\text{in}}{2}\right) \leq \left(1.25 * 3.50\text{in} + \frac{0.75\text{in}}{2}\right) =$$

$$a' = (2.68\text{in}, 4.75\text{in}) = 2.68\text{in}$$

$$t_C = \sqrt{\frac{4Bb'}{\phi p F_u}} = \sqrt{\frac{4 * 49.38\text{kips} * 3.13\text{in}}{\phi * 5.25\text{in} * 65\text{ksi}}} = 1.345\text{in}$$

$$\alpha = \frac{1}{\delta}\left[\frac{T}{B}\left(\frac{t_c}{t}\right)^2 - 1\right] \quad \text{where } 0 \le \alpha \le 1$$

$$\alpha = \frac{1}{0.845}\left[\frac{25\text{kips}}{49.38\text{kps}}\left(\frac{1.345\text{in}}{0.605\text{in}}\right)^2 - 1\right] = 1.778$$

$0 \le 1.778 \le 1$, therefore α = 1.0

$$q = B\left[\delta\alpha\rho\left(\frac{t}{t_c}\right)^2\right] = 49.38\text{kips} * \left[0.845 * 1.0 * 1.166 * \left(\frac{0.605\text{in}}{1.345\text{in}}\right)^2\right] = 9.844\text{kips}$$

Prying Force in Bolt, q = 13.02kips

Total Bolt Force T_{actual} = 25kips + 9.844kips = **34.844kips** $\le$ **49.38kips Bolt**

OK!!

Alternatively, determine available bolt force.

$$\alpha' = \frac{1}{\delta(1+\rho)}\left[\left(\frac{t_c}{t}\right)^2 - 1\right] = \frac{1}{0.845 * (1 + 1.166)}\left[\left(\frac{1.345\text{in}}{0.605\text{in}}\right)^2 - 1\right] = 2.154$$

$Q = 1$ when $\alpha' < 0$,

$Q = \left(\frac{t}{t_c}\right)^2 (1 + \delta\alpha')$ when $0 \le \alpha' \le 1$,
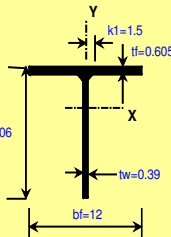
$Q = \left(\frac{t}{t_c}\right)^2 (1 + \delta)$ when $\alpha' > 1$ => $Q = \left(\frac{0.605\text{in}}{1.345\text{in}}\right)^2 (1 + 0.845) = 0.373$

$T_{available} = BQ = 49.38\text{kips} * 0.373 = $ **18.44kips**

Figure B-1 shows a screen shot of the spreadsheet that was developed to confirm the AISC[4] provisions calculations.

AISC Beam Properties

WT Shapes

(diagram: Y axis, k1=1.5, tf=0.605, d=6.06, tw=0.39, bf=12, X axis)

WT6X32.5		
A =	9.54	in.^2
d =	6.060	in.
tw =	0.390	in.
bf =	12.000	in.
tf =	0.605	in.
k =	1.2000	in.
k1 =	1.5000	in.
Ix =	20.60	in.^4
Sx =	4.06	in.^3
rx =	1.470	in.
Iy =	87.20	in.^4
Sy =	14.50	in.^3
ry =	3.020	in.
Zx =	7.50	in.^3
Zy =	22.00	in.^3
J =	1.09	in.^4
Cw =	2.97	in.^6
a =	2.66	in.
Wno =	0.00	in.^2
Sw =	0.00	in.^4
Qf =	0.00	in.^3
Qw =	0.00	in.^3

Checks	SYM.	Explanation	Units		
		First Anaylsis were prying action does not apply based on thickness			
	Fu	65.00	ksi	Tensile Strength	
	Fy	50.00	ksi	Yield Strength	
	T	25.00	kips	Required strength, rut or rat per bolt	
75in,	B	49.38	kips	Availible Tension per Bolt (φrn so say no SF, same as T)	
OK	b	3.50	in	Distance Edge Web to Center Bolt	
	b'	3.13	in	Fig 9-4	
	a	2.31	in	Distance Center Bolt to edge of flange	
	a'	2.680	in	Fig 9-4	
	db	0.75	in	Bolt Diameter	
		0.0625	in	Bolt Hole Tolarence 1/16 or 1/8	
	pe	11.07	in	Zoetemeijer (1974) Equivalent Length	
	pe	10.43	in	Thornton and Kane	
	p	5.25	in	2b (max) ≤ s	
	s	5.25	in	Bolt Spacing	
	g	7.50	in	Gauge Distance	
	tmin	**0.957**	in	Minimum Flange thickness to Neglect prying action forces	AISC 9-20b
OK	tw	0.390	in	Web Thickness	
		Second Anaylsis of Prying Action with Prying force applied			
	tf	0.605	in	Thickness of the Flange	
	T	17.84	kips	Tensile Force with preliminary thickness chosen (T max)	AISC 9-22b
Flange Thickness Not Adequ	tmin	**0.704**	in	Acceptable Fitting Strength and Stiffness and Bolt Strength	AISC 9-23b
	δ	0.845			AISC 9-24
OK	α'	1.000			
	α	1.000000	actual	Check 0 ≤ α ≤ 1; Possibly OK if States Connection not Adequate	AISC 9-29
	a'	2.68			AISC 9-27
	β	0.84			AISC 9-25
	ρ	1.166			AISC 9-26
	d'	0.813	in	Hole Width along length of fitting (Bolt Hole in Flange)	
OK	q	**9.848**	kips	Prying force per bolt	AISC 9-28
	tc	**1.345**	in	Minimum Thickiness to prevent prying action	AISC 9-30b
		Avaiable Tensile Strength per Bolt with Prying Action			
	α'	2.153			AISC 9-35
	Q	0.373			AISC 9-32,33,34
OK	Tactual	**34.848**	kips	Actual Bolt Tensile Load	AISC 9-31
Prying Action Occurs	Tavail	18.44	kips	Q*B	

Figure B-1: Prying Calculation Spreadsheet 1.5b.

Prying Action Calculations for WT6x32.5 @ Bolt Spacing of 2.0b, 2.5b, 3.0b, 4.0b:

Tributary Length for Specimens 2.0b, 2.5b, 3.0b, 4.0b

$$p = \max 2b, \text{ but } \leq s, = \max(2.0 * 3.5\text{in}, 3.5\text{in} \leq 7.0\text{in}) = 7.0\text{in}$$

$$p = \max 2b, \text{ but } \leq s, = \max(2.0 * 3.5\text{in}, 3.5\text{in} \leq 8.75\text{in}) = 7.0\text{in}$$

---

[4] AISC. 2011.

$p = \max 2b, \text{ but } \leq s, = \max(2.0 * 3.5\text{in}, 3.5\text{in} \leq 10.50\text{in}) = 7.0\text{in}$

$p = \max 2b, \text{ but } \leq s, = \max(2.0 * 3.5\text{in}, 3.5\text{in} \leq 14.00\text{in}) = 7.0\text{in}$

Note: Based on AISC[5] 14th ed. two calculations for prying action need to be considered, 1.5b and 2.0b, since 2.0b, 2.5b, 3.0b, 4.0b all have the same tributary length, which will result in the same amount of prying force.

$$t_{min} = \sqrt{\frac{4Tb'}{\phi p F_u}} = \sqrt{\frac{4 * 25\text{kips} * 3.13\text{in}}{1.0 * 7.00\text{in} * 65\text{ksi}}} = 0.829\text{in}$$

$$T \leq \frac{\phi F_u t^2 p}{2b} = \frac{1.0 * 65ksi * (0.605in)^2 * 7.00in}{2 * 3.5in} = 23.79\text{kips}$$

$$\delta = 1 - \frac{d'}{p} = 1 - \frac{0.8125in}{7.00in} = 0.884$$

$$\rho = \frac{b'}{a'} = \frac{3.13\text{in}}{2.68\text{in}} = 1.17$$

$$\beta = \frac{1}{\rho}\left(\frac{B}{T} - 1\right) = \frac{1}{1.17}\left(\frac{49.38\text{kips}}{25\text{kips}} - 1\right) = 0.82$$

α' = 1.0 if β ≥ 1 = the lesser of 1 and $\frac{1}{\delta}\left(\frac{\beta}{1-\beta}\right)$ if β < 1

$$\alpha' = \min\left(1.0, \frac{1}{\delta}\left(\frac{\beta}{1-\beta}\right)\right) = \min\left(1.0, \frac{1}{0.845}\left(\frac{0.84}{1-0.84}\right)\right) = \min(1.0, 6.23)$$

$\alpha' = 1.0$

---

[5] AISC. 2011.

$$t_{min} = \sqrt{\frac{4Tb'}{\phi p F_u (1 + \delta\alpha')}} = \sqrt{\frac{4 * 25\text{kips} * 3.13\text{in}}{\phi * 5.25\text{in} * 65\text{ksi} * (1 + 0.845 * 1.0)}} = 0.704\text{in}$$

$$a' = \left(a + \frac{d_b}{2}\right) \leq \left(1.25b + \frac{d_b}{2}\right) = \left(2.31\text{in} + \frac{0.75\text{in}}{2}\right) \leq \left(1.25 * 3.50\text{in} + \frac{0.75\text{in}}{2}\right) =$$

$$a' = (2.68\text{in}, 4.75\text{in}) = 2.68\text{in}$$

$$t_c = \sqrt{\frac{4Bb'}{\phi p F_u}} = \sqrt{\frac{4 * 49.38\text{kips} * 3.13\text{in}}{\phi * 7.00\text{in} * 65\text{ksi}}} = 1.165\text{in}$$

$$\alpha = \frac{1}{\delta}\left[\frac{T}{B}\left(\frac{t_c}{t}\right)^2 - 1\right] \quad \text{where } 0 \leq \alpha \leq 1$$

$$\alpha = \frac{1}{0.884}\left[\frac{25\text{kips}}{49.38\text{kips}}\left(\frac{1.165\text{in}}{0.605\text{in}}\right)^2 - 1\right] = 0.9924$$

$$0 \leq 0.9924 \leq 1 \text{ therefore } \alpha = 0.9924$$

$$q = B\left[\delta\alpha\rho\left(\frac{t}{t_c}\right)^2\right] = 49.38\text{kips} * \left[0.884 * 0.9924 * 1.166 * \left(\frac{0.605\text{in}}{1.165\text{in}}\right)^2\right] = 13.6\text{kips}$$

Prying Force in Bolt, q = 13.6kips

Total Bolt Force T_{actual} = 25kips + 13.6kips = **38.6kips ≤ 49.38kips Bolt OK!!**

Alternatively, determine available bolt force.

$$\alpha' = \frac{1}{\delta(1 + \rho)}\left[\left(\frac{t_c}{t}\right)^2 - 1\right] = \frac{1}{0.884 * (1 + 1.166)}\left[\left(\frac{1.165\text{in}}{0.605\text{in}}\right)^2 - 1\right] = 1.414$$

Q = 1 when α' < 0 ,

$$Q = \left(\frac{t}{t_c}\right)^2 (1 + \delta\alpha') \ \text{ when } 0 \le \alpha' \le 1 \, ,$$

$$Q = \left(\frac{t}{t_c}\right)^2 (1 + \delta) \text{ when } \alpha' > 1 \ => Q = \left(\frac{0.605\text{in}}{1.165\text{in}}\right)^2 (1 + 0.884) = 0.508$$

$$T_{available} = BQ = 49.38\text{kips} * 0.508 = \mathbf{25.09\text{kips}}$$

Figure B-2 shows a screen shot of the prying force spreadsheet which confirms the hand calculations are correct.

	AISC Beam Properties		Checks	SYM.	Explanation	Units			
					First Anaylsis were prying action does not apply based on thickness				
	WT Shapes			Fu	65.00	ksi	Tensile Strength		
				Fy	50.00	ksi	Yield Strength		
	k1=1.5			T	25.00	kips	Required strength, rut or rat per bolt		
	tf=0.605		75in,	B	49.38	kips	Availible Tension per Bolt (φrn so say no SF, same as T)		
			OK	b	3.50	in	Distance Edge Web to Center Bolt		
				b'	3.13	in	Fig 9-4		
	X			a	2.31	in	Distance Center Bolt to edge of flange		
d=6.06				a'	2.680	in	Fig 9-4		
	tw=0.39			db	0.75	in	Bolt Diameter		
					0.0625	in	Bolt Hole Tolarence 1/16 or 1/8		
	bf=12			pe	11.94	in	Zoetemeijer (1974) Equivalent Length		
				pe	11.30	in	Thornton and Kane		
				p	7.00	in	2b (max) ≤ s		
				s	7.00	in	Bolt Spacing		
	WT6X32.5			g	7.50	in	Gauge Distance		
A =	9.54	in.^2		tmin	**0.829**	in	Minimum Flange thickness to Neglect prying action forces	AISC 9-20b	
d =	6.060	in.	OK	tw	0.390	in	Web Thickness		
tw =	0.390	in.							
bf =	12.000	in.					**Second Anaylsis of Prying Action with Prying force applied**		
tf =	0.605	in.		tf	0.605	in	Thickness of the Flange		
k =	1.2000	in.		T	23.79	kips	Tensile Force with preliminary thickness chosen (T max)	AISC 9-22b	
k1 =	1.5000	in.	OK	tmin	**0.604**	in	Acceptable Fitting Strength and Stiffness and Bolt Strength	AISC 9-23b	
Ix =	20.60	in.^4		δ	0.884			AISC 9-24	
Sx =	4.06	in.^3	OK						
rx =	1.470	in.		α'	1.000				
Iy =	87.20	in.^4		α	0.991495	actual	Check 0 ≤ α ≤ 1; Possibly OK if States Connection not Adequate	AISC 9-29	
Sy =	14.50	in.^3		a'	2.68			AISC 9-27	
ry =	3.020	in.		β	0.84			AISC 9-25	
Zx =	7.50	in.^3		ρ	1.166			AISC 9-26	
Zy =	22.00	in.^3		d'	0.813	in	Hole Width along length of fitting (Bolt Hole in Flange)		
J =	1.09	in.^4	OK	q	**13.616**	kips	Prying force per bolt	AISC 9-28	
				tc	**1.165**	in	Minimum Thickness to prevent prying action	AISC 9-30b	
Cw =	2.97	in.^6							
a =	2.66	in.							
Wno =	0.00	in.^2					**Avaiable Tensile Strength per Bolt with Prying Action**		
Sw =	0.00	in.^4		α'	1.413			AISC 9-35	
Qf =	0.00	in.^3		Q	0.508			AISC 9-32,33,34	
Qw =	0.00	in.^3							
			OK	Tactual	**38.616**	kips	Actual Bolt Tensile Load	AISC 9-31	
			OK	Tavail	25.10	kips	Q*B		

Figure B-2: Prying Calculation Spreadsheet 2.0b, 2.5b, 3.0b, 4.0b.

Appendix C: Shop Drawings

The following Figures show the shop drawings of which was submitted to German Town Iron and Steel, which was the company that donated the steel for the project.

Figure C-1: Base Plate.
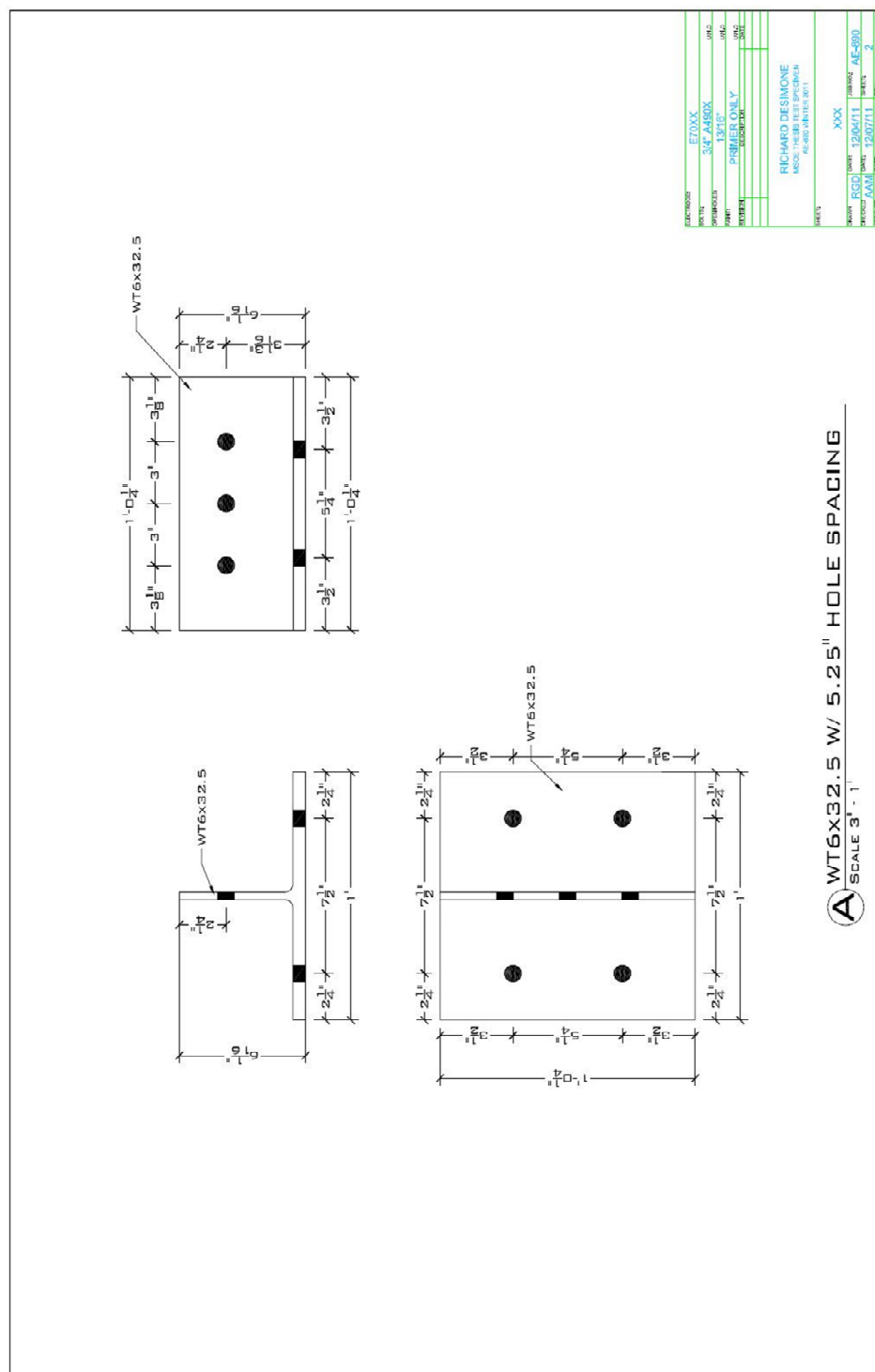
Figure C-2: WT6x32.5 with 1.5b Bolt Spacing.
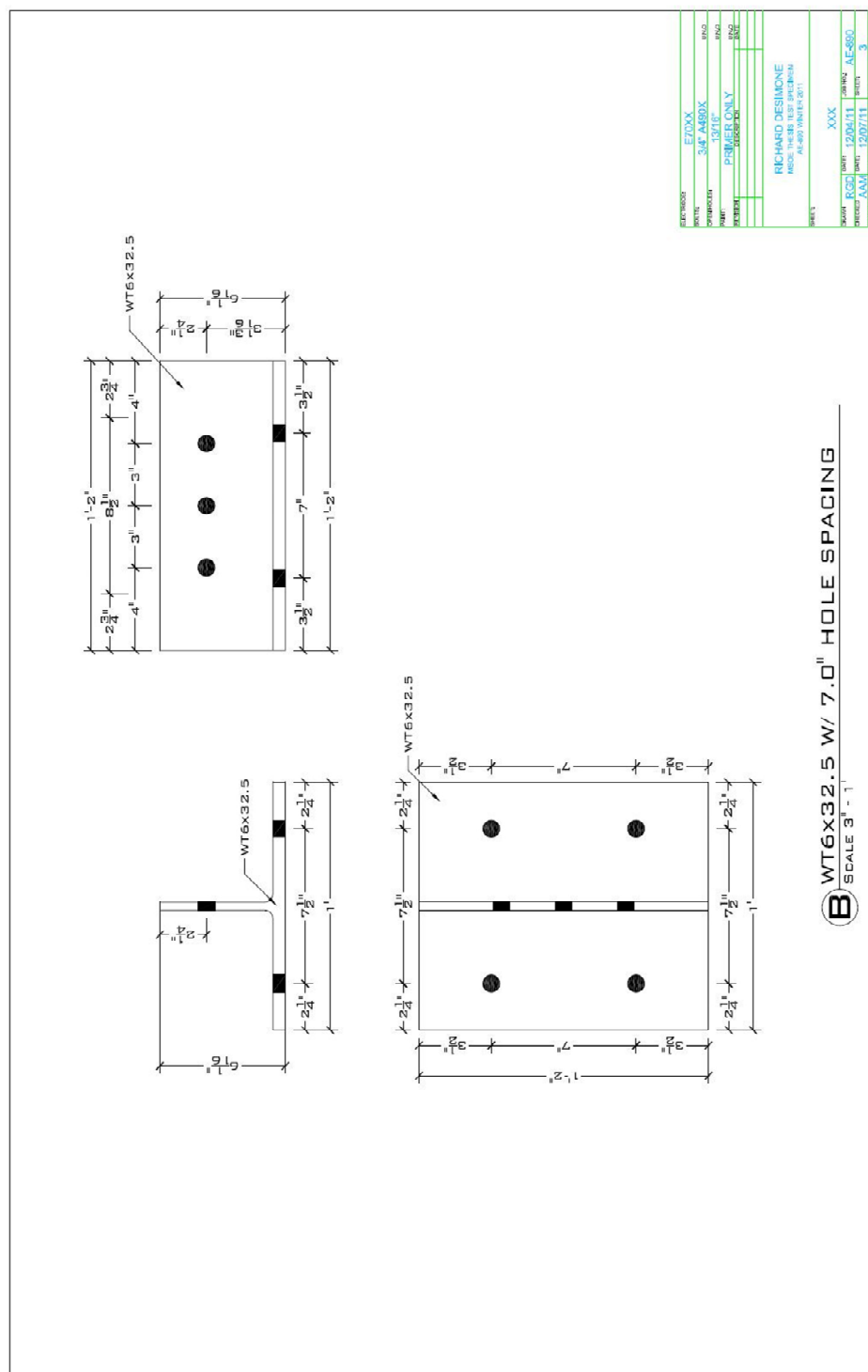
Figure C-3: WT6x32.5 with 2.0b Bolt Spacing.
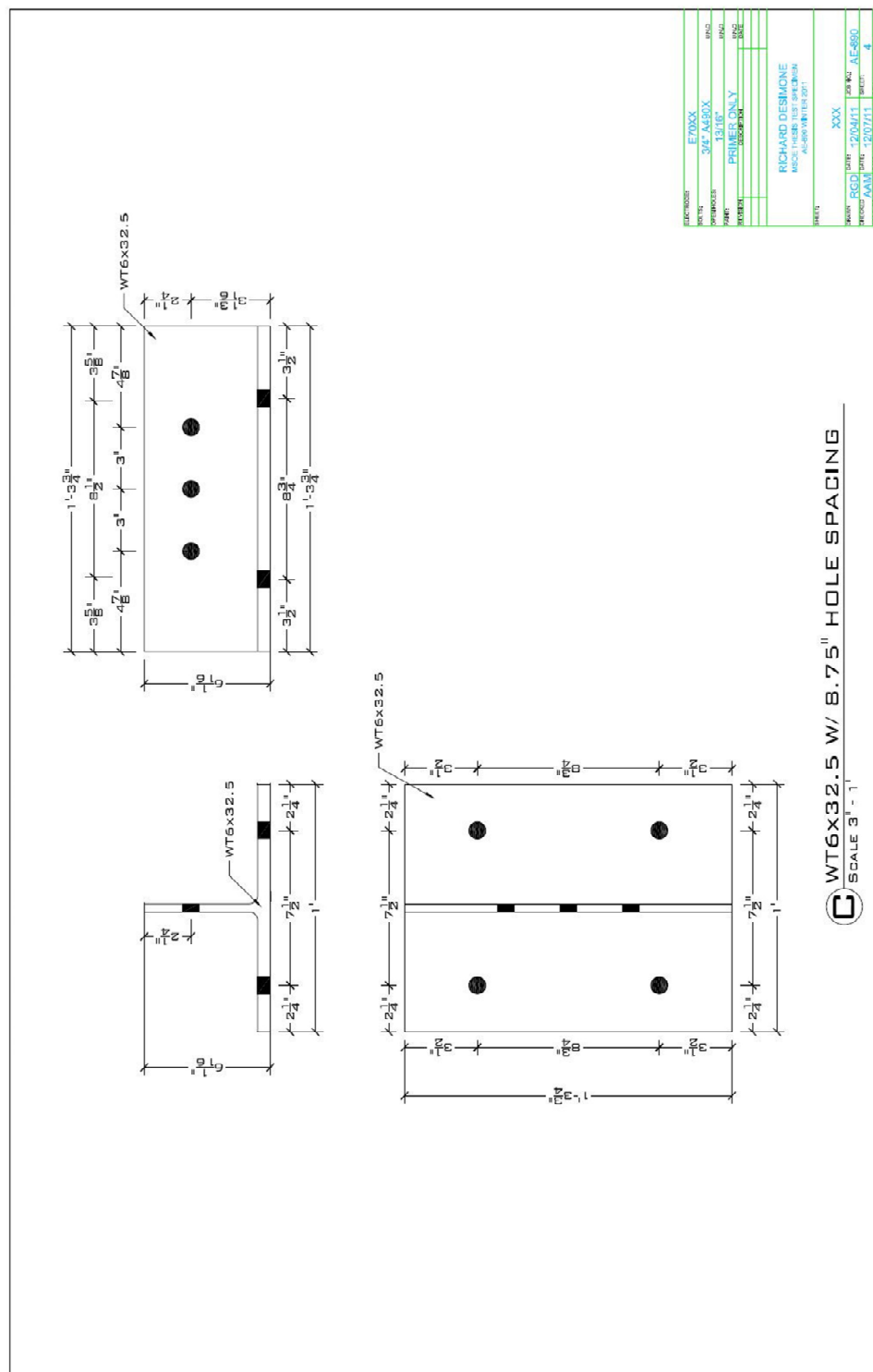
Figure C-4: WT6x32.5 with 2.5b Bolt Spacing.
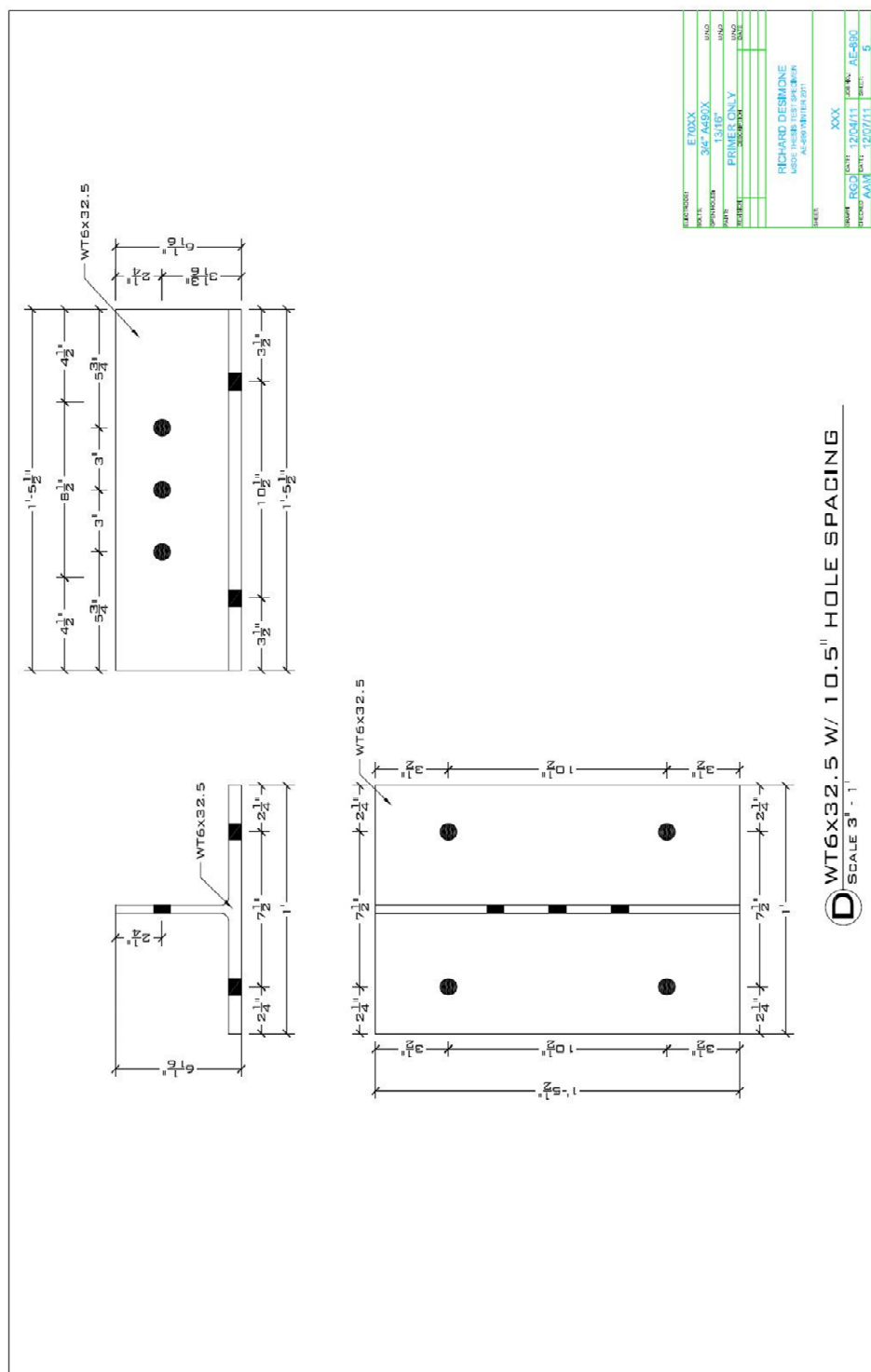
Figure C-5: WT6x32.5 with 3.0b Bolt Spacing.
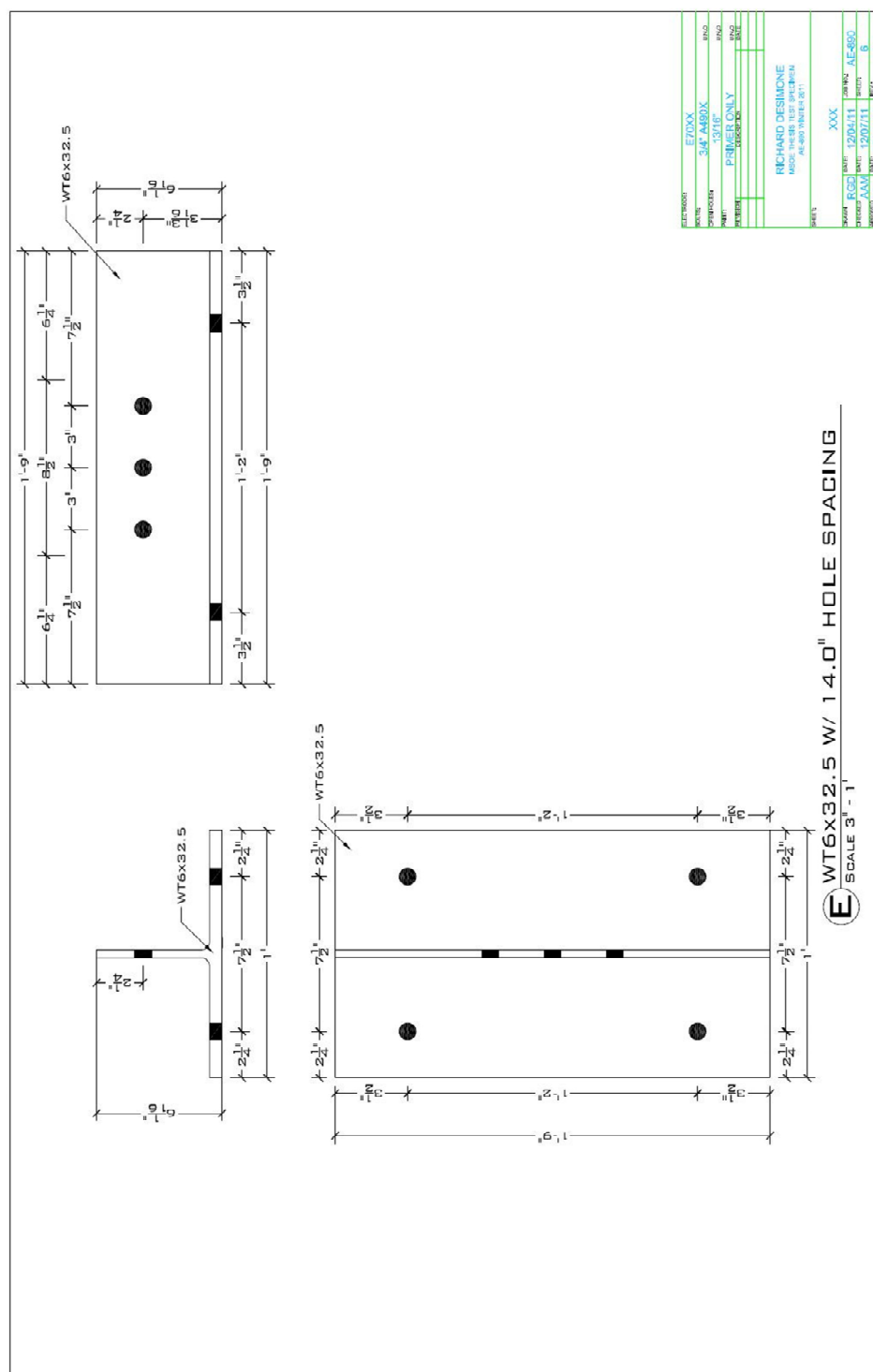
Figure C-6: WT6x32.5 with 4.0b Bolt Spacing.
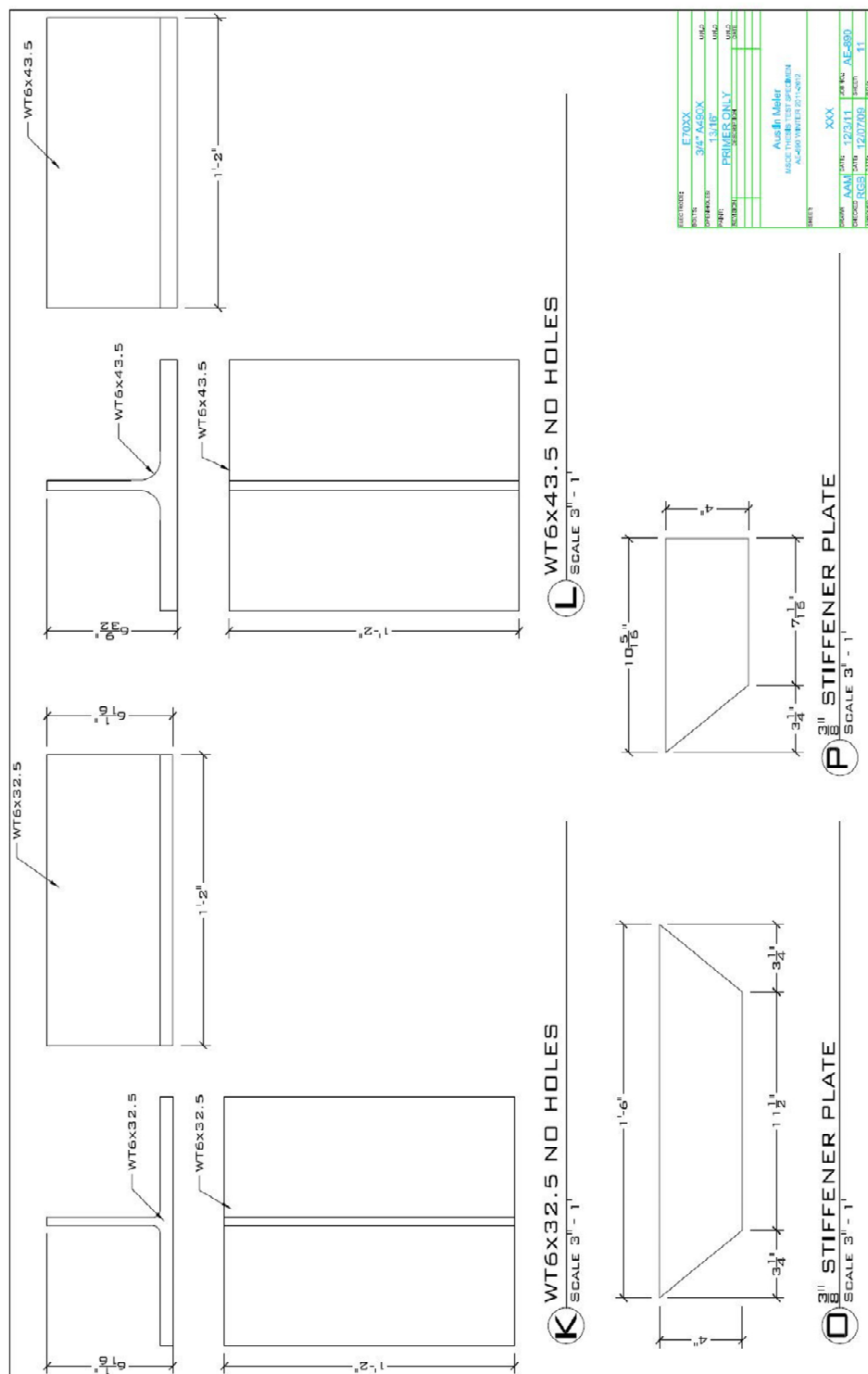
Figure C-6: WT6x32.5 ASTM8 Test Specimens.

Appendix D: Instrumented Bolt Procedure

The follow two Figures show the instruction manual on how to properly install the strain gages in the bolts, courtesy of Tokyo Sokki Kenkyujo Company.
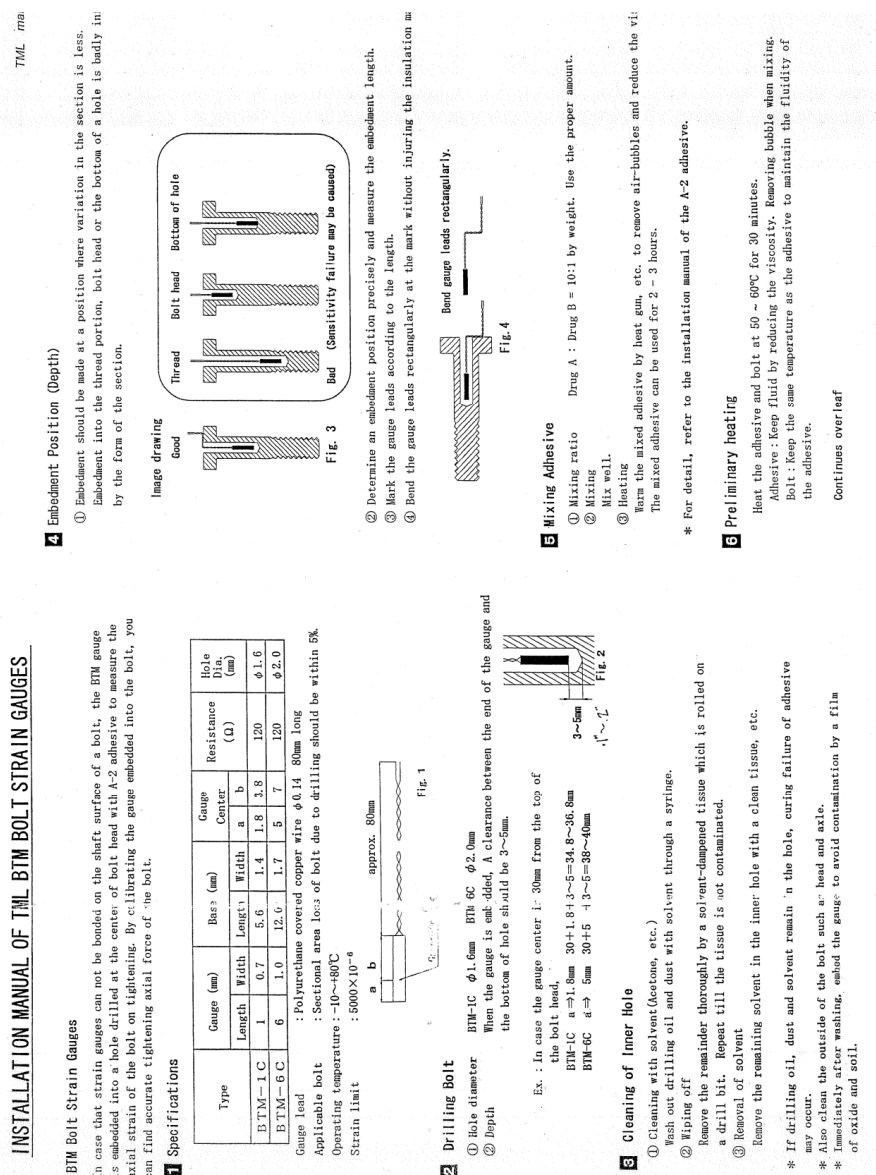
Figure D-1: Installation Manual BTM Strain Gages page 1-2[6].

---

[6] Tokyo Sokki Kenkyujo Co., Ltd. Installation Manual.

7 Pouring of Mixed Adhesive

① With use of syringe
· Enter the mixed adhesive into the syringe.
· Insert the syringe to reach the bottom of the drilled hole.
· Apply the mixed adhesive into the hole from the bottom fully.
  Take care not to produce air bubbles in the hole by adjusting the pulling-up speed of the syringe and pouring speed. When drawing up the syringe from the adhesive, take care not to make air bubbles remain in the hole.
* A specific needle of 1.8mm dia. is available for embedding BTM-6C, not for BTM-1C.

Insert 1   Pour 2   Fill 3

Air bubbles
Bad
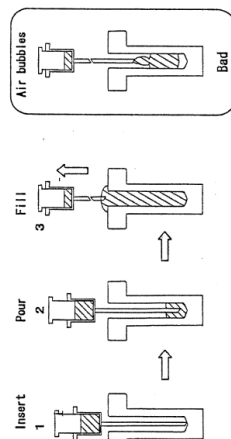
Fig. 5

② With use of vacuum pump
· Make a fence using vinyl tape around bolt head for adhesive pond.
· Pour the mixed adhesive. (For example, proper quantity should be 4 to 5 grams for a drilled hole of 2.0mm in diameter and 50mm in depth.)
· Put bolt into desiccator and create a vacuum for 15 to 20 minutes to get a level at 1 to 10Pa. The time to create vacuum depends upon desiccator volume and pump but vacuum work must be completed within 30 minutes in respect of pot life.
· After completion, remove the fence, and take off an excess adhesive.

Making fence 1   Poring A-2   Vacuum desiccator 3   Fill 4   Complete 5

Vacuum pump
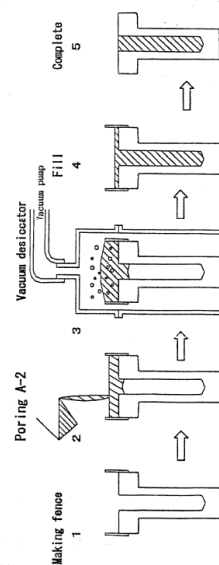
Fig. 6

8 Inserting Gauge

① Apply the mixed adhesive to the bolt gauge.
② Insert the gauge into the hole to put the bent part of gauge leads on the bolt
· The gauge should be placed at the center of hole. Take care not to bend or pl the gauge eccentrically or at the bottom.
· When inserting the gauge, take care not to develop air bubbles.
③ Allow the adhesive to cure for 12 hours at room temperature. (In this state, th adhesive does not harden.)

Image Drawing
Good   Bend   Eccentric   At the bottom
Bad (Sensitivity failure is eased.)
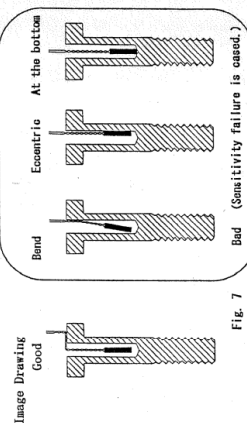
Fig. 7

9 Hot Curing

Cure with the bolt standing in electric furnace for 3 hours at 140°C. Temperature should be raised after placing the bolt in the furnace.

* Quick temperature elevation should be avoided: otherwise air bubbles or crack will occur.

10 Connection

After cooling the bolt, wire the gauge to instrument for measurement.
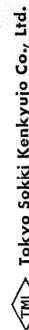
<TML> **Tokyo Sokki Kenkyujo Co., Ltd.**
8-2 Minami-ohi 6-chome, Shinagawa-ku, Tokyo, 140-8560 Japan
TEL 03-3763-5611 FAX 03-3763-6128
E-mail:sales@tokyosokki.co.jp

Figure D-1: Installation Manual BTM Strain Gages page 3-4[7].

---

[7] Tokyo Sokki Kenkyujo Co.

Appendix E: Experiment Assembly Schematic Drawings

The following Figures show a schematic design of how the test Specimen's will be connecting into the testing frame. The Figure's also indicate the location of the strain gage within the instrumented bolts.
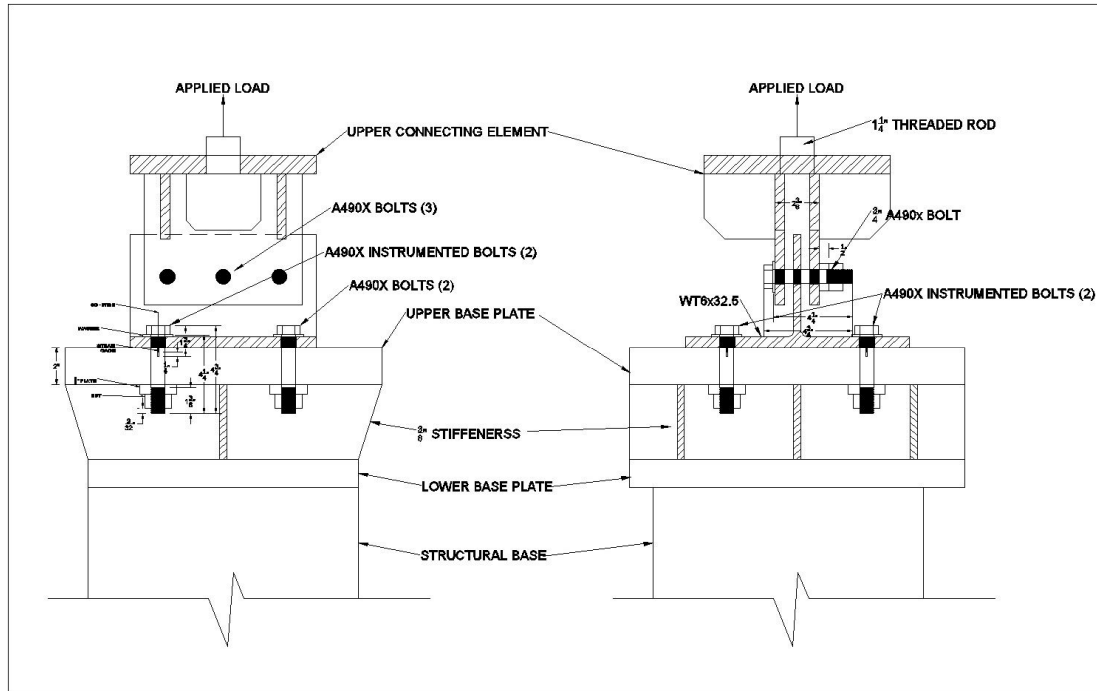
Figure E-1: Fully Bolted WT6x32.5 Specimen.
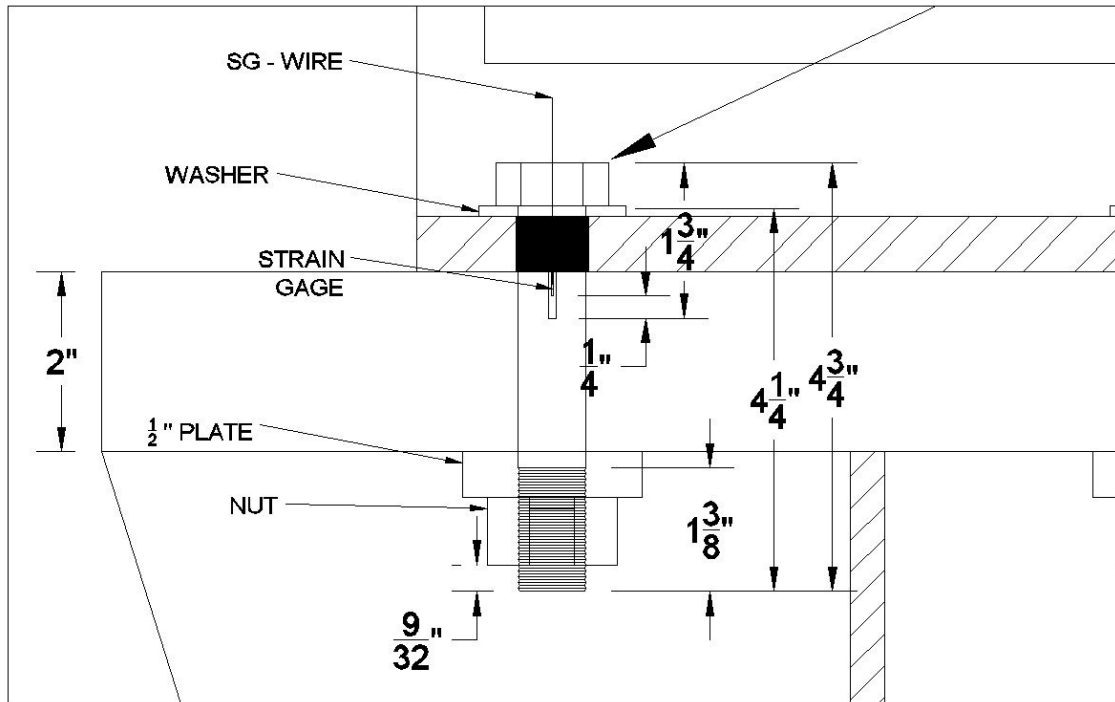
Figure E-2: Instrumented Bolt.

Appendix F: Testing Protocol Checklist

The testing protocol was the checklist used in the lab to confirm consistency

between experiments and was as follows:

Testing Protocol

Test Assembly

Confirm Load Cell is Fully Lowered (All the way down) From Previous Test

Correct Specimen size and spacing selected.

Specimen properly labeled and visible

Specimen placed on Base Plate

>   Center Specimen on BP by measuring four sides

Install loaded Bolts on right side through BP

>   Top: Head of Bolt – 1 Normal Washer

>   Underside: 2"x2"x1/2" PL, Regular Nut

>   Hand Tighten (Pre-Tensioned Later)

Install non-loaded bolts on left side through BP

>   Head of Bolt: 1 Normal Washer

>   Thread Side: 2"x2"x1/2" PL, Regular Nut

>   Hand Tighten (Pre-Tensioned Later)

Confirm Specimen is Centered on BP

Install 3 A490X Bolts Connecting Upper Connection and Specimen Web

>   Head of Bolt: 2 Normal Washer

>   Thread side: 3 Regular Washers, Regular Nut

Snug Tighten (1/4 to 1/2 Turn of wrench after hand tightened)

LVDTs correctly placed and secured (TBD)

Take Pictures

Software (Labview) Setup

Instrumented bolt #1 strain gage (Front Right) properly secured to channel 0.

Instrumented bolt #2 strain gage (Front Left) properly secured to channel 1.

Open Labview

Re-name Testing File (Ex: **Specimen Size_Specimen Spacing _Pretensioning**)

Strain gage factors correct

LVDTs properly attached to receiver (Channels TBD)

Run Pretension Test

Pretension Loaded Bolts (Strain ~300 = 3.8k, ~400 = 5.1k)

Pretension non-loaded bolts to approximately the same amount of turn as loaded

bolts)

Confirm LVDT's are Reading

Stop Pretension Test (Confirmed Saved Data)

Plaster Paris applied

Take Pictures

Final Testing Checks

Protective shield in place

Specimen Labeled index card on Protective Shield

Camera/Video properly placed and recording

Experiment Test

Re-name Testing File (Ex: **Specimen Size_Specimen Spacing**)

Run Test

Slowly Apply Load through Load cell (TBD Frequency, etc.)

Load until ~100k is applied or Failure occurs (WT6x43.5 / WT6x32.5 will vary)

Take pictures at Max loading

Stop Test (Confirm Saved Data)

Unload Load cell so Specimen can be removed

Disconnect all Strain Gages/LVDT's

Unbolt Specimen.

After Specimen Removed, Place bolts through same bolt holes of Specimen for keeping

Record any observations as deem necessary

Fully Lower Load Cell (All the way Down) for next experiment

Appendix G: Experimental Graphs and Spreadsheets

Figure G-1 shows the required values for which were needed to determine the experimental prying forces, tributary/effective length, and alpha, α.

WT6x32.5 Specimen Properties	

Material Properties

Modulus Of Elasticity				WT Tensile Strength		
(A490x Bolt)				(From ASTM E8-04 Test)		
E	29000	ksi		Fu	70.214	ksi

Bolt Area				Flange Thickness		
Dia	0.7455	in		t	0.6050	in
A	0.4317	in^2				

Prying Action Variables

Dist. Web Edge to Bolt Line				Ratio b'/a'	
b'	3.1250	in		ρ	1.1660

LRFD Safety Factor				Bolt Hole Width	
(Take as 1.0 for Experiment)				d'	0.8125
φ	0.9000				

Experimental Variables

Experimental Applied Load		
Load	Varies	kips

Total Bolt Force				Prying Force per Bolt		
T	Varies	kips		q	Varies	kips

Measured Bolt Strain				Bolt Stress		
ε	Varies	strain		σ	Varies	ksi

Figure G–1: General and Material Properties per each Specimen.

Each Specimen below shows the same Figures per each Specimen. The first three Figures for each Specimen show the first three and last four lines from the spreadsheet data file of which was used to determine the experimental values for which was considered for analysis. Finally, some additional plots of which were not included in the main body are shown.

WT6x32.5 at Bolt Spacing 1.5b:

WT6x32.5 Specimen 1.5b				
Experimental Values (Strain Gage 1, Front Right)				
Stress	Bolt Force	Prying Force	Tributary Length	Ratio ($M_{bolt\ Line}/M_{web}$)
$\varepsilon E = \sigma$	$\sigma A = T$	$q = T - \dfrac{Load}{4}$	$p = \dfrac{[T\rho - q]4b'}{\rho \phi F u t^2}$	$\alpha = \dfrac{q}{\left[(p - d')\rho \dfrac{\phi F u t^2}{4b'}\right]}$
(ksi)	(Kips)	(Kips)	(in)	(Ratio)
Max	Max	Max	Max	Max
91.174	39.360	14.373	8.174	1.121
Data	Data	Data	Data	Data
-0.118	-0.051	-0.075	0.043	0.0407262
0.011	0.005	-0.019	0.020	0.0101160
0.119	0.051	0.027	0.000	-0.0140447

90.489	39.065	14.112	6.251	1.0824183
90.826	39.210	14.223	6.221	1.0969441
90.685	39.149	14.196	6.215	1.0959863
91.174	39.360	14.373	6.158	1.1214929

Figure G-2: Data Results Specimen 1.5b Bolt 1.

WT6x32.5 Specimen 1.5b				

Experimental Values (Strain Gage 2, Front Left)				
Stress	Bolt Force	Prying Force	Tributary Length	Ratio ($M_{bolt\ Line}/M_{web}$)
$\varepsilon E = \sigma$	$\sigma A = T$	$q = T - \dfrac{Load}{4}$	$p = \dfrac{[T\rho - q]4b'}{\rho \phi F u t^2}$	$\alpha = \dfrac{q}{\left[(p - d')\rho \dfrac{\phi F u t^2}{4b'}\right]}$
(ksi)	(Kips)	(Kips)	(in)	(Ratio)
Max	Max	Max	Max	Max
95.731	41.328	16.340	8.578	1.506
Data	Data	Data	Data	Data
-0.090	-0.039	-0.063	0.038	0.0339335
0.093	0.040	0.016	0.005	-0.0083509
-0.068	-0.030	-0.054	0.034	0.0287727
94.927	40.981	16.028	5.451	1.4411613
95.275	41.131	16.143	5.420	1.4615749
95.199	41.098	16.145	5.402	1.4671685
95.731	41.328	16.340	5.337	1.5062692

Figure G-3: Data Results Specimen 1.5b Bolt 2.

WT6x32.5 Specimen 1.5b				
Experimental Values (Strain Gage Average)				
Stress	Bolt Force	Prying Force	Tributary Length	Ratio ($M_{bolt\ Line}/M_{web)}$
$\varepsilon E = \sigma$	$\sigma A = T$	$q = T - \dfrac{Load}{4}$	$p = \dfrac{[T\rho - q]4b'}{\rho\phi Fut^2}$	$\alpha = \dfrac{q}{\left[(p-d')\rho\dfrac{\phi Fut^2}{4b'}\right]}$
(ksi)	(Kips)	(Kips)	(in)	(Ratio)
Max	Max	Max	Max	Max
93.452	40.344	15.357	8.367	1.298
Data	Data	Data	Data	Data
-0.104	-0.045	-0.069	0.041	0.0373188
0.052	0.023	-0.002	0.012	0.0007974
0.025	0.011	-0.013	0.017	0.0069090
92.708	40.023	15.070	5.851	1.2475647
93.051	40.171	15.183	5.820	1.2646763
92.942	40.124	15.170	5.809	1.2664808
93.452	40.344	15.357	5.748	1.2978849

Figure G-4: Data Results Specimen 1.5b Bolt Average.
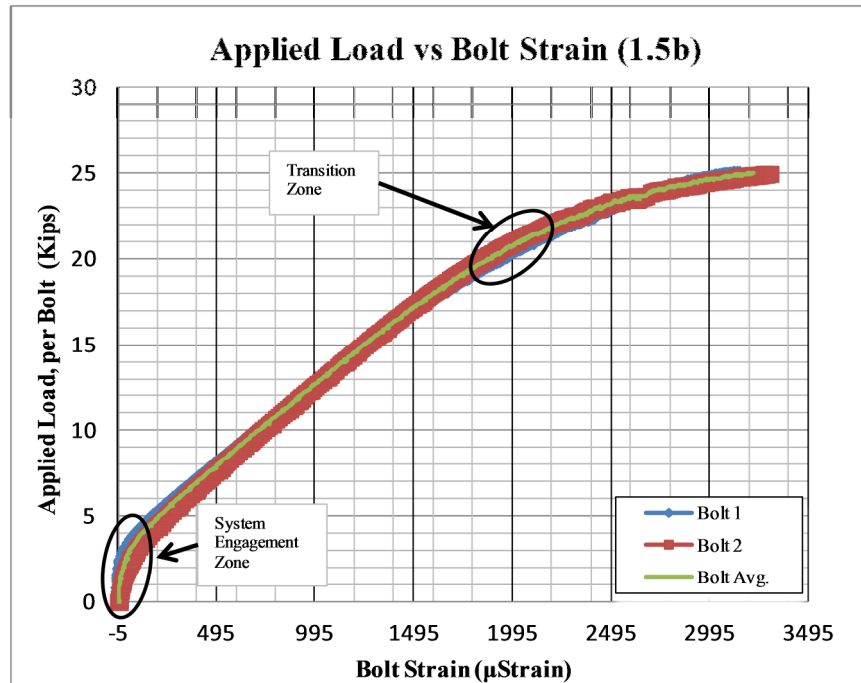
Figure G-5: Applied Load versus Bolt Strain Specimen 1.5b.
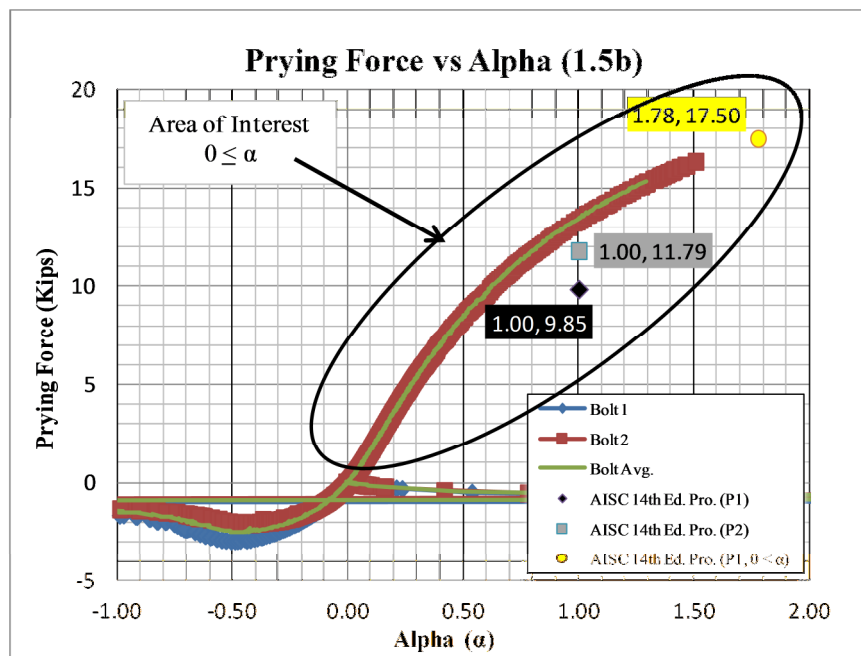
Figure G-6: Prying Force versus Alpha Specimen 1.5b.

Figure G-7: Effective Length versus Alpha Specimen 1.5b.

Figure G-8: Effective Length versus Alpha Specimen 1.5b.

WT6x32.5 at Bolt Spacing 2.0b

WT6x32.5 Specimen 2.0b				
Experimental Values (Strain Gage 1, Front Right)				
Stress	Bolt Force	Prying Force	Tributary Length	Ratio ($M_{bolt\ Line}/M_{web}$)
$\varepsilon E = \sigma$	$\sigma A = T$	$q = T - \dfrac{Load}{4}$	$p = \dfrac{[T\rho - q]4b'}{\rho\phi F u t^2}$	$\alpha = \dfrac{q}{\left[(p-d')\rho\dfrac{\phi F u t^2}{4b'}\right]}$
(ksi)	(Kips)	(Kips)	(in)	(Ratio)
Max	Max	Max	Max	Max
73.741	31.835	6.847	9.593	0.337
Data	Data	Data	Data	Data
0.052	0.023	-0.014	0.023	0.0072644
-0.002	-0.001	-0.037	0.033	0.0198175
0.074	0.032	-0.139	0.141	0.0861389
73.427	31.699	6.821	9.255	0.3370267
73.416	31.694	6.780	9.290	0.3336022
73.351	31.666	6.762	9.293	0.3325859
73.741	31.835	6.847	9.297	0.3366090

Figure G-9: Data Results Specimen 2.0b Bolt 1.

WT6x32.5 Specimen 2.0b				

Experimental Values (Strain Gage 2, Front Left)				
Stress	Bolt Force	Prying Force	Tributary Length	Ratio ($M_{bolt\ Line}$/M_{web})
$\varepsilon E = \sigma$	$\sigma A = T$	$q = T - \dfrac{Load}{4}$	$p = \dfrac{[T\rho - q]4b'}{\rho \phi F u t^2}$	$\alpha = \dfrac{q}{\left[(p - d')\rho \dfrac{\phi F u t^2}{4b'}\right]}$
(ksi)	(Kips)	(Kips)	(in)	(Ratio)
Max	Max	Max	Max	Max
70.976	30.641	5.656	9.883	0.264
Data	Data	Data	Data	Data
0.064	0.027	-0.009	0.021	0.0046648
0.010	0.004	-0.032	0.031	0.0171527
0.085	0.037	-0.134	0.139	0.0828470

70.727	30.533	5.656	9.741	0.2642221
70.683	30.515	5.600	9.782	0.2604431
70.629	30.491	5.587	9.783	0.2597820
70.976	30.641	5.653	9.795	0.2625221

Figure G-10: Data Results Specimen 2.0b Bolt 2.

WT6x32.5 Specimen 2.0b				
Experimental Values (Strain Gage Average)				
Stress	Bolt Force	Prying Force	Tributary Length	Ratio ($M_{bolt\ Line}/M_{web}$)
$\varepsilon E = \sigma$	$\sigma A = T$	$q = T - \dfrac{Load}{4}$	$p = \dfrac{[T\rho - q]4b'}{\rho\phi Fut^2}$	$\alpha = \dfrac{q}{\left[(p-d')\rho\dfrac{\phi Fut^2}{4b'}\right]}$
(ksi)	(Kips)	(Kips)	(in)	(Ratio)
Max	Max	Max	Max	Max
72.359	31.238	6.250	9.704	0.300
Data	Data	Data	Data	Data
0.058	0.025	-0.011	0.022	0.0059629
0.004	0.002	-0.035	0.032	0.0184833
0.080	0.034	-0.136	0.140	0.0844904
72.077	31.116	6.238	9.498	0.2996056
72.050	31.104	6.190	9.536	0.2959910
71.990	31.079	6.174	9.538	0.2951616
72.359	31.238	6.250	9.546	0.2985097

Figure G-11: Data Results Specimen 2.0b Bolt Average.
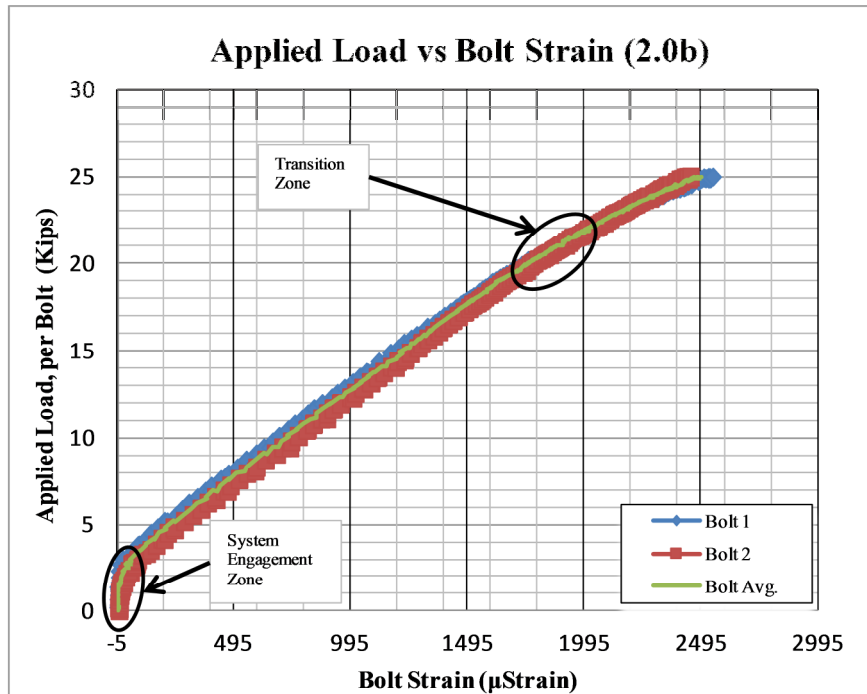
Figure G-12: Applied Load versus Bolt Strain Specimen 2.0b.
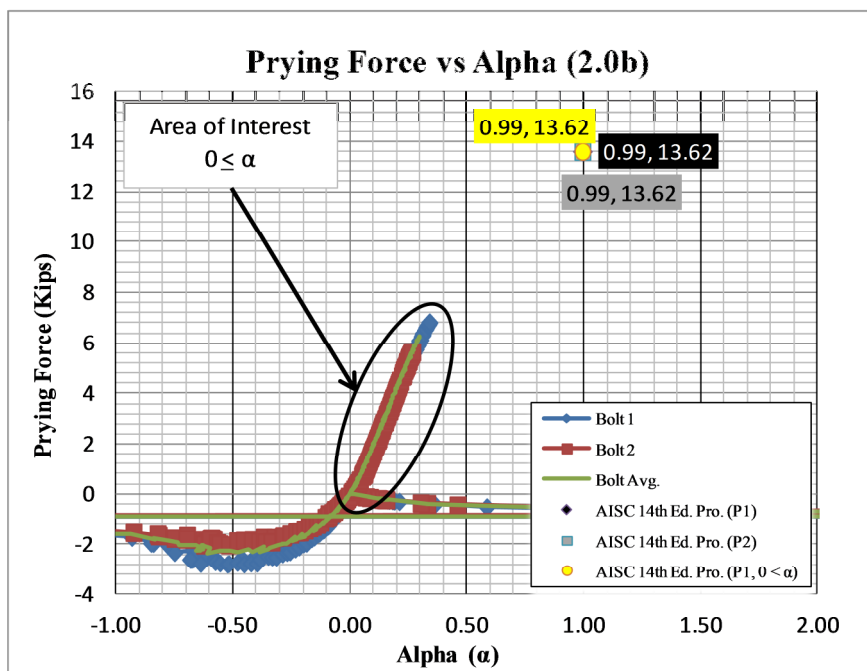
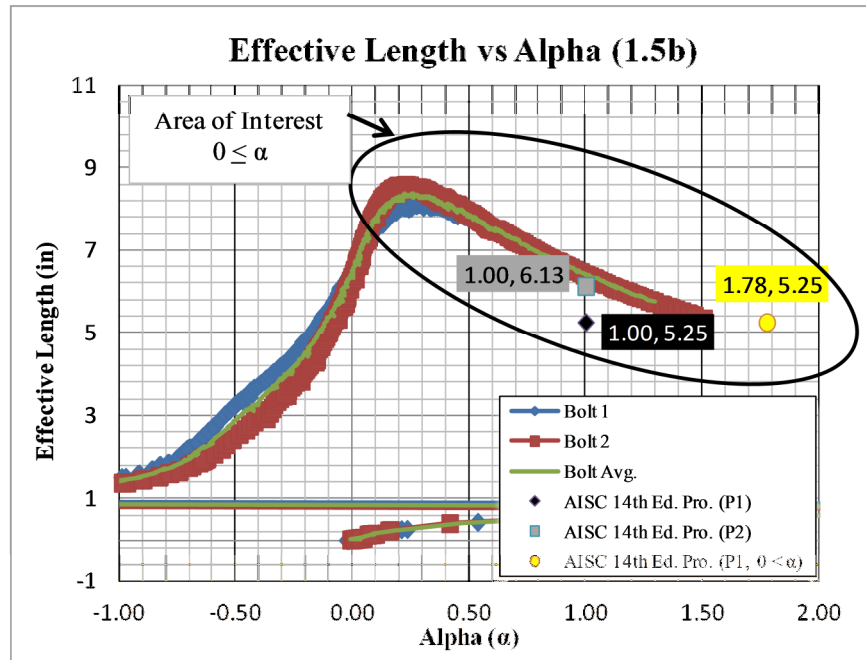**Figure G-13: Prying Force versus Alpha Specimen 2.0b.**

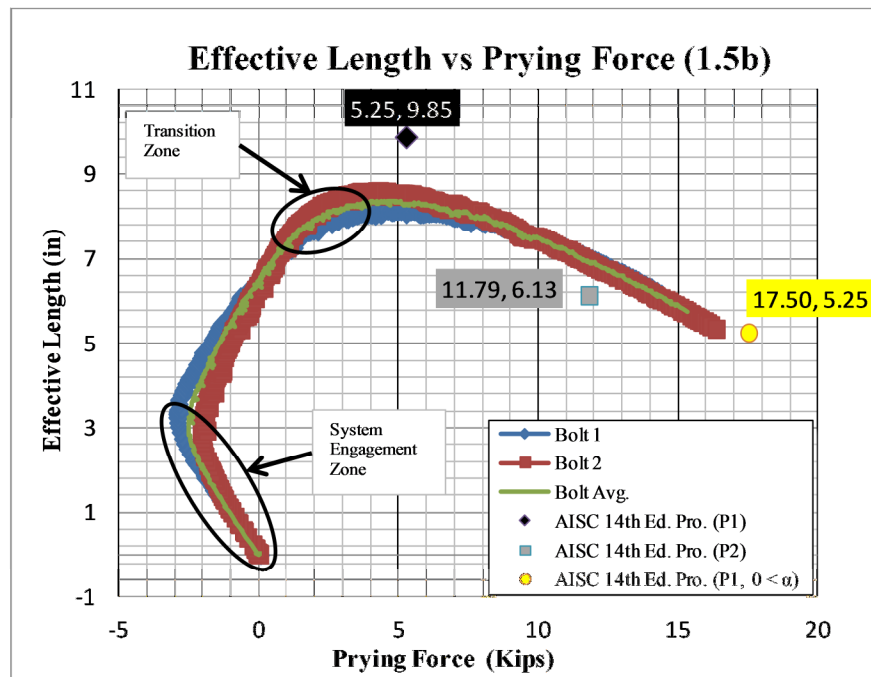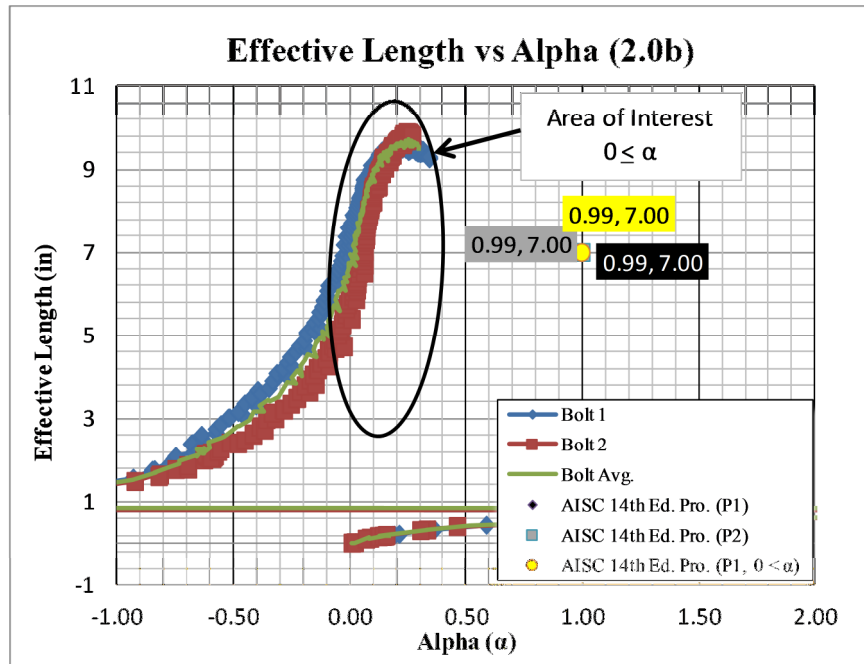**Figure G-14: Effective Length versus Alpha Specimen 2.0b.**

WT6x32.5 at Bolt Spacing 2.5b:

WT6x32.5 Specimen 2.5b				
Experimental Values (Strain Gage 1, Front Right)				
Stress	Bolt Force	Prying Force	Tributary Length	Ratio ($M_{bolt\ Line}/M_{web)}$
$\varepsilon E = \sigma$	$\sigma A = T$	$q = T - \dfrac{Load}{4}$	$p = \dfrac{[T\rho - q]4b'}{\rho \phi F u t^2}$	$\alpha = \dfrac{q}{\left[(p - d')\rho \dfrac{\phi F u t^2}{4b'}\right]}$
(ksi)	(Kips)	(Kips)	(in)	(Ratio)
Max	Max	Max	Max	Max
73.177	31.978	6.990	9.250	0.346
Data	Data	Data	Data	Data
-0.207	-0.091	-0.188	0.126	0.1141130
0.117	0.051	-0.022	0.045	0.0119676
-0.142	-0.062	-0.257	0.202	0.1758122
72.916	31.864	6.933	9.234	0.3433581
73.068	31.930	6.965	9.238	0.3448205
73.057	31.926	6.972	9.228	0.3455615
73.177	31.978	6.990	9.238	0.3460750

Figure G-15: Data Results Specimen 2.5b Bolt 1.

WT6x32.5 Specimen 2.5b

Experimental Values (Strain Gage 2, Front Left)

Stress	Bolt Force	Prying Force	Tributary Length	Ratio ($M_{bolt\ Line}/M_{web}$)
$\varepsilon E = \sigma$	$\sigma A = T$	$q = T - \dfrac{Load}{4}$	$p = \dfrac{[T\rho - q]4b'}{\rho \phi F u t^2}$	$\alpha = \dfrac{q}{\left[(p-d')\rho \dfrac{\phi F u t^2}{4b'}\right]}$
(ksi)	(Kips)	(Kips)	(in)	(Ratio)
Max	Max	Max	Max	Max
65.136	28.464	3.477	10.707	0.147
Data	Data	Data	Data	Data
0.121	0.053	-0.044	0.066	0.0247635
-0.062	-0.027	-0.100	0.077	0.0567606
0.165	0.072	-0.123	0.146	0.0770810
64.963	28.388	3.457	10.684	0.1460702
65.006	28.407	3.442	10.707	0.1450888
65.028	28.417	3.463	10.692	0.1462244
65.136	28.464	3.477	10.703	0.1466157

Figure G-16: Data Results Specimen 2.5b Bolt 2.

WT6x32.5 Specimen 2.5b				
Experimental Values (Strain Gage Average)				
Stress	Bolt Force	Prying Force	Tributary Length	Ratio ($M_{bolt\ Line}/M_{web)}$)
$\varepsilon E = \sigma$	$\sigma A = T$	$q = T - \dfrac{Load}{4}$	$p = \dfrac{[T\rho - q]4b'}{\rho\phi F u t^2}$	$\alpha = \dfrac{q}{\left[(p-d')\rho\dfrac{\phi F u t^2}{4b'}\right]}$
(ksi)	(Kips)	(Kips)	(in)	(Ratio)
Max	Max	Max	Max	Max
69.156	30.221	5.233	9.977	0.238
Data	Data	Data	Data	Data
-0.043	-0.019	-0.116	0.096	0.0675720
0.027	0.012	-0.061	0.061	0.0338791
0.011	0.005	-0.190	0.174	0.1242832
68.940	30.126	5.195	9.959	0.2368966
69.037	30.169	5.203	9.972	0.2369438
69.043	30.171	5.218	9.960	0.2379197
69.156	30.221	5.233	9.970	0.2383652

Figure G-17: Data Results Specimen 2.5b Bolt Average.
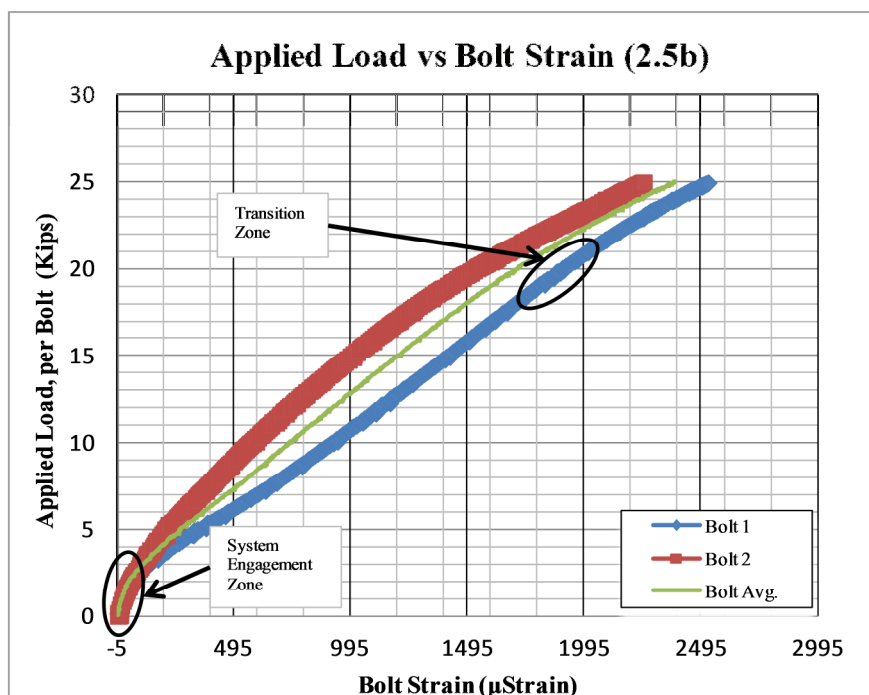
Figure G-18: Applied Load versus Bolt Strain Specimen 2.5b.
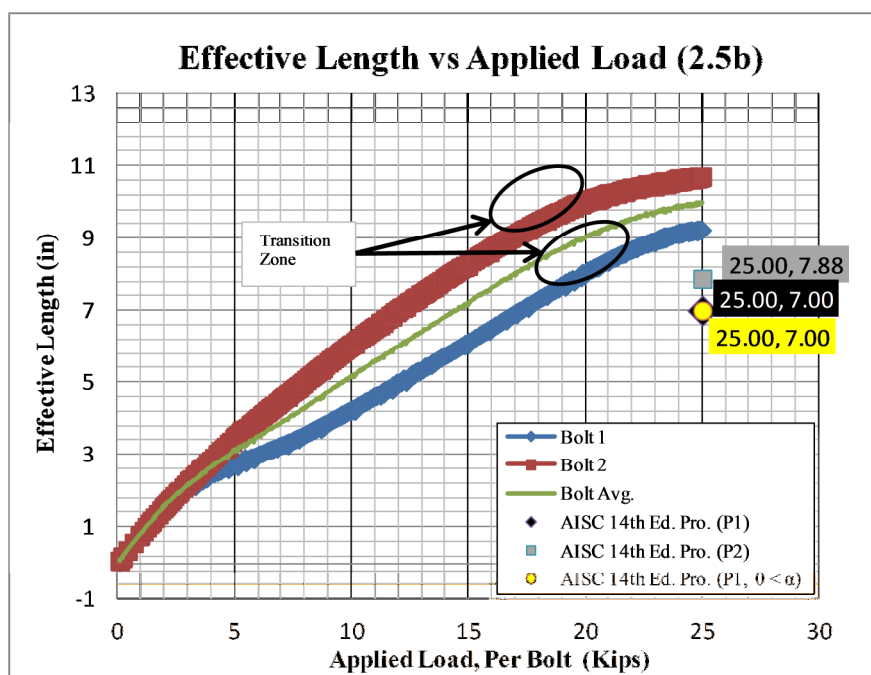
Figure G-19: Effective Length versus Applied Load Specimen 2.5b.
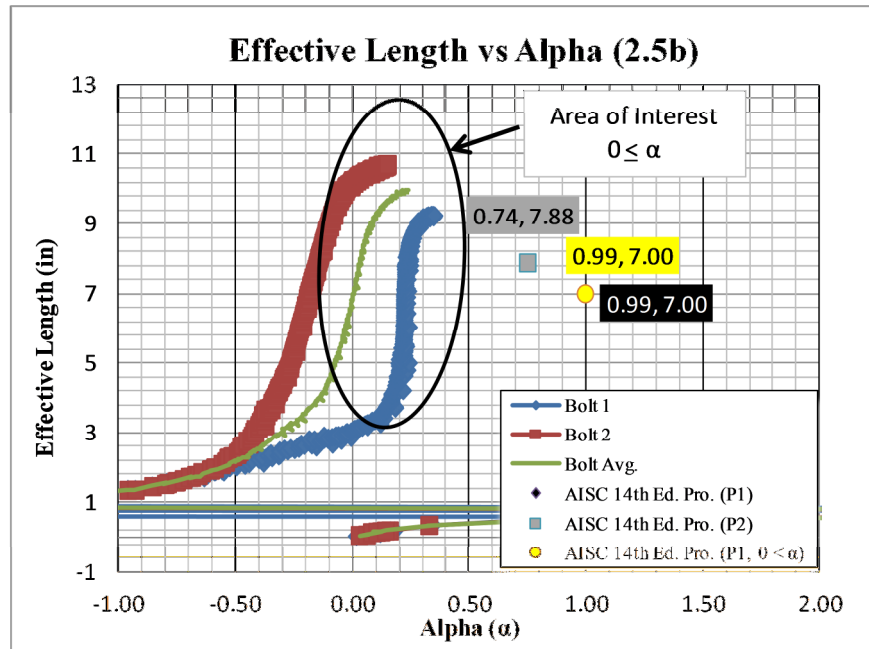
Figure G-20: Effective Length versus Alpha Specimen 2.5b.

WT6x32.5 at Bolt Spacing 3.0b

WT6x32.5 Specimen 3.0b				
Experimental Values (Strain Gage 1, Front Right)				
Stress	Bolt Force	Prying Force	Tributary Length	Ratio ($M_{bolt\ Line}/M_{web}$)
$\varepsilon E = \sigma$	$\sigma A = T$	$q = T - \dfrac{Load}{4}$	$p = \dfrac{[T\rho - q]4b'}{\rho\phi Fut^2}$	$\alpha = \dfrac{q}{\left[(p-d')\rho\dfrac{\phi Fut^2}{4b'}\right]}$
(ksi)	(Kips)	(Kips)	(in)	(Ratio)
Max	Max	Max	Max	Max
62.273	26.884	1.999	11.381	0.080
Data	Data	Data	Data	Data
0.152	0.066	0.042	-0.006	-0.0211879
-0.096	-0.041	-0.066	0.039	0.0353647
0.087	0.038	0.014	0.006	-0.0070345
62.176	26.842	1.947	11.296	0.0774655
62.143	26.828	1.850	11.377	0.0730411
62.013	26.772	1.816	11.381	0.0716675
62.273	26.884	1.896	11.362	0.0749756

Figure G-21: Data Results Specimen 3.0b Bolt 1.

WT6x32.5 Specimen 3.0b

Experimental Values (Strain Gage 2, Front Left)				
Stress	Bolt Force	Prying Force	Tributary Length	Ratio ($M_{bolt\ Line}/M_{web}$)
$\varepsilon E = \sigma$	$\sigma A = T$	$q = T - \dfrac{Load}{4}$	$p = \dfrac{[T\rho - q]4b'}{\rho \phi F_u t^2}$	$\alpha = \dfrac{q}{\left[(p - d')\rho \dfrac{\phi F_u t^2}{4b'}\right]}$
(ksi)	(Kips)	(Kips)	(in)	(Ratio)
Max	Max	Max	Max	Max
61.601	26.594	1.658	11.504	0.065
Data	Data	Data	Data	Data
0.044	0.019	-0.005	0.014	0.0026263
0.055	0.024	0.000	0.012	0.0001935
0.109	0.047	0.023	0.002	-0.0118018
61.428	26.519	1.624	11.431	0.0638020
61.439	26.524	1.546	11.504	0.0603102
61.385	26.500	1.544	11.494	0.0603120
61.601	26.594	1.606	11.483	0.0627870

Figure G–22: Data Results Specimen 3.0b Bolt 2.

WT6x32.5 Specimen 3.0b				
Experimental Values (Strain Gage Average)				
Stress	Bolt Force	Prying Force	Tributary Length	Ratio ($M_{bolt\ Line}/M_{web}$)
$\varepsilon E = \sigma$	$\sigma A = T$	$q = T - \dfrac{Load}{4}$	$p = \dfrac{[T\rho - q]4b'}{\rho\phi Fut^2}$	$\alpha = \dfrac{q}{\left[(p-d')\rho\dfrac{\phi Fut^2}{4b'}\right]}$
(ksi)	(Kips)	(Kips)	(in)	(Ratio)
Max	Max	Max	Max	Max
61.937	26.739	1.829	11.441	0.073
Data	Data	Data	Data	Data
0.098	0.042	0.018	0.004	-0.0094239
-0.021	-0.009	-0.033	0.025	0.0174753
0.098	0.042	0.018	0.004	-0.0094239
61.802	26.680	1.786	11.363	0.0705901
61.791	26.676	1.698	11.440	0.0666377
61.699	26.636	1.680	11.437	0.0659595
61.937	26.739	1.751	11.423	0.0688465

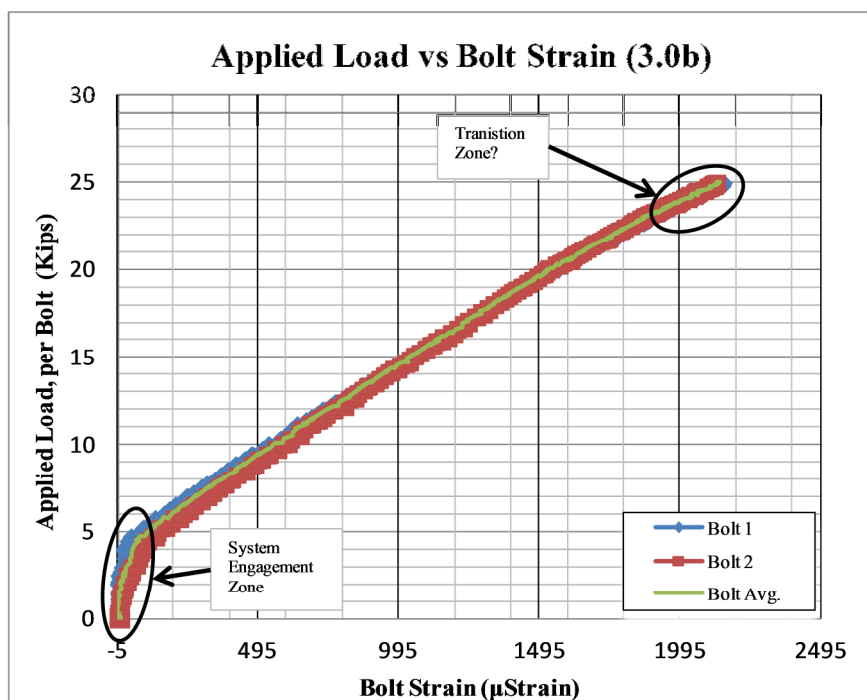**Figure G-23: Data Results Specimen 3.0b Bolt Average.**

Figure G-24: Applied Load versus Bolt Strain Specimen 3.0b.
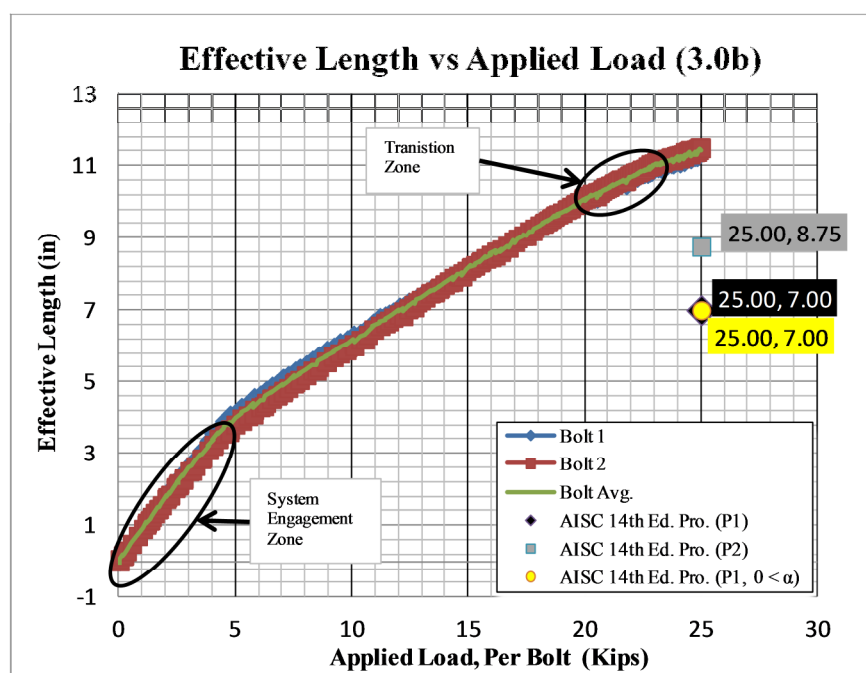
Figure G-25: Effective Length versus Applied Load Specimen 3.0b.

WT6x32.5 at Bolt Spacing 4.0b

WT6x32.5 Specimen 4.0b				
Experimental Values (Strain Gage 1, Front Right)				
Stress	Bolt Force	Prying Force	Tributary Length	Ratio ($M_{bolt\ Line}/M_{web}$)
$\varepsilon E = \sigma$	$\sigma A = T$	$q = T - \dfrac{Load}{4}$	$p = \dfrac{[T\rho - q]4b'}{\rho \phi F u t^2}$	$\alpha = \dfrac{q}{\left[(p - d')\rho \dfrac{\phi F u t^2}{4b'}\right]}$
(ksi)	(Kips)	(Kips)	(in)	(Ratio)
Max	Max	Max	Max	Max
55.942	24.151	-0.002	12.642	-0.030
Data	Data	Data	Data	Data
0.030	0.013	-0.011	0.016	0.0058027
0.019	0.008	-0.016	0.018	0.0082629
-0.078	-0.034	-0.058	0.036	0.0309653
55.552	23.982	-0.993	12.562	-0.0352503
55.812	24.095	-0.883	12.517	-0.0314718
55.141	23.805	-1.178	12.642	-0.0415333
55.206	23.833	-1.155	12.635	-0.0407413

Figure G-26: Data Results Specimen 4.0b Bolt 1.

WT6x32.5 Specimen 4.0b

Experimental Values (Strain Gage 2, Front Left)				
Stress	Bolt Force	Prying Force	Tributary Length	Ratio ($M_{bolt\ Line}/M_{web}$)
$\varepsilon E = \sigma$	$\sigma A = T$	$q = T - \dfrac{Load}{4}$	$p = \dfrac{[T\rho - q]4b'}{\rho\phi F_{ut}^2}$	$\alpha = \dfrac{q}{\left[(p - d')\rho\dfrac{\phi F_{ut}^2}{4b'}\right]}$
(ksi)	(Kips)	(Kips)	(in)	(Ratio)
Max	Max	Max	Max	Max
65.775	28.395	3.408	10.827	0.143
Data	Data	Data	Data	Data
-0.009	-0.004	-0.028	0.023	0.0148423
0.002	0.001	-0.023	0.022	0.0123500
0.002	0.001	-0.023	0.022	0.0123500

65.525	28.288	3.312	10.766	0.1388191
65.601	28.321	3.343	10.754	0.1402513
65.233	28.161	3.179	10.825	0.1324280
65.254	28.171	3.183	10.826	0.1326074

Figure G-27: Data Results Specimen 4.0b Bolt 2.

WT6x32.5 Specimen 4.0b

Experimental Values (Strain Gage Average)				
Stress	Bolt Force	Prying Force	Tributary Length	Ratio ($M_{bolt\ Line}/M_{web)}$)
$\varepsilon E = \sigma$	$\sigma A = T$	$q = T - \dfrac{Load}{4}$	$p = \dfrac{[T\rho - q]4b'}{\rho \phi Fut^2}$	$\alpha = \dfrac{q}{\left[(p - d')\rho \dfrac{\phi Fut^2}{4b'}\right]}$
(ksi)	(Kips)	(Kips)	(in)	(Ratio)
Max	Max	Max	Max	Max
60.859	26.273	1.286	11.734	0.050
Data	Data	Data	Data	Data
0.011	0.005	-0.020	0.020	0.0103023
0.011	0.005	-0.020	0.020	0.0103023
-0.038	-0.016	-0.041	0.029	0.0215728
60.539	26.135	1.160	11.664	0.0445823
60.707	26.208	1.230	11.636	0.0473978
60.187	25.983	1.000	11.734	0.0382106
60.230	26.002	1.014	11.730	0.0387505

Figure G-28: Data Results Specimen 4.0b Bolt Average.

Applied Load vs Bolt Strain (4.0b)

Applied Load, per Bolt (Kips) — vertical axis
Bolt Strain (μStrain) — horizontal axis

System Engagement Zone

Bolt 1
Bolt 2
Bolt Avg.
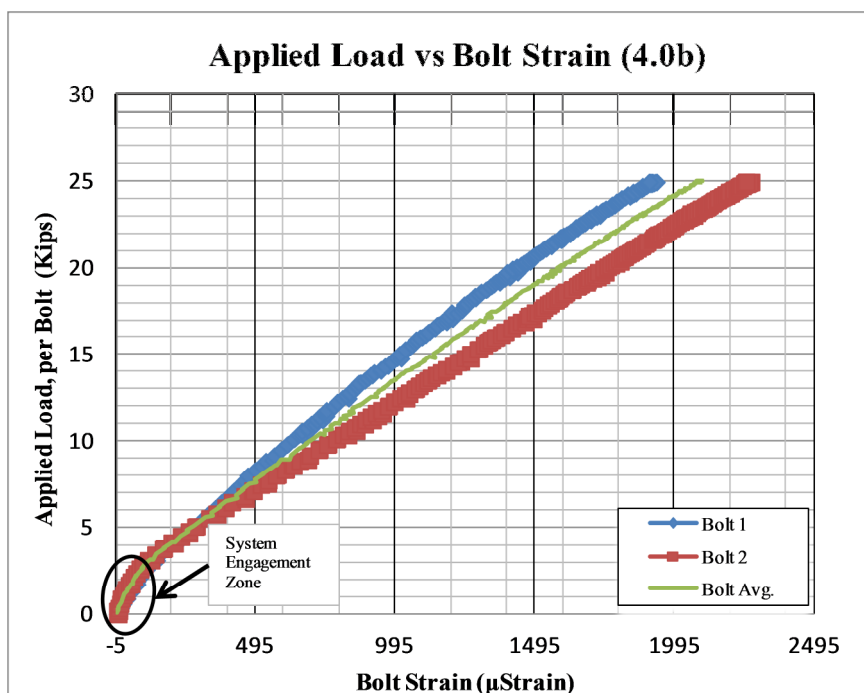
Figure G-29: Applied Load versus Bolt Strain Specimen 4.0b.

Effective Length vs Applied Load (4.0b)

Effective Length (in) — vertical axis
Applied Load, Per Bolt (Kips) — horizontal axis

25.00, 10.50
25.00, 7.00
25.00, 7.00

System Engagement Zone

Bolt 1
Bolt 2
Bolt Avg.
AISC 14th Ed. Pro. (P1)
AISC 14th Ed. Pro. (P2)
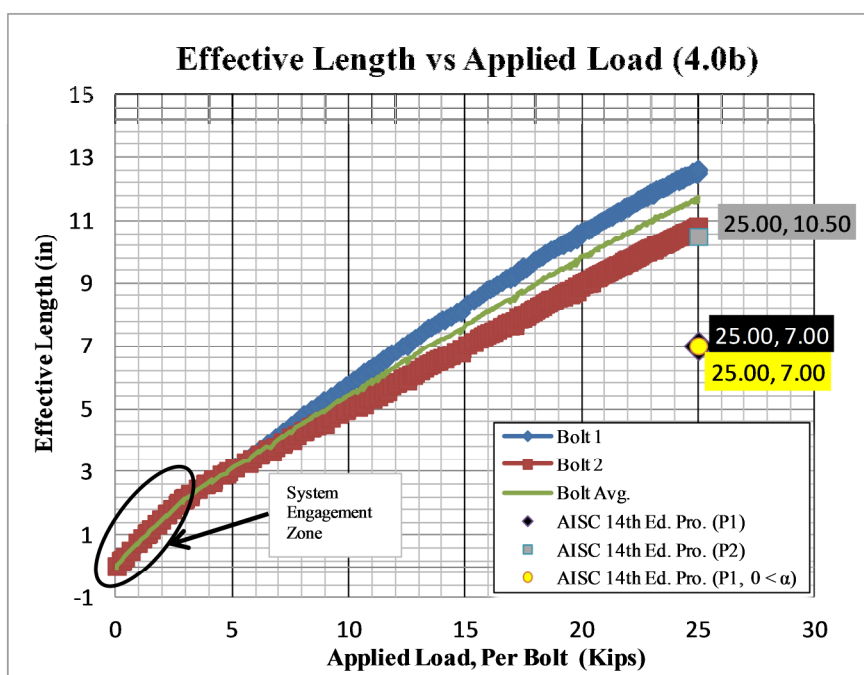AISC 14th Ed. Pro. (P1, $0 < \alpha$)

Figure G-30: Effective Length versus Applied Load Specimen 4.0b.

The following shows the steps of which Equation (25) and (26) where derived. The derivation was important because the experimental values for tributary length and alpha, α, were extracted from them.

Derivation of Equations (25) and (26)

Prying Force Provision and solve for Alpha:

$$q = B \left[\delta \alpha \rho \left(\frac{t}{t_c} \right)^2 \right] \tag{G-1}$$

$$q = B \left[\delta \alpha \rho \left(\frac{t}{\sqrt{\frac{4Bb'}{pFu}}} \right)^2 \right] \tag{G-2}$$

$$q = B \left[\delta \alpha \rho \frac{t^2}{\frac{4Bb'}{pFu}} \right] \tag{G-3}$$

$$q = B \left[\delta \alpha \rho \frac{pFut^2}{4Bb'} \right] \tag{G-4}$$

$$q = \delta \alpha \rho \frac{pFut^2}{4b'} \tag{G-5}$$

$$\alpha = \frac{q}{\left[\delta \rho \frac{pFut^2}{4b'} \right]} \tag{G-6}$$

$$\alpha = \frac{q}{\left[(1 - \frac{d'}{p}) \rho \frac{pFut^2}{4b'} \right]} \tag{G-7}$$

$$\alpha = \frac{q}{\left[\left(p - \frac{pd'}{p} \right) \rho \frac{Fut^2}{4b'} \right]} \tag{G-8}$$

$$\alpha = \frac{q}{\left[(p - d') \rho \frac{Fut^2}{4b'} \right]} \tag{G-9}$$

Equation (G-9) is Equation (26) in the text.

Alternate Alpha Provision with p as variable:

$$\alpha = \frac{1}{\delta}\left[\frac{T}{B}\left(\frac{t_c}{t}\right)^2 - 1\right] \tag{G-10}$$

$$\alpha = \frac{1}{\delta}\left[\frac{T}{B}\left(\frac{\sqrt{\frac{4Bb'}{pFu}}}{t}\right)^2 - 1\right] \tag{G-11}$$

$$\alpha = \frac{1}{\delta}\left[\frac{T}{B}\frac{\frac{4Bb'}{pFu}}{t^2} - 1\right] \tag{G-12}$$

$$\alpha = \frac{1}{\delta}\left[\frac{T}{B}\frac{4Bb'}{pFut^2} - 1\right] \tag{G-13}$$

$$\alpha = \frac{1}{\delta}\left[T\left(\frac{4b'}{pFut^2}\right) - 1\right] \tag{G-14}$$

Try Setting (G-6) = (G-14):

$$\frac{q}{\left[\delta\rho\frac{pFut^2}{4b'}\right]} = \frac{1}{\delta}\left[T\left(\frac{4b'}{pFut^2}\right) - 1\right] \tag{G-15}$$

$$\frac{q}{\left[\rho\frac{pFut^2}{4b'}\right]} = T\left(\frac{4b'}{pFut^2}\right) - 1 \tag{G-16}$$

$$\frac{q4b'}{[\rho pFut^2]} = T\left(\frac{4b'}{pFut^2}\right) - 1 \tag{G-17}$$

$$q4b' = \left[T\left(\frac{4b'}{pFut^2}\right) - 1\right][\rho pFut^2] \tag{G-18}$$

$$q4b' = \left[T\left(\frac{4b'\rho pFut^2}{\phi pFut^2}\right) - \rho pFut^2\right] \tag{G-19}$$

$$q4b' = [T4b'\rho - \rho pFut^2] \tag{G-20}$$

$$\rho p F u t^2 = [T4b'\rho - q4b'] \tag{G-21}$$

$$p = \frac{[T4b'\rho - q4b']}{\rho F u t^2} \tag{G-22}$$

$$p = \frac{[T\rho - q]4b'}{\rho F u t^2} \tag{G-23}$$

Equation (G-23) is Equation (25) in the text.

NOTE: Equation Verified by comparing to that of the prying Force Calculations.

Appendix H: Uniaxial Tension Test Stress versus Strain Plots

The following tables are from the uniaxial tension testing and show the stress versus strain plots for the web and flange test specimen.
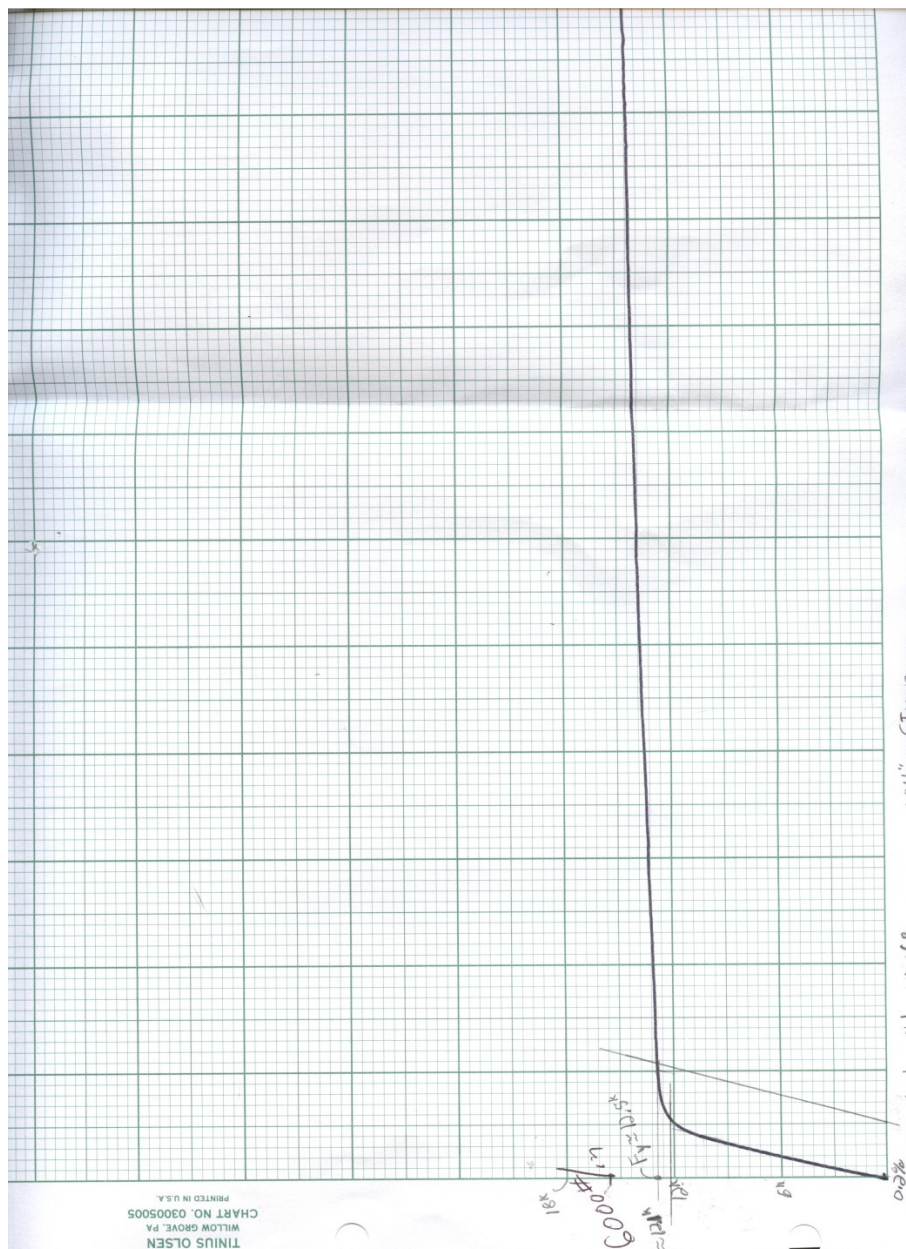

Figure H-1: Stress versus Strain Plot for the Stem Dogbone Specimen.

Figure H-2: Stress versus Strain Plot for the Flange Dogbone Specimen.

Appendix I: Copyright Permissions

The following is an email stating that inserting the installation manual found in

Appendix D is acceptable.

```
-----Original Message-----
From: Texas Measurements [mailto:sales@straingage.com]
Sent: Friday, May 04, 2012 8:55 AM
To: Meier, Austin A.
Subject: Re: FW: Cited Work for Master's Project

Good morning Austin,

We are happy to give permission to scan a copy of the installation guide into
your thesis' Appendix. Thank you for asking, and good luck with your thesis.

Sincerely,
Amy Persyn
Office Manager

Texas Measurements, Inc.
Tel: 979-764-0442
Fax: 979-696-2390
Email: sales@straingage.com
Web: www.straingage.com



Meier, Austin A. wrote:
>
> Hello,
>
> I tried sending this to the actual manufacturers email address but got
> an "undeliverable" error so I thought I could send it to the supplier
> then. I dealt with Harry Jones with this transaction/sale. Below
> summarizes my situation. Feel free to contact me at this email or my
> cell phone is 920-203-2906. Thank you.
>
> *From:* Meier, Austin A.
> *Sent:* Thursday, May 03, 2012 8:31 PM
> *To:* 'sales@tokyosokki.co.jp'
> *Subject:* Cited Work for Master's Project
> Hello,
>
> I am currently a Graduate student at the Milwaukee School of
> Engineering working on my thesis for Structural Engineering. Earlier
> in the year my partner and I purchased TML Bolt Strain Gages from
> Texas Measurements which got the strain gages from your company. What
> my question is, is that in our thesis papers we have an Appendix
> section in which we would like to use a scan copied of this
> installation instruction guide (2 pages total) to better demonstrate
> how we installed these strain gages, would you have any disagreement
> to us putting this directly into our paper? We would give full
> reference and credit of course to your company. If so, please let me
> know and I can send an agreement mandated by our library advisor and
> if you would like us not to do this it is no problem at all. I look
> forward to hearing back from you. Thank you for your time.
>
> *Austin Meier*
>
> Milwaukee School of Engineering '12
>
> Architectural Engineering B.S. &
>
> Structural Engineering M.S.
>
> meieraa@msoe.edu <mailto:meieraa@msoe.edu>
>
> http://173.193.254.108-static.reverse.softlayer.com/web-2010/web_image
> s/school_logos/w_200/msoe200.jpg
```

Structural Engineering

Capstone Report Approval Form

Master of Science in Structural Engineering -- MSST

Milwaukee School of Engineering

This capstone report, titled "Effects of Bolt Spacing on Prying Action in Thin Flanged Specimens" submitted by the student Richard G. DeSimone, has been approved by the following committee:

Faculty Advisor: _____ Date: _____

Dr. Christopher Raebel, Ph.D., P.E., S.E.

Faculty Member: _____ Date: _____

Dr. Hans-Peter Huttelmaier, Ph.D., P.E.

Faculty Member: _____ Date: _____

Professor Michael Kempfert, M.S., P.E.